February 2020

Irish Water
CRU Water Services Innovation Fund

Climate Change Adaptation – Linking science with industry and customer needs – Identification of Climate Sensitive Catchments

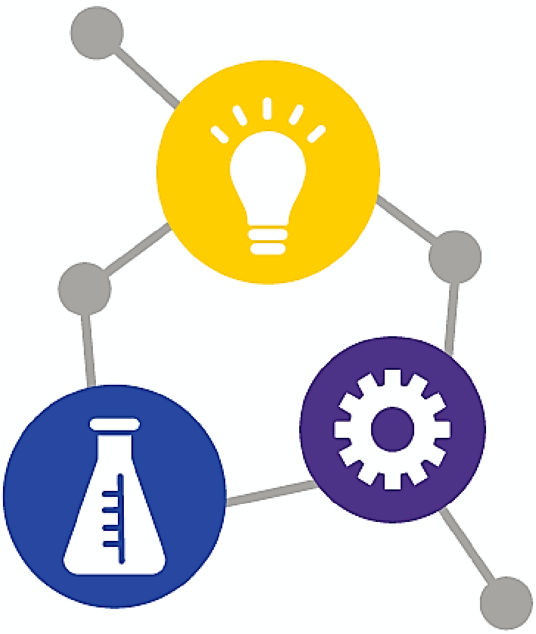

Commission for Regulation of Utilities (CRU) Water Services Innovation Fund

Climate Change Adaptation – Linking science with industry and customer needs – Identification of Climate Sensitive Catchments

Attached is *Identification of climate sensitive catchments: Water Resources and Climate Change Adaptation* produced for Irish Water by Dr Ciaran Broderick and Dr Conor Murphy of the Irish Climate Analysis and Research UnitS (ICARUS), Department of Geography, Maynooth University.

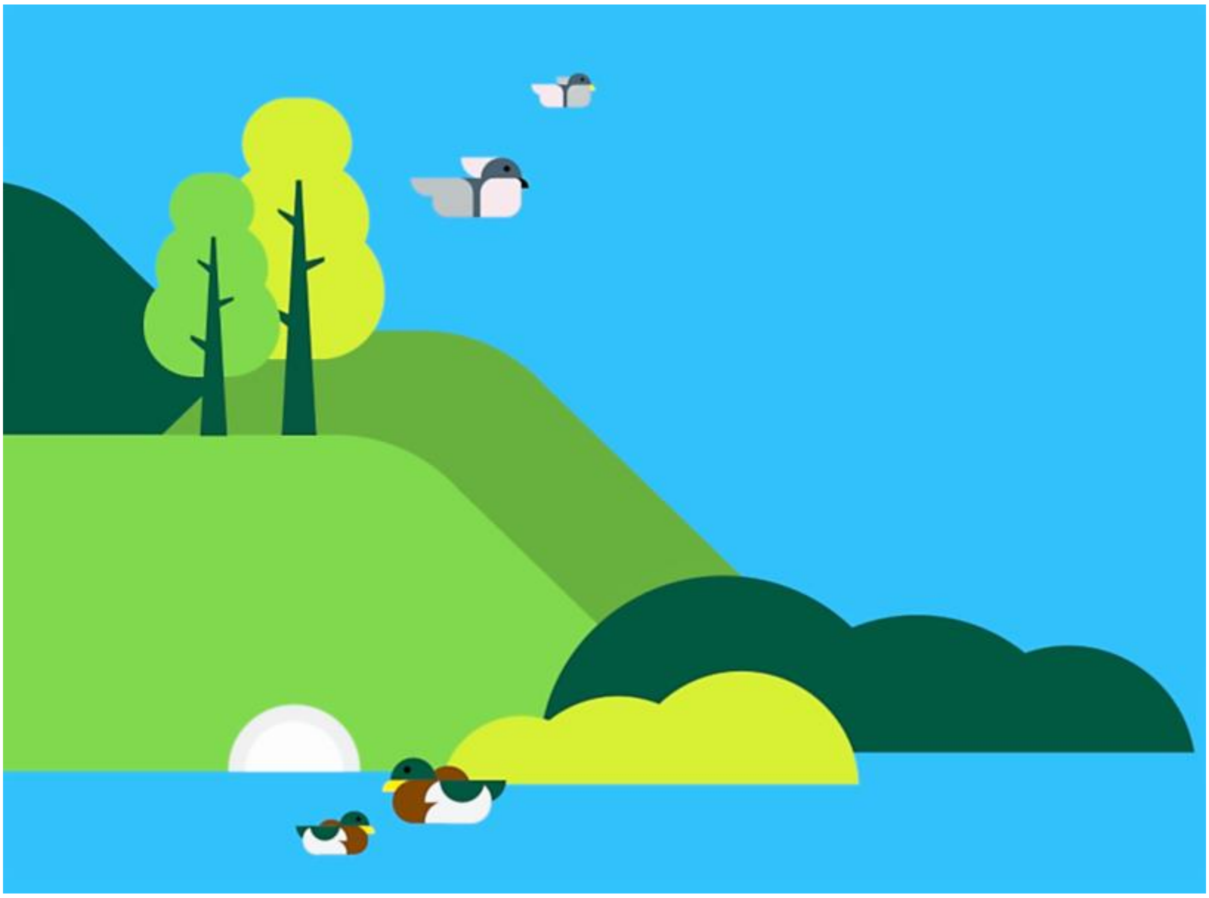

IRISH WATER

PO Box 860, South City Delivery office, Cork City, Ireland

Telephone: Callsave 1800 278 278 / International +353 1 707 2828

Website: www.water.ie

ACKNOWLEDGEMENTS

This report is published as part of the Commission for Regulation of Utilities (CRU) Water Services Innovation Fund.

In 2015, the CRU established the Water Services Innovation Fund. The Innovation Fund allows Irish Water to explore innovative technologies and approaches through projects that would not otherwise be funded as part of its normal operating costs or Investment Plans. By their nature, innovation projects may not succeed, however, for a project to be approved, Irish Water must demonstrate that it has a reasonable chance of delivering defined, tangible benefits for Irish Water's customers and that these benefits outweigh the cost of the project. Projects must be designed to deliver improvements in at least one of the following areas:

- Provision of safe, secure, and reliable water services;
- Increased understanding of customer behaviours and their drivers and effective customer engagement;
- Enhanced energy savings in the provision of water services;
- Achievement of relevant environmental standards and the objectives of the Water Framework Directive;
- Mitigation of negative climate change impacts;
- Provision of water services in an economic and efficient manner; *and*
- Improved conservation of water resources.

DISCLAIMER

Identification of climate sensitive catchments: Water Resources and Climate Change Adaptation

Dr Ciaran Broderick & Dr Conor Murphy

Report prepared by Irish Climate Analysis and Research UnitS (ICARUS), Department of Geography, Maynooth University for Irish Water

Foreword

Climate change is projected to have a significant impact on our water services. Reduced rainfall with a growing population and economy may put increased pressure on our water supplies and receiving waters. In order to reduce and manage the risks associated with climate change Irish Water has committed to using best available techniques to assess the vulnerability of water and wastewater services to climate change[1].

The project brought together the expertise within Irish Water and academia to develop innovative tools for informing decision making to maximise benefit to the customer and to maintain a sustainable water service. A sustainable water service is fundamental to the ability of Irish Water to achieve our objectives to 'provide safe and reliable water, maximise the value to Irish Water's customers from available resources, provide efficient and economic management of water and wastewater supply assets, support social and economic growth, protect and enhance the environment' and meet customer expectations. To this end, the project provided:

- A review of best available techniques to assess the vulnerability of water resources to climate change;
- An assessment of the sensitivity of 206 river catchments to low flows caused by climate change; and
- Decision tools to aid water resources managers make risk based decisions regarding climate change vulnerability.

This work represents a thorough and detailed look at the issue of how climate change is likely to impact river flows in Ireland. It is to Irish Water's knowledge the most detailed assessment of the issue yet. Findings of this research will assist Irish Water in understanding impacts of climate change on Irish catchments and water quality. These findings are being used to assess the sustainability of existing and future abstractions for public supplies as part of the development of Irish Water's National Water Resources Plan. This will help to inform investment in our present and future asset base. This research will help Irish Water to strengthen the resilience of water and wastewater services to climate change and provide a safe and reliable water service in the future.

Potential future work in the area of climate change and water resource planning include the following topics

[1]Irish Water Climate Change Policy IW-AMT-POL-010

1) Collect additional hydrological and catchment information to assess climate change vulnerability for all strategically important river catchments, groundwater influenced river catchments, groundwater/lake resources, heavily modified water bodies and wastewater services.
2) Use additional hydrological modelling and catchment information to improve and develop additional response surfaces and approaches to climate assessment. The scenario neutral approach could be extended to other flow indices.
3) Test the resilience of major water supply systems to historical droughts and climate change.
4) Investigate the effect of climate change on the intensity, persistence and location of drought.
5) Develop and implement tools such as seasonal hydrological forecasting to assist water managers in longer term planning.
6) Develop drought monitoring and prediction tools for Ireland.
7) Assess the sensitivity of water quality, particularly water temperature, to climate change.
8) Investigate future design rainfall.

To address the above, collaboration of state agencies such as ESB and OPW will be required.

Table of Contents

List of Tables 10

List of Figures 10

Glossary of Terms & Abbreviations 15

Non-Technical Summary 16

1. Summary of Key Findings 18

1.1 Introduction 18

1.2 Take home messages

1.2.1 Five catchment sensitivity types 19

1.2.3 The importance of hydrological model uncertainty 21

1.2.4 The importance of temperature change to low flows 21

1.2.5 Risk based allowances for climate change planning 22

1.3 Limitations and priorities for future work 22

2. Approaches to Adaptation in the Water Sector 25

2.1 Introduction 25

2.2 Approaches in industry 29

2.2.1 England and Wales 30

2.2.2 Netherlands 32

2.2.3 Germany 33

2.2.4 Denver Water, Colorado 35

2.3 Recommended approach to adaptation 36

2.4 Summary of data requirements for robust adaptation approaches 36

3. Methods - Developing a Scenario Neutral (SN) Approach for Low Flows 38

3.1 Introduction to the Senario-Neutral (SN) framework 38

3.2 Application of Senario-Neutral (SN) method to low flows 43

3.3 The sensitivity domain 44

3.4 Rainfall runoff models employed 43

3.5 Weather Generator (WG) 46

3.6 Low flow indicators 47

3.7 Clustering catchment types 47

3.8 Classification Trees (CT) for ungauged catchments 48

3.9 Datasets employed 49

3.9.1 Observed climate data 49

3.9.2 Catchment data 49
3.9.3 Climate model projections 54
3.10 Results 52
3.10.1 Rainfall-runoff model development 55
3.10.2 CMIP projected climate changes 53
3.10.3 A typology of catchment sensitivity 54
3.10.4 Response surface typologies 80
3.10.5 Interpretation of catchment clusters 82
3.10.6 Discriminant analysis 84
3.10.7 Catchment exposure to projected climate changes 86

3.11 Conclusion 89

References 92
Appendix 96

List of Tables

Table 1.1 Allowances (Percent change) for Q95 low flows in Irish catchments assuming a 2°C rise in annual mean temperature.

Table 2.1 Examples of adaptation frameworks from academic literature.

Table 2.2 Overview of data requirements for robust adaptation.

Table 3.1 List of available Physical Catchment Descriptors (PCDs) derived for the Flood Studies Update (FSU). Also show is the range in values for 206 catchments included in the FSU and values for the 35 catchments used in this study.

Table 3.2 Mean gradient (*y* and *x*-axis respectively) and slope of the +2°C centroid response surface for each rainfall-runoff model. Also shown is the ID number of catchments assigned to each cluster.

Table A1 Physical attributes of the catchment sample used for low flow sensitivity testing. Also listed are the NSE efficiency score for the median simulations from the GLUE procedure estimated for the calibration and validation period for each rainfall-runoff model.

Table A2 Global Climate Model simulations obtained from CMIP5 archive.

Table A3 Group membership for each of the 206 catchments included in the FSU. Catchments are classified according to their physical attributes using the decision rules specified in Figure 3.12.

List of Figures

Figure 1.1 Distribution of catchments falling into each of the 5 sensitivity types (a-e) identified. For ungauged locations, commonly available physical catchment descriptors available from the Flood Studies Update can be used to associate any catchment with a sensitivity type. The user simply needs to follow the decision tree provided.

Figure 2.1 Economic Balance of supply and demand (von Christierson *et al.*, 2010).

Figure 2.2 Traditional versus ATP approaches to adaptation (Kwadijk *et al., 2012).*

Figure 3.1 Contrasting 'top-down' and 'bottom-up' approaches to climate impact assessment.

Figure 3.2 Schematic of methodology used to develop response surfaces for a sample of Irish catchments.

Figure 3.3 Weather generator performance in reproducing the statistical attributes of station scale temperature and precipitation estimated for the period 1976-2005.

Figure 3.4 The location, boundaries and identification number of the catchment sample used to derive low flow response surfaces.

Figure 3.5 Observed and model simulated hydrological signatures estimated for each catchment using the period for which observed flow data is available.

Figure 3.6 Boxplots showing percent changes in the mean annual amount (harmonic mean) and seasonality (harmonic amplitude) of the precipitation cycle described using a single phase harmonic function (equation 1). Plots are developed using GCM simulations from the CMIP5 archive stored at a monthly resolution for all 206 catchments (FSU). Changes are examined for three future time horizons (2010-2039; 2040-2069 and 2070-2099) relative to the 1976-2005 reference and for four different RCP scenarios. Also shown are absolute changes in mean annual temperature for all catchments projected by the CMIP5 ensemble (°C; a).

Figure 3.7 Response surfaces showing changes (%) in the magnitude of the Q95 low flow indicator for incremental changes (5%) in harmonic parameters representing the mean amount (-40% to +40%; x-axis) and seasonality (0% to 50%; y-axis) of the annual precipitation cycle. Surfaces are developed for each of the 47 catchments using the median NAM simulation. Overlain on each plot are changes (%) in the harmonic mean and amplitude projected for the 2080s under all 4 RCPs by each member of the CMIP5 ensemble. Surfaces relate to a +2°C increase in mean annual temperature relative to 1976-2005.

Figure 3.8 As in Figure 7 except for GR4J.

Figure 3.9 As in Figure 7 except for HBV.

Figure 3.10 Response surfaces showing changes (%) in the magnitude of the QAS low flow indicator for incremental changes (5%) in harmonic parameters representing the mean amount (-40% to +40%; x-axis) and seasonality (0% to 50%; y-axis) of the annual precipitation cycle. Surfaces are developed using the median HBV simulation. Overlain on each plot are changes (%) in the harmonic mean and amplitude projected for the 2080s under all 4 RCPs by each member of the CMIP5 ensemble. Surfaces relate to a +4°C (top row), +2°C (middle row) and +0° (bottom row) increase in mean annual temperature.

Figure 3.11 The centroid of five clusters for each rainfall runoff model (GR4J, HBV and NAM) showing the composite response surface relating to a 2°C temperature increase. Response surfaces show change (%) in Q95 for percent changes n the mean amount (-40% to +60%; *x*-axis) and seasonality (0% to 120%; *y*-axis) of the annual precipitation cycle. For plotting purposes the range is constrained between -100% and +100%.

Figure 3.12 The centroid of five clusters for each rainfall runoff model (GR4J, HBV and NAM) showing the composite response surface relating to a 2°C temperature increase. Response surfaces show change (%) in Q95 for percent changes n the mean amount (-40% to +60%; *x*-axis) and seasonality (0% to 120%; *y*-axis) of the annual precipitation cycle. For plotting purposes the range is constrained between -100% and +100%.

Figure 3.13 Classification of (206) catchments from the FSU into one of five different sensitivity types according to their climatological and physical attributes.

Figure 3.14 Percent of CMIP5 projections (y-axis) which exceed climate change allowances of 0% - 40% (relative to baseline period 1976-2005; x-axis) calculated for each catchment type (a-e) and rainfall-runoff model. Thresholds relate to a temperature scenario of +2°C relative to baseline conditions. Climate risk exposure based on the CMIP5 ensemble is calculated using projections for all 206 catchments and the corresponding centroid relating to their sensitivity type (Figure 3.11). Plots show the exposure of each type to projected climate and the adequacy of different adaptive thresholds. The 20% reduction allowance is emphasised using the black line. Combined threshold calculated for RCP4.5, RCP6 and RCP8.5 over the period 2040-2069 and 2070-2099 are shown in the upped row. The second, third and fourth row show thresholds for the period 2070-2099 relating to RCP4.5, RCP6 and RCP8.5 respectively.

Figure A1 Response surfaces showing changes (%) in the magnitude of the Q95 low flow indicator for incremental changes (5%) in harmonic parameters representing the mean amount (-40% to +40%; x-axis) and seasonality (0% to 50%; y-axis) of the annual precipitation cycle. Surfaces are developed for each of the 47 catchments using the median NAM simulation. Overlain on each plot are changes (%) in the harmonic mean and amplitude projected for the period 2010-2039 under all 4 RCPs by each member of the CMIP5 ensemble. Surfaces relate to a +0°C increase in mean annual temperature relative to 1976-2005.

Figure A2 As in Figure A1. except for GR4J.

Figure A3 As in Figure A1 except for HBV.

Figure A4 Response surfaces showing changes (%) in the magnitude of the Q95 low flow indicator for incremental changes (5%) in harmonic parameters representing the mean amount (-40% to +40%; *x*-axis) and seasonality (0% to 50%; *y*-axis) of the annual precipitation cycle. Surfaces are developed for each of the 47 catchments using the median NAM simulation. Overlain on each plot are changes (%) in the harmonic mean and amplitude projected for the period 2040-2069 under all 4 RCPs by each member of the CMIP5 ensemble. Surfaces relate to a +0°C increase in mean annual temperature relative to 1976-2005.

Figure A5 As in Figure A4. except for GR4J.

Figure A6 As in Figure A4 except for HBV.

Figure A7 Response surfaces showing changes (%) in the magnitude of the Q95 low flow indicator for incremental changes (5%) in harmonic parameters representing the mean amount (-40% to +40%; *x*-axis) and seasonality (0% to 50%; *y*-axis) of the annual precipitation cycle. Surfaces are developed for each of the 47 catchments using the median NAM simulation. Overlain on each plot are changes (%) in the harmonic mean and amplitude projected for the period 2070-2099 under all 4 RCPs by each member of the

CMIP5 ensemble. Surfaces relate to a +0°C increase in mean annual temperature relative to 1976-2005.

Figure A8 As in Figure A7. except for GR4J.

Figure A9 As in Figure A7 except for HBV.

Figure A10 Response surfaces showing changes (%) in the magnitude of the Q95 low flow indicator for incremental changes (5%) in harmonic parameters representing the mean amount (-40% to +40%; *x*-axis) and seasonality (0% to 50%; *y*-axis) of the annual precipitation cycle. Surfaces are developed for each of the 47 catchments using the median NAM simulation. Overlain on each plot are changes (%) in the harmonic mean and amplitude projected for the period 2010-2039 under all 4 RCPs by each member of the CMIP5 ensemble. Surfaces relate to a +2°C increase in mean annual temperature relative to 1976-2005.

Figure A11 As in Figure A10. except for GR4J.

Figure A12 As in Figure A10 except for HBV.

Figure A13 Response surfaces showing changes (%) in the magnitude of the Q95 low flow indicator for incremental changes (5%) in harmonic parameters representing the mean amount (-40% to +40%; *x*-axis) and seasonality (0% to 50%; *y*-axis) of the annual precipitation cycle. Surfaces are developed for each of the 47 catchments using the median NAM simulation. Overlain on each plot are changes (%) in the harmonic mean and amplitude projected for the period 2040-2069 under all 4 RCPs by each member of the CMIP5 ensemble. Surfaces relate to a +2°C increase in mean annual temperature relative to 1976-2005.

Figure A14 As in Figure A13. except for GR4J.

Figure A15 As in Figure A13 except for HBV.

Figure A16 Response surfaces showing changes (%) in the magnitude of the Q95 low flow indicator for incremental changes (5%) in harmonic parameters representing the mean amount (-40% to +40%; x-axis) and seasonality (0% to 50%; y-axis) of the annual precipitation cycle. Surfaces are developed for each of the 47 catchments using the median NAM simulation. Overlain on each plot are changes (%) in the harmonic mean and amplitude projected for the period 2010-2039 under all 4 RCPs by each member of the CMIP5 ensemble. Surfaces relate to a +4°C increase in mean annual temperature relative to 1976-2005.

Figure A17 As in Figure A16. except for GR4J.

Figure A18 As in Figure A16 except for HBV.

Figure A19 Response surfaces showing changes (%) in the magnitude of the Q95 low flow indicator for incremental changes (5%) in harmonic parameters representing the mean amount (-40% to +40%; *x*-axis) and seasonality (0% to 50%; *y*-axis) of the annual precipitation cycle. Surfaces are developed for each of the 47 catchments using the median NAM simulation. Overlain on each plot are changes (%) in the harmonic mean and amplitude projected for the period 2040-2069 under all 4 RCPs by each member of the CMIP5 ensemble. Surfaces relate to a +2°C increase in mean annual temperature relative to 1976-2005.

Figure A20 As in Figure A19. except for GR4J.

Figure A21 As in Figure A19 except for HBV.

Figure A22 Response surfaces showing changes (%) in the magnitude of the Q95 low flow indicator for incremental changes (5%) in harmonic parameters representing the mean amount (-40% to +40%; *x*-axis) and seasonality (0% to 50%; *y*-axis) of the annual precipitation cycle. Surfaces are developed for each of the 47 catchments using the median NAM simulation. Overlain on each plot are changes (%) in the harmonic mean and amplitude projected for the period 2070-2099 under all 4 RCPs by each member of the CMIP5 ensemble. Surfaces relate to a +4°C increase in mean annual temperature relative to 1976-2005.

Figure A23 As in Figure A22. except for GR4J.

Figure A24 As in Figure A22 except for HBV.

Figure A25 Percent of CMIP5 projections (y-axis) which exceed climate change allowances of 0% - 40% (relative to baseline period 1976-2005; x-axis) calculated for each catchment type (a-e) and rainfall-runoff model. Thresholds relate to a temperature scenario of +0°C relative to baseline conditions. Climate risk exposure based on the CMIP5 ensemble is calculated using projections for all 215 catchments and the corresponding centroid relating to their sensitivity type (Figure 3.11). Plots show the exposure of each type to projected climate and the adequacy of different adaptive thresholds. The 20% reduction allowance is emphasised using the black line. Combined threshold calculated for RCP4.5, RCP6 and RCP8.5 over the period 2040-2069 and 2070-2099 are shown in the upped row. The second, third and fourth row show thresholds for the period 2070-2099 relating to RCP4.5, RCP6 and RCP8.5 respectively.

Glossary of Terms and Abbreviations	
Abbreviation or Term	**Definition or Meaning**
ICARUS	Irish Climate Analysis and Research UnitS
CRU	Commission for Regulation of Utilities
Q95	The flow rate equaled or exceeded 95% of the time
OPW	Office of Public Works
EPA	Environmental Protection Agency
PCD	Physical Catchment Descriptors
FSU	Flood Studies Update
SN	Scenario-Neutral
CMIP5	Couple Model Intercomparison Project Phase 5
SAAR	Standard Annual Average Rainfall
ALLUV	Proportional extent of floodplain alluvial deposit
SAAPE	Standardised Annual Average Potential Evapotranspiration
NAM	NedborAfstromnings Model
GR4J	Génie Rural à 4 paramètres Journalier
HBV	Hydrologiska Byråns Vattenbalansavdelning Model
BFI	Baseflow Index
RCP	Representative Concentration Pathway
IPCC	Intergovernmental Panel on Climate Change
WRMP	Water Resource Management Plans
OFWAT	Office of Water Services
EA	Environment Agency
DEFRA	Department for Environment, Food and Rural Affairs
UKWIR	UK Water Industry Research
EBSD	Economic Balance of Supply and Demand
WRZ	Water Resource Zones
ATP	Adaption Tipping Point
RBD	River Basin District
RBMP	River Basin Management Plans
UCRB	Upper Colorado River Basin
SCRA	Shoshone Call Relaxation Agreement
WGEN	Weather Generator
PET	Potential Evapotranspiration
GLUE	Generalized Likelihood Uncertainty Estimation
NSE	Nash Sutcliffe Efficiency
WG	Weather Generator
GCM	Global Climate Model
WeaGets	Weather Generator École de Technologie Supérieure
CH	Calinski-Harabasz
CT	Classification Trees
CF	Change Factors
ID	Identification
RC	Runoff Coefficient
HMWB	Heavily Modified Water Body

Non-Technical Summary

Identification of climate sensitive catchments: Water Resources and Climate Change Adaptation

This project was undertaken to gain better understanding of how river flows may change due to climate change and enable better planning for such changes.

The traditional way of looking at the climate change impacts for catchments is to take a 'top down' approach. This approach downscales climate models, forced by different greenhouse gas (GHG) emissions scenarios to run hydrological models for a catchment. This can result in considerable uncertainties at the catchment scale which can hinder decisions making and planning.

This project applied a 'bottom up' methodology to understand the sensitivity of Irish catchments to change in low flows associated with climate change. By examining the potential responses of catchments to plausible changes in climate from a number of climate models, five difference catchment sensitivity types were identified. Climate change projections were then used to examine risk based allowances for changes in low flows across the different catchment types.

206 river catchments were included in the study and were characterised into 5 catchment sensitivity types (a) to (e) as illustrated in Figure 1 below.

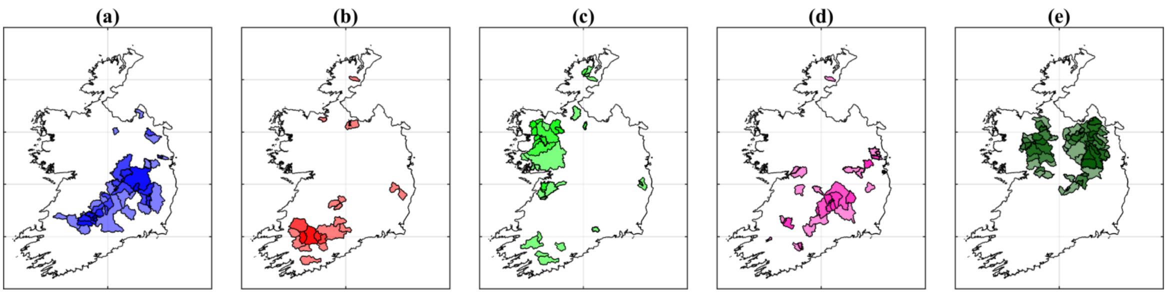

The sensitivity of low flows across catchments to two key types of change were examined; changes in annual mean rainfall and change in the seasonality of rainfall (wetter winters and dryer summer). These were selected given relative confidence in climate models in capturing such large scale features.

Of the five catchment sensitivity types (a), (d) and (e) are generally located in the midlands and east and are characterised as drier, low lying, and possess greater natural storage to offset reduced summer precipitation. These catchments, while still projected to have reductions in flow, are less affected by changes in seasonality of rainfall. Catchment types (b) and (c) are situated in wetter areas of the country particularly along the western seaboard and uplands. They have generally poor natural storage capacity and in turn most sensitivity to changes in the seasonality of rainfall due to climate change.

The main report quantifies the potential reduction in future low flows for various climate scenarios and concluded that in some instances flows during dry weather (Q95%ile) may reduce by in excess of 30% from the middle of this century. A look-up table giving risk based design allowances for flows for each catchment category for various climate scenarios is included as an appendix to the main report.

The findings of this research will assist in understanding impacts of climate change on Irish catchments and water quality which will be impacted on by lower flows and higher temperatures. These findings are being used in the National Water Resources Plan to assess the sustainability of existing and future abstractions for public supplies.

1. Summary of Key Findings

1.1 Introduction

The water sector is likely to face considerable challenges with climate change through increases in floods and low flows and greater variability in water resources. The sector is also key to society and the economy. Changes in low flows are likely to further impact on water quality, water temperature and riverine ecosystems. For those tasked with managing our water resources climate change presents complex logistical and adaptation challenges. Our uncertainty regarding the exact magnitude and timing of future changes means these difficulties are particularly acute where decisions regarding capital investment in long life infrastructure are required. This is particularly the case in Ireland given the lack of previous research to explore the underlying sensitivity of Irish catchments to climate change.

This research examined the climate change sensitivity of river catchments with good quality flow and catchment information. To do this, observed flow records were obtained from gauged locations administered by the Office of Public Works (OPW; http://waterlevel.ie/) and Environmental Protection Agency (EPA; http://www.epa.ie/hydronet/). Information on the physical characteristics (Physical Catchment Descriptors; PCDs) of the catchments were taken from the OPW Flood Studies Update (FSU) - Table 1; Mills *et al.*, 2014). Heavily modified river catchments such as the Liffey and Shannon were not included in scope of this study due to lack of good quality information at the time.

Conventionally climate change assessment has followed a ‘top-down’ framework whereby hydrological models trained to simulate a given catchment or water supply system are forced using climate projections. Model projections relative to present day conditions are used to establish the hydrological response to future climate. Decisions are then made based on adapting to projected impacts. However, this method has a number of drawbacks. Often, selected climate models only represent a small subset of the range of plausible future change. Consequently an over-reliance on model output may result in failure to recognize and plan for important impacts which fall outside the trajectory of change described. Non-linearity in how catchments respond to altered climate forcing further heightens the risk of top-down approaches failing to highlight vulnerabilities across a wider range of possible impacts. In addition, considering large ensembles can result in bewilderingly wide ranges of uncertainty if not treated in a risk based manner. Hence application of scenario-led approaches for risk-based planning decisions is vulnerable to over-confidence in particular climate outcomes.

In light of these limitations, what are referred to as Scenario-Neutral (SN) approaches are increasingly employed to evaluate potential climate change impacts on water and environmental systems. Such approaches start with understanding the sensitivity of the system of interest (hence 'bottom-up'). Typically this involves testing the responsiveness of a key indicator (e.g. low flows, Q95) to incremental adjustments in key climate variables (e.g. temperature, rainfall), across a plausible range of change. SN approaches can also reveal which variables most impact local systems and how antecedent conditions can influence sensitivity, potentially helping to refine decision making. The framework can also be adapted to examine the effect of different climate and hydrological model uncertainties. Within the SN approach climate model simulations are only used to provide guidance on the possible future risks. For instance, by mapping climate model projections onto the sensitivity domain, exposure to climate risk (as defined by current climate ensembles) can be established.

Here we apply the SN method to (i) Establish the sensitivity of Irish catchments to changes in low flows, and; (ii) To explore the exposure of Irish catchments to the full range of change contained in the CMIP5 ensemble of climate models. Together, these objectives can be used to establish guidance/allowances for climate change based on catchment sensitivity to inform adaptation planning in the water sector. Our findings also shed light on the importance of using different hydrological model structures when assessing future low flows and the sensitivity of future low flows to changes in temperature. Full details of the methods and results from our study can be found in main report. Here we provide a brief overview of key findings.

1.2 Take Home Messages

1.2.1 Five catchment sensitivity types

By assessing the sensitivity of low flows (Q95) across 35 catchments to changes in the annual amount and seasonality (wetter winters, drier summers) of precipitation, we identify 5 sensitivity types (a-e). There is a geographical pattern to the location of these catchment types (Figure 3.1.1). This is most evident in the difference between catchment type c and d and reflects a general east-west gradient across the country. Generally catchment types a, d and e are situated on the east coast and midlands region. Catchment sensitivity types b and c are located along the furthermost south/north-western perimeter of the catchment sample and in upland areas. Catchment type d is most sensitive to changes in annual mean precipitation. Greatest decreases in Q95 relating to changes in seasonality are associated with catchment types b and c. Catchment type a, while sensitive to changes in annual precipitation, is highlighted as the least sensitive to changes in the seasonal distribution of precipitation. When changes in seasonality and mean amount are considered together - catchment type d is the most sensitive and type b the least.

In hydrological terms changes in the annual amount and seasonality of precipitation are likely to have a greater impact on catchments which have a shorter memory (i.e. predominantly upland type systems with an impermeable geology and thin peaty soils). As they possess greater storage capacity, catchments with a longer memory (i.e. lowland type systems with permeable geology providing abundant long-term storage) have a low flow regime which is less sensitive to the impacts of inter-annual and inter-seasonal precipitation changes. Overall, catchments characterised as runoff-dominated have a low flow regime which is more sensitive to drier summers (i.e. increased seasonality). For example, despite an increase of up to ~20% in total annual precipitation, catchment types b and c indicate a pronounced decrease in Q95 under an amplified seasonal cycle. While the same behaviour is evident in catchment types a, d and e, owing to their greater natural storage, the impact on Q95 (under the same conditions) is much reduced. Catchment types a, d and e are indicative of more slowly responding drier catchments in the midlands and east. Catchments belonging to types (e) and (d) are differentiated based on evaporative losses, with those in the midlands and south (d) experiencing the greatest losses.

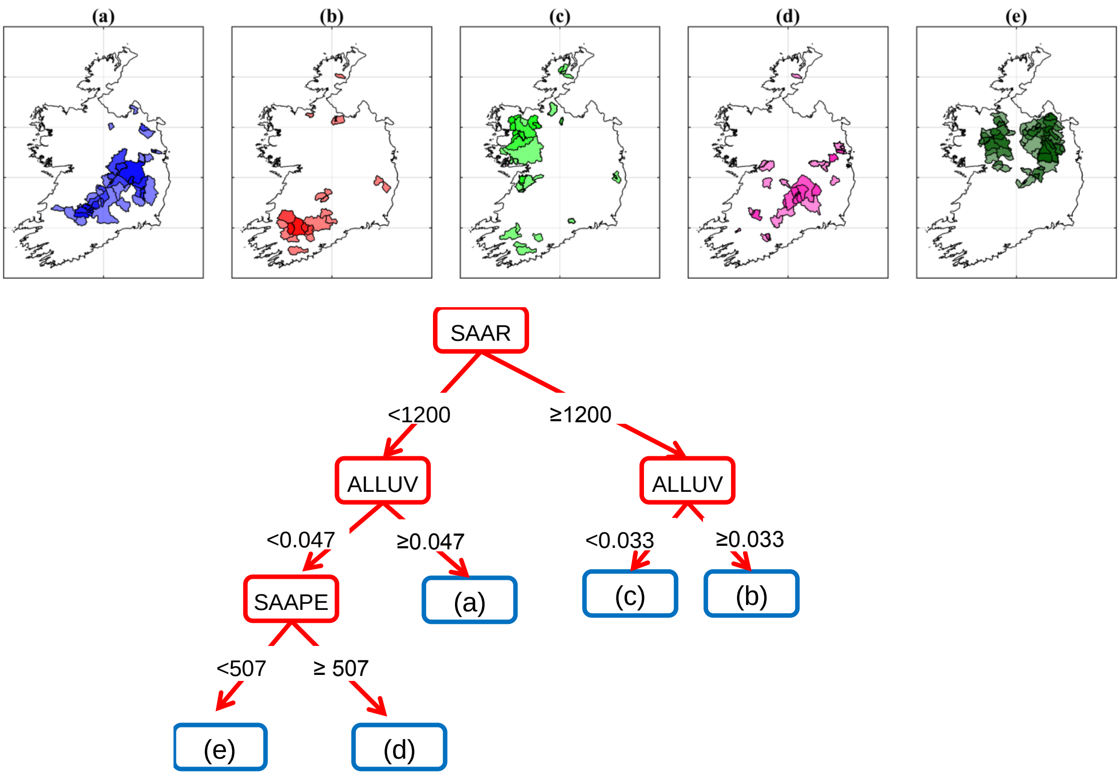

Figure 1.1 Distribution of catchments falling into each of the 5 sensitivity types (a-e) identified. For ungauged locations, commonly available physical catchment descriptors available from the Flood Studies Update can be used to associate any

catchment with a sensitivity type. The user simply needs to follow the decision tree provided.

1.2.2 Extension to ungauged locations

A key success of the SN method is its extension to ungauged locations. Climatology and physical catchment characteristics combine to influence hydrological processes at different spatio-temporal scales and ultimately determine the sensitivity of low flows to changes in climate. Establishing a connection between catchment sensitivity types and commonly available physical catchment descriptors produced by the Flood Studies Update (FSU) enables extrapolation to ungauged or poorly observed catchments. Through a discriminant analysis we derive the decision tree in Figure 1.1 to associate any ungauged catchment with a catchment sensitivity type. The first distinction between catchment sensitivity types is related to differences in Standard Annual Average Rainfall (SAAR). Catchments with greater precipitation (types c and b) are designated as more sensitive to changes in seasonality. Drier catchments are associated with types a, d and e. ALLUV indicates the proportion or extent of floodplain alluvial deposits and is indicative of poorly draining soil. For wetter catchments (>1200mm/yr^{-1}) this predictor distinguishes between type c and b. For drier catchments it also distinguishes between catchment types e/d and a. A final distinction between catchment types e and d is made based on evaporative losses using the Standardised Annual Average Potential Evapotranspiration (SAAPE) descriptor.

1.2.3 The importance of hydrological model uncertainty

The analysis employs three different and widely used hydrological models (NAM, GR4J, HBV). Results show that sensitivity to climate change is influenced by hydrological model choice. In terms of climate exposure GR4J and HBV typically suggest greater reductions in low flows than simulated by the NAM model. Model results show GR4J generally performs better than NAM and HBV for the majority of catchments, particularly those with a lower Baseflow Index (BFI). Given the importance of hydrological model uncertainty it is strongly recommended that assessments of low flows under climate change should use an ensemble of hydrological model structures as done here. Derived climate change allowances (below in section 1.2.5) also recognize the importance of hydrological model uncertainty and are tailored to visualize specific model outputs.

1.2.4 The importance of temperature change to low flows

Catchment sensitivity to changes in annual rainfall totals and seasonality was assessed for different magnitudes of temperature change. The main results presented are for an annual mean temperature increase of 2°C relative to the period 1976-2005. This temperature scenario is selected given that it is a good approximation of temperature change for individual catchments across different representative concentration pathways (RCP) or emissions scenarios, particularly for the 2080s under RCP 6.0 and RCP 4.5. It is important to note that results are sensitive to changes in temperature given greater evaporative loses at higher temperatures. Therefore in the main report, we estimate climate exposure and reductions in low flows for an annual mean temperature increase of 4°C (consistent with upper end change for RCP 8.5 by the end of the century). Assessment shows substantially greater exposure (i.e. reductions in low flows) for this higher temperature scenario.

1.2.5 Risk based allowances for climate change planning

Using the SN approach risk based allowances were extracted for low flows across catchment sensitivity types. These were derived by overlaying projected changes from the CMIP5 ensemble of climate models onto catchment response surfaces. These allowances are not prescriptive and it is up to Irish Water to decide on how to use them best for decision purposes. It may be that more stringent allowances are employed for high risk/value decisions and lower allowances for less critical situations.

Allowances are provided for a scenario of 2°C warming (relative to 1976-2005) in Table 1.1. For each catchment sensitivity type, allowances are presented for (i) 2080s under RCP 8.5 (left most table); (ii) 2080s under a middle of the road RCP 4.5 (central table), and (iii) all RCPs for the latter half of the century (2040-2099) (right most table). In each case allowances are extracted for individual hydrological models and the average across each hydrological model. The derived allowances are risk based relative to the full CMIP5 ensemble. For instance, the *central 50th* allowance represents the percent reduction in Q95 as represented by up to half of the CMIP5 ensemble. Similarly the *upper 75th* allowance represents the reduction in Q95 as simulated by up to 75 percent of CMIP5 climate models. Given that the CMIP5 ensemble is under representative of the plausible range of change in future rainfall we also derive an *upper* + allowance which exceeds by 5 percent the upper range reduction in Q95 as simulated by the CMIP5 archive.

1.3 Limitations and priorities for future work

This work represents a comprehensive assessment of climate change sensitivity and low flows in Ireland. However, a number of limitations and assumptions exist. There is an under-representation of small upland and urban catchments in the sample used. A larger more diverse sample of catchments may affect the identification of catchment types and regionalization to ungauged catchments. While the SN approach has many advantages it is restricted to examining precipitation changes along two dimensions, in this case changes in annual mean and the seasonality of precipitation. It is possible that changes in additional aspects of the precipitation regime (e.g. persistence of dry periods) are also likely to influence future low flows and future work should explore this. In addition, it is assumed that the hydrological models used provide a reliable simulation of low flow behaviour under climate conditions which diverge greatly from the observed period used for model calibration. The approach developed is also restricted to examining sensitivity to changes in low flows (Q95).

Given the importance of a well-adapted and resilient water sector to economy and society it is crucial that water managers continue to develop the tools and datasets necessary to underpin effective decision making in response to climate change. This work represents just one contribution. Recent work has highlighted the significant and prolonged droughts that have occurred historically, while summer 2018 served to highlight the vulnerability of water supplies. It is recommended that future work priorities may require collaboration of state agencies to address topics as outlined below:

1. Collect additional hydrological and catchment information, especially for groundwater and strategically important river catchments
2. Use additional hydrological models and catchment information to improve and develop additional response surfaces and approaches to climate assessment. The scenario neutral approach could be extended to other flow indices
3. Testing the resilience of major water supply systems to historical droughts and climate change
4. Investigate the effect of climate change on the intensity, persistence and location of drought
5. Development of tools such as seasonal hydrological forecasting to assist water managers in longer term planning. Such capacity is currently being developed at Maynooth University under the SFI funded HydroCast project
6. Assessment of the sensitivity of water quality, particularly water temperature, to climate change
7. Development of drought monitoring and prediction tools for Ireland

Table 1.1 Allowances (Percent change) for Q95 low flows in Irish catchments assuming a 2°C rise in annual mean temperature

	2080's 2 °C RCP8.5			
Catchment Type A	**GR4J**	**HBV**	**NAM**	**Mean**
Upper+	-40	-38	-38	-38
Upper	-35	-33	-33	-33
Upper 75th	-25	-23	-20	-23
Central 50th	-15	-13	-9	-12
Lower 25th	-5	-4	0	-3
Catchment Type B				
upper +	-65	-55	-43	-54
upper	-60	-50	-38	-49
upper 75th	-45	-38	-30	-38
central 50th	-33	-28	-20	-27
lower 25th	-23	-18	-13	-18
Catchment Type C				
upper +	-50	-50	-55	-52
upper	-45	-45	-50	-47
upper 75th	-35	-35	-41	-37
central 50th	-26	-25	-28	-26
lower 25th	-16	-14	-14	-15
Catchment Type D				
upper +	-40	-48	-43	-44
upper	-35	-43	-38	-39
upper 75th	-24	-32	-27	-28
central 50th	-18	-23	-18	-19
lower 25th	-7	-10	-3	-7
Catchment Type E				
upper +	-43	-55	-38	-45
upper	-38	-50	-33	-40
upper 75th	-27	-33	-23	-28
central 50th	-18	-20	-13	-17
lower 25th	-8	-8	-5	-7

	2080's 2 °C RCP4.5			
Catchment Type A	**GR4J**	**HBV**	**NAM**	**Mean**
Upper+	-40	-40	-32	-37
Upper	-35	-35	-28	-33
Upper 75th	-18	-18	-15	-17
Central 50th	-13	-11	-8	-11
Lower 25th	-5	-4	-2	-4
Catchment Type B				
upper +	-55	-50	-45	-50
upper	-50	-45	-40	-45
upper 75th	-33	-28	-23	-28
central 50th	-25	-23	-18	-22
lower 25th	-18	-13	-10	-14
Catchment Type C				
upper +	-50	-50	-57	-52
upper	-45	-45	-52	-47
upper 75th	-27	-25	-31	-28
central 50th	-20	-17	-20	-19
lower 25th	-13	-10	-9	-11
Catchment Type D				
upper +	-40	-47	-45	-44
upper	-35	-42	-40	-39
upper 75th	-18	-25	-21	-21
central 50th	-13	-18	-12	-14
lower 25th	-5	-7	-3	-5
Catchment Type E				
upper +	-43	-48	-38	-43
upper	-38	-43	-33	-38
upper 75th	-19	-23	-18	-20
central 50th	-13	-14	-12	-13
lower 25th	-5	-3	-3	-4

	2040-2099 2 °C RCP 4.5, 6.0, 8.5			
Catchment Type A	**GR4J**	**HBV**	**NAM**	**Mean**
Upper+	-40	-40	-38	-39
Upper	-35	-35	-33	-34
Upper 75th	-21	-18	-17	-19
Central 50th	-13	-12	-11	-12
Lower 25th	-5	-3	-3	-4
Catchment Type B				
upper +	-60	-55	-45	-53
upper	-55	-50	-40	-48
upper 75th	-36	-32	-26	-31
central 50th	-28	-24	-20	-24
lower 25th	-20	-15	-13	-16
Catchment Type C				
upper +	-50	-50	-60	-53
upper	-45	-45	-55	-48
upper 75th	-30	-29	-34	-31
central 50th	-22	-20	-23	-22
lower 25th	-15	-13	-12	-13
Catchment Type D				
upper +	-40	-50	-45	-45
upper	-35	-45	-40	-40
upper 75th	-22	-28	-23	-24
central 50th	-15	-20	-15	-17
lower 25th	-8	-12	-5	-8
Catchment Type E				
upper +	-43	-48	-38	-43
upper	-38	-43	-33	-38
upper 75th	-23	-38	-20	-27
central 50th	-15	-18	-13	-15
lower 25th	-8	-8	-5	-7

2. Approaches to Adaptation in the Water Sector

2.1 Introduction

In determining 'best practice' for adaptation within the Irish Water Sector, a review of approaches taken by climate experts presents several frameworks which can be adopted when developing climate change adaptation strategies. These approaches are broadly separated into two categories, namely 'top-down' or scenario led approaches and 'bottom-up' or vulnerability led approaches. The Intergovernmental Panel on Climate Change (IPCC) (2014) highlights how the 'top-down' approach works, whereby climate models are run to generate projections of future climate and subsequently inform policy through the development of scenario-impact research. This is a standard method in climate science and the impacts literature. However, the propagation of uncertainty throughout the 'top-down' modelling process, due to the various assumptions and limitations of models, results in climate information of limited utility for decision makers attempting to develop robust adaptation strategies. The uncertainties in 'top-down' approaches are unlikely to be overcome in the near future; adaptation work has begun to adopt approaches, which incorporate elements of 'bottom-up' approaches to climate change adaptation.

In contrast to 'top-down' approaches, 'bottom-up' approaches aim to understand and identify the various processes which contribute to existing vulnerability within the system in question. 'Bottom-up' approaches place greater emphasis on the study of social and/or physical systems and their thresholds, in order to identify the system's ability to cope with ranges of plausible change. Subsequently, factors, which affect adaptive capacity (i.e. the potential for adaptation, such as politics, economics, income, social capital, location and technology, etc.) (IPCC, 2014), are investigated with the aim of developing policy which reduces current vulnerabilities and increases resilience. The main benefits of 'bottom-up' approaches include the ability to incorporate the uncertainty associated with scenario driven 'top-down' approaches, however this approach can also be problematic due to the inability to assess the robustness of adaptation actions under changing climate conditions.

As such, approaches taken in academic literature aim to identify synergies between 'top-down' and 'bottom-up' approaches to adaptation, in order to develop frameworks which integrate climate science with decision making processes. The application of these approaches can be used to explore key vulnerabilities while maximising information from climate models to develop greater understanding of system exposure and the appraisal of robust adaptation options. Several of these frameworks have been developed, examples of which are provided in Table 2.1.

Table 2.1 Examples of adaptation frameworks from academic literature

Framework	Description	Further information
Adaptive Policymaking/ Adaptive Management	A dynamic framework based on four principles: (i) adaptation to short-term climate variability should be prioritised as a foundation for reducing variability to long term change (ii) adaptation should take place at a relevant scale (iii) adaptation should occur in a developmental context (iv) adaptation strategies and how stakeholders implement strategies are equally important.	Walker *et al.* (2013) Burton *et al.* (2005)
Decision Scaling	A dynamic framework which aims to link 'bottom-up' vulnerabilities with tailored climate information. An iterative, phased approach which ends when climate risks have been addressed, if not continued assessment is completed. Generalised the phases include (i) stakeholder engagement to identify system performance indicators and a portfolio of adaptation option, (ii) developing system models, (iii) simulating the system and identifying performance metrics and (iv) evaluation of adaptation options through stress testing.	Poff *et al.* (2015) Ray and Brown (2015) Brown *et al.* (2012) Wilby and Murphy (In press)
Information-Gap Theory	A iterative and static method for identifying adaptation options which are robust under severe uncertainty by (i) developing a model of uncertainty, (ii) developing a system model, (iii) identification of adaptation strategies, (iii) setting performance requirements and (iv) evaluating robustness	Matrosov *et al.* (2013) Korteling *et al.* (2012) Hall *et al.* (2012)

Framework	Description	Further information
	of strategies under a range of plausible future conditions. Aims to develop strategies which 'satisfice' adaptation requirements under a range of future conditions.	
Robust Decision Making	A iterative and static method for identifying adaptation options which are robust under severe uncertainty by (i) creating a portfolio of adaptation options, (ii) characterises uncertainties and trade-offs for adaptation options (iii) identification of candidate strategy, (iii) characterisation of candidate strategy vulnerability through exploratory modelling and (iv) assessing options, for improving an adaptation strategy. Aims to develop a strategy which 'satisfices' adaptation requirements under a range of future conditions. Differs from information-gap theory in the sequencing of analysis and technical methodology.	Matrosov *et al.* (2013) Weaver *et al.* (2012) Hall *et al.* *(2012)* Wilby and Murphy (In press)
Real Options Analysis	A dynamic framework which explores future scenarios with the aim of incorporating flexibility into decision making processes by identifying how current decision may limit adaptation and attempts to increase the ability to react to future change through monitoring and learning. This approach to climate change adaptation is primarily utilised in examining monetary benefits and flexibility of adaptation options.	Woodward *et al.* (2013)

There are several differences between the adaptation approaches illustrated in Table 2.1, such as:

(i) The treatment of uncertainty, which can be seen by comparing information-gap methods, which use non-traditional methods to sample wider ranges of uncertainty

(Korteling *et al.*, 2012), to adaptive policymaking whereby adaption over time is emphasised in order to reduce uncertainties through the timing of adaptation actions;

(ii) Adaptation aims, for example, real options analysis provides a framework for identifying adaptation strategies which place greater emphasis on cost effectiveness in contrast to approaches, such as adaptive management, which considers the cost benefits but prioritises the broader effectiveness of adaptation strategies; and

(iii) Adaptation strategies outcomes, as shown by Beh *et al.* (2015) who distinguish between frameworks based on whether they result in static (rigid) or dynamic (open-ended) adaptive strategies. Wilby and Murphy (in press) explore static and dynamic approaches, by comparing robust decision making and decision scaling, while also providing real world examples.

While there may appear to be many adaptation frameworks to choose from in decision making under uncertainty, in practice, they all have essentially five key elements:

1. Coherent descriptions of plausible ranges of change in future climatic and non-climatic pressures
2. A model of the system of interest (e.g. catchment or water resource system)
3. A set of thresholds or limits which determine the vulnerability of the system (e.g. low flow threshold which should not be surpassed or threshold of minimum deployable yield which needs to be maintained)
4. Portfolios of potential adaptation options (identified by relevant stakeholders in water resources management including local community, agriculture, industry, health services, etc.)
5. Indicators of decision outcomes (which give a measure of success of identified adaptation options relative to the plausible ranges of change assessed)

The general idea is to ‘stress test’ the system with, and without, the adaptation(s) under the given set of pressures (climatic and non-climatic) and to then compare the resulting vulnerability or performance indicators against baseline conditions. Where vulnerability is found to exist a preferred adaptation strategy is one which is robust to the range of pressures imposed (i.e. reduces vulnerability), yet may still entail trade-offs between various objectives such as population growth, agricultural demand, etc.

Determining 'best practice' for adaptation is best achieved by identifying these commonalties and incorporating them into the approach to be taken in the Irish water sector. The primary objective of a climate adaptation plan should be to develop a framework which tests vulnerability to a wide range of plausible climatic and non-climatic futures and emphasises adaptation strategies which are not overly reliant on specific model predictions of future climate, but are robust against a range of plausible future changes. Even large ensembles of climate models present a lower bound estimation of future climate uncertainty, at best. Wilby and Dessai (2010) highlight that uncertainty is a key variable when considering climate change adaptation and therefore it is sensible to pursue robust decision making and decision centric frameworks which facilitate dealing with uncertainty to identify adaptation options which perform well over a wide range of future conditions. Subsequently, modelling carried out for the purpose of climate change adaptation should be exploratory, not deterministic in nature. Exploratory models can be used to stress-test system sensitivity and identified adaptation options, which can be achieved through the use of 'scenario-neutral' approaches, such as that of Prudhomme *et al.* (2010) and/or decision scaling (Brown *et al*. 2012). Secondary benefits of this approach include the potential to reduce the monetary costs, the computational resources and the technical expertise associated with climate models.

Developing portfolios of potential adaptation options is also sensible as water management is a cross-sectoral issue. As such it will require stakeholder engagement in order to identify candidate strategies which are acceptable across relevant sectors. Wilby and Dessai (2010) suggest that adaptation options should preferably be (i) 'low-regret', in that adaptation should yield benefits regardless of changes in future climate and (ii) flexible, in that they can be reversed, altered or improved to prevent managers becoming 'locked-in' to a single adaptation pathway. This can be achieved by adopting an iterative and dynamic approach to adaptation which reduces uncertainty over time through continued monitoring and learning.

2.2 Approaches in industry

In order to determine 'best practice' for adaptation in the Irish water sector an investigation of the approaches and methods currently being implemented by water managers in different countries, at the time of writing, was completed. Several countries have been examined including France, Spain, Australia, Scotland, Northern Ireland and Germany. To demonstrate the variation in approaches, three case studies are examined: (i) England and Wales, (ii) the Netherlands, and (iii) Denver Water, Colorado. Each case study provides an overview of the adaptation frameworks, adaptation goals and methodologies water managers are using to adapt to climate change.

2.2.1 England and Wales

Water companies in England and Wales are required to provide evidence of their long-term ability to maintain a balance between the demand and supply of water under future climatic conditions. The water sector in England and Wales incorporate climate change into adaptation planning through an adaptive management framework (Table 2.1). This framework seeks to identify and adapt to current system vulnerabilities while continuing to monitor the system in order to learn and improve adaptation options. This framework is facilitated through the development of Water Resource Management Plans (WRMPs). These WRMPs cover a 25 year planning period and must be updated every 5 years. WRMPs embed climate change, along with non-climatic stressors, in the planning process. Stakeholder engagement is an important aspect of this approach, as including relevant actors in the planning process, produces practical information of interest for decision makers.

In a report by the Environmental Agency, von Christierson *et al.* (2013) provide an overview of the approaches to climate change adaptation for the water sector in England and Wales. In this report they highlight that climate change is typically included in planning through forecasts of supply and demand, known as the Economic Balance of Supply and Demand (EBSD) (Figure 2.1). The general working order for this approach is to:

1. Define Water Resource Zones (WRZs)
2. Perform sensitivity testing to identify vulnerable WRZs
3. Evaluate current system performance using baseline supply and demand
4. Forecast supply under future conditions
5. Forecast demand under future conditions
6. Develop portfolios of feasible options based on supply/demand surpluses/deficits
7. Options appraisal

More detailed information on the methods used for sensitivity testing and forecasting supply under future conditions can be found on the UKWIR website (https://www.ukwir.org/). Downing *et al.* (2003) provides a methodology for estimating changes in water demand under future climate conditions. This approach for examining the effects of climate change on the supply/demand balance is primarily 'top-down' scenario lead, whereby change factors are used to adjust historical data. This approach could be criticised for relying heavily on the modelling process or for the use of change factors which fail to account for changes in the timing of flow patterns. The scenario neutral approach for assessing catchment sensitivity to climate change in this work will provide a more suitable assessment of plausible ranges of change for incorporation into adaptive management approaches. Portfolios of feasible options are dependent on circumstance and therefore vary between water companies. However, each water companies' portfolio of adaptation options can be accessed as WRMPs and are publicly available (http://www.water.org.uk/policy/water-resources/water-company-plans). For England and Wales the appraisal of options is carried out on a cost benefit basis, with several companies employing real options analysis as a method for investigating potential adaptations options.

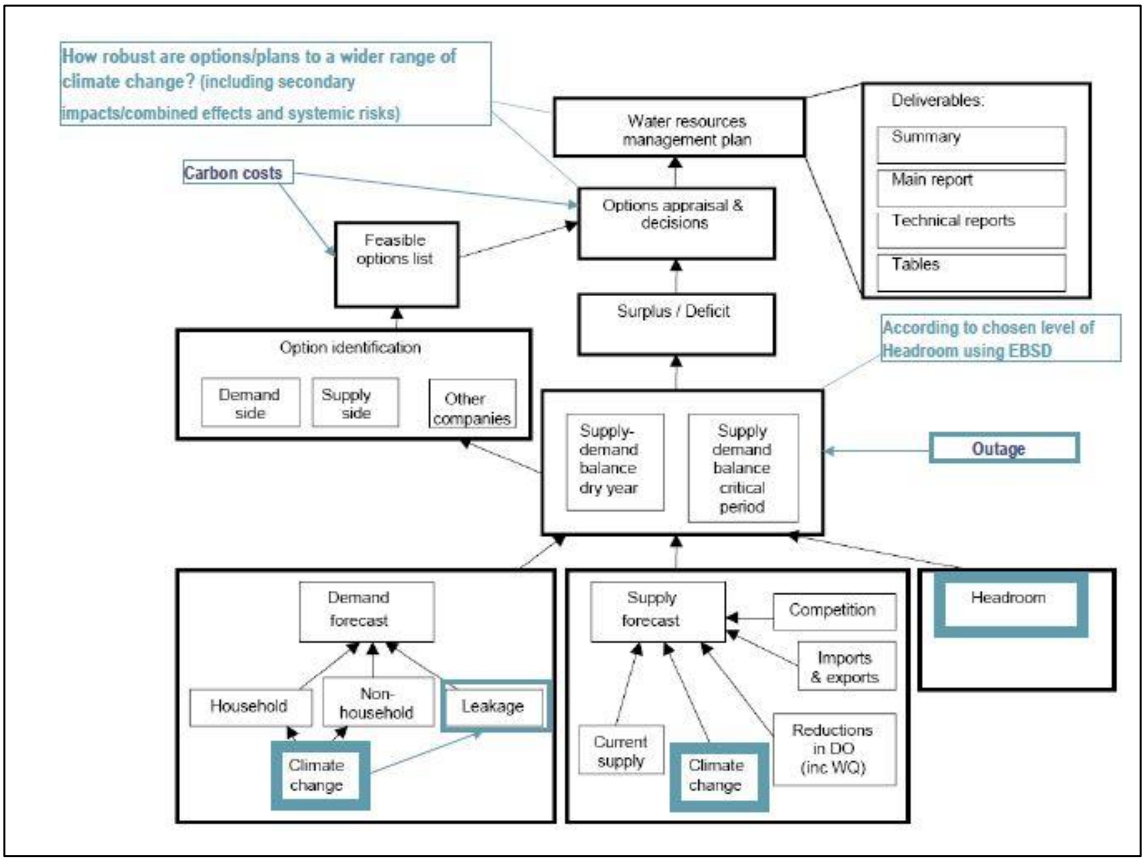

Figure 2.1 Economic Balance of supply and demand (von Christierson *et al.*, 2010)

2.2.2 Netherlands

Water resource managers in the Netherlands have adopted a relatively new approach to climate change adaptation. This approach, known as Adaptation Tipping Points (ATP) or Adaptation Pathways, can be described as a variation of adaptive policymaking/management as it shares several characteristics such as considering climate change in a developmental context and prioritising short term adaptation as a means for providing flexibility for future adaptation. This framework was adopted by Dutch water managers in order to move away from 'top-down' approaches. Ranger *et al.* (2013) describe this approach as a 'decision-centric' approach to adaptation which aims to develop dynamic robustness. As illustrated in Figure 2.2, the ATP approach to adaptation begins by investigating how much change current systems can cope with. The identification of 'tipping points' is central to this approach. In the context of ATP, Kwadijk *et al.* (2010) define these 'tipping points' as points where the magnitude of change, due to climate change, is such that current management strategies no longer function at an acceptable level.

ATP approaches to adaptation focus on identifying whether or not a system requires adaptive measures, and if so, when those measures will be necessary. If an ATP is likely to occur, water managers can then develop new adaptation strategies and appraise their ability to increase a systems ability to cope with change. This presents a framework which is more independent of climate models when compared to traditional approaches, and can even be done without them, but Walker *et al.* (2013) notes that models are often used to explore the timing of adaptation actions. This approach also enables water managers to consider non-climate related stressors, such as economic, societal or political factors, which may result in an ATP being exceeded. Subsequently, the catalyst for adaptation within this framework is not dependent on projections of future climate, which can sometimes limit action, but on the failure of a system to meet required levels of service.

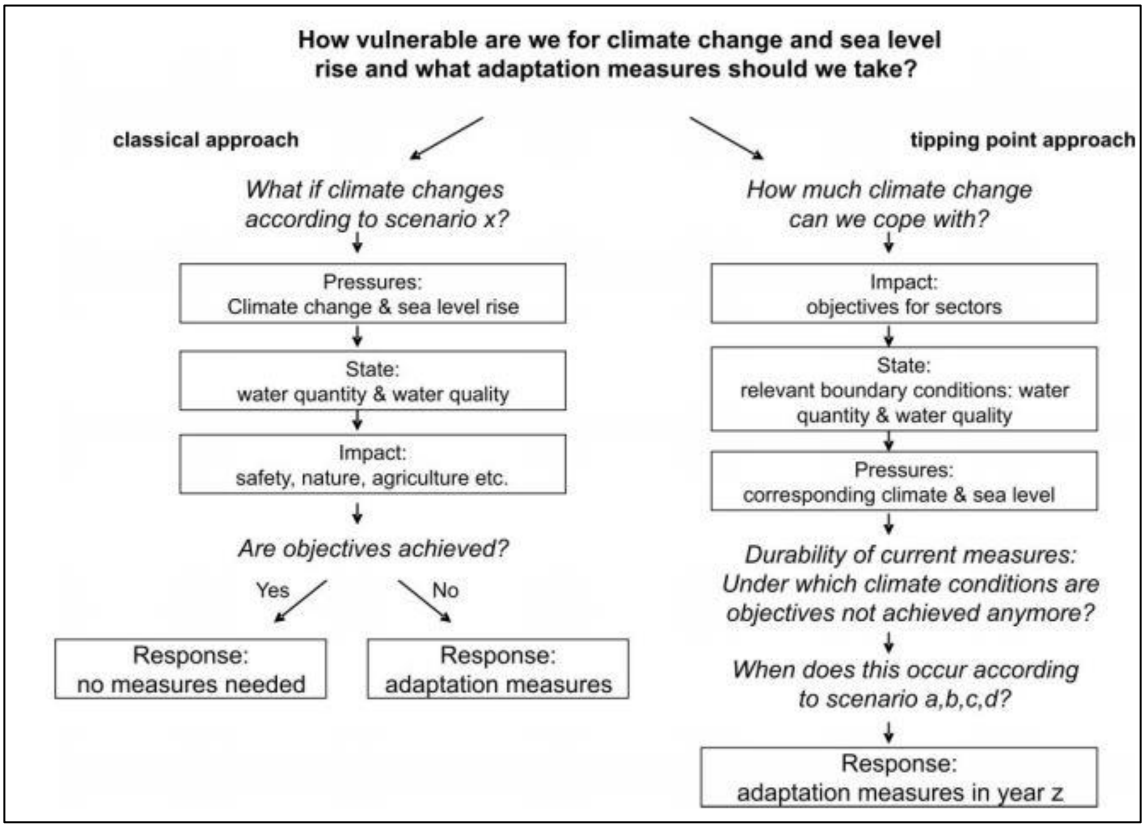

Figure 2.2 Traditional versus ATP approaches to adaptation (Kwadijk *et al., 2012)*

In their case study investigating the application of ATP to the Netherlands, Kwadijk *et al.* (2010) provide a brief overview of the methods for determining ATPs. They use various studies (hydrological, ecological and impact studies, etc.) to examine the sensitivity of different systems to changes in both climate change and sea level rise. They then use climate change projections to estimate the earliest and latest dates at which a management strategy for a particular system is no longer viable. Simultaneously, this framework provides a secondary benefit, in that it enables managers to determine the urgency for adaptation measures by identifying climate change impacts which may be experienced sooner than others and when these issues may be expected. As a result, this adaptation framework develops an adaptation pathway which evolves as more knowledge of the system is discovered.

2.2.3 Germany

In a study investigating changes in future climate, Zebisch *et al.* (2005) conclude that air temperatures and precipitation regimes in Germany are likely to experience change. It is also expected that these changes will result in negative impacts on both social and natural systems. Despite the uncertainties associated with future climate change, decision makers in Germany have recognised the need to develop strategic approaches for adapting to climate change. This process is further complicated by the large numbers of stakeholders and cross-sectoral relationships which must be considered. While water managers in Germany are tasked with managing 10 river basin districts (RBDs), several of these RBDs share borders with other countries. Therefore, water managers in Germany are adopting approaches which require stakeholder consultation, in order to define adaptation objectives and develop potential adaptation measures.

The German Federal Government describes their Adaptation Action Plan framework as a suitable approach for adapting to climate change. In a report on this approach (BMU, 2008), they describe how the government will promote cross-sectoral discussion regarding adaptation strategies, identify the risks that Germany faces as a result of climate change, ensure climate change becomes an integral issue in the planning process and create suitable conditions for strengthening adaptive capacity. The framework employed in Germany is in line with guidelines provided by the European Commission for river basin management under changing climate. As such, water managers in Germany have developed river basin management plans (RBMPs) using these guiding principles described in European Commission (2009) report on river basin management. Examples of these guidelines include:

- Understanding the assumptions, and associated uncertainties, made in the modelling process
- Using a wide range of climate projections or scenarios for river basin management
- Favouring adaptation options which are robust against a range of future conditions
- Favouring adaptation options which provide flexibly
- Identifying 'best-practice' based on current climate research
- Evaluating and improving monitoring networks
- Including knowledge and data from key stakeholders
- Developing cross-sectoral partnerships
- Developing programmes of adaptation options
- Carrying out sensitivity tests and cost benefit analyses to evaluate adaptation options

The approach taken to adaptation in Germany incorporates several of the priority approaches suggested by academic literature. The German water sector is another example where water managers are attempting to develop adaptation methods which aim to avoid adaptation which is based solely on projections of future climate, but instead attempt to extract valuable insights from climate information in order to support robust adaption.

2.2.4 Denver Water, Colorado

Denver Water is a municipal utility responsible for supplying water resources to a population of approximately ~4.5 million people. While regional rivers represent one source of water for Denver, the primary water source for the area originates as runoff from snowmelt in mountain areas. The majority of climate projections for Colorado indicate that future air temperatures will increase, which will affect both the magnitude and timing of the melt season. Projections of future change in precipitation regimes, and subsequently river flows, in the region are highly uncertain (Yates *et al.,* 2015). The reliability of water resources in Denver is reliant on the ability to divert and store runoff in reservoirs, particularly in the Upper Colorado River Basin (UCRB), which accounts for the large majority of storage capacity (Wilby and Murphy, in press). The uncertainty surrounding the future climate of Denver paired with the fact that Denver is a region which experiences recurrent drought, has resulted in a need for Denver Water to develop cost-effective methods for adapting to both long-term and short-term climate change.

Subject to Colorado water laws, access to these reservoirs is subject to a prior appropriation system, a system which provides senior parties priority access to a water resource over other parties. Yates *el al.* (2015) draws attention the Shoshone Call Relaxation Agreement (SCRA), whereby Denver Water have an agreement with energy company Xcel Energy, in which Xcel Energy forego their rights to call water to their Shoshone Power Plant, if certain conditions are met. A more detailed account of the agreement can be found in Yates *et al.* (2015). This approach to adaptation is similar to decision scaling approaches described in academic literature. The steps which can be found in the development of the Shoshone Call Relaxation Agreement compares to those of decision scaling:

1. Stakeholder engagement to arrive at shared understanding of management options

2. Building a model of the physical and legal system which governs water resources in the UCRB
3. Simulating the systems and extracting performance metrics
4. Stress-testing the system with/without the identified adaptation option(s)

The approach taken by Denver Water illustrates a 'low-regret' and innovative approach to climate change adaptation. Using a decision scaling framework, Denver Water were able to engage stakeholders and develop a viable adaptation strategy, which exploits synergies between water management and the power sector, and explore the robustness of adaptation options under a range of future scenarios.

2.3 Recommended approach to adaptation

The examples of England and Wales, the Netherlands and Denver Water, Colorado demonstrate how water management requires inclusive approaches and how determining plausible changes in critical parameters under climate change underpin successful adaptation. Water managers in various water industries are taking steps to move away from traditional 'top-down' deterministic modelling approaches to adaptation. Across each case study, decision makers' favoured exploratory approaches which test system vulnerability and assess the robustness of adaptation strategies, under a range of future climates using methods such as stress-testing or decision-scaling analyses. Similarly, each framework emphasizes the importance of an iterative process, incorporating non-climate stressors and engaging stakeholders in the planning process. In general, the main differences between adaptation frameworks is related to the stage at which climate change information is introduced to the planning process and the method by which it is included. As such, an approach to adaption which satisfies these criteria, such as that of decision scaling or scenario neutral approaches, currently represents 'best practice' for adapting to climate change in the water sector.

2.4 Summary of data requirements for robust adaptation approaches

Implementing robust decision making approaches for adaptation requires diverse datasets. A critical question is how to determine what are plausible or likely ranges of climate change? Too often, thinking is limited to the information available from climate model experiments. In Ireland, climate model experiments are limited to constrained sets of climate projections which undoubtedly underestimate the uncertainties in likely changes. This work will access a much wider range of climate projections as outlined below and make them available for robust decision making and water planning. Yet, there are actually many sources of information to turn to when bounding climate stress tests, including: (i) paleo-climatic records of extreme events that may even pre-date civilization; (ii) historical and archival evidence of weather conditions before systematic measurements began; (iii) documentary weather records built from multiple sources of data; and (iv) observations from the modern instrumental era.

While investigating approaches to climate change in various water industries and in academic literature, observational data and model data were the primary sources of information used. The type of observational and model data required was dependent on the location, the adaptation approach employed and the system of interest. Table 2.2 illustrates a high level summary of the data used in academic literature and various water industries. It is noted that relative to other countries Ireland has significantly less long-term and historic data on our water resources systems. Collating the necessary data for adaption planning is a key step in increasing adaptive capacity and therefore should be an early priority in adaptation planning. In general, improving observational records through expanding monitoring networks, quality assuring data and using historical or documentary sources to extend observational records can contribute to improved analyses. As priority approaches to adaptation advocate for iterative approaches, whereby learning through time to increase system knowledge and reduce the uncertainty horizons, improving monitoring networks provides a 'low-regret' approach to increasing adaptive capacity. Similarly, developing a database of demographic, policy and consumption data will be useful in incorporating non-climatic stressors into adaptation planning.

Table 2.2 Overview of data requirements for robust adaptation

Data	Variable	Description	Potential Usage
Meteorological	Temperature Precipitation Evaporation Humidity	Long records of quality assured daily or sub-daily data	▪ Investigating past and current climate variability ▪ Developing climate models ▪ Identifying links between meteorological and hydrological phenomena
Hydrometric	River flow Groundwater Soil moisture	Long records of quality assured daily or sub-daily data	▪ Developing rainfall-runoff models ▪ Estimating water supply under future climate conditions

			▪ Sensitivity testing
Model	Temperature Precipitation Evaporation Humidity River flow Groundwater Soil moisture	Matching data for observational records	▪ Develop scenarios of future climate ▪ Stress-test adaptation strategies ▪ Estimating uncertainty ▪ Improve understanding of physical processes ▪ Identify tipping points
Demographic	Population	Current population numbers, age, gender, etc.	▪ Estimations of population growth ▪ Identify non-climatic stressors ▪ 'Bottom-up vulnerability' research ▪ Changes in water demand
Policy	Abstraction Storage Headroom	Information regarding water available for use, abstraction licenses, current allowances for shortages, etc.	▪ Developing models of water systems ▪ Develop policy based adaptation strategies ▪ Appraisal of current management strategies
Consumer	Domestic water use Non-Domestic water use	Household usage, industry usage, agricultural usage, etc.	▪ Forecasting water demand under future climate conditions ▪ Developing policy for reducing demand
Physical	Land use Digital Elevation Model Area	Land use maps, physical descriptors	▪ Modelling physical system ▪ Improving understanding of physical processes

3. Methods - Developing a Scenario Neutral (SN) Approach for Low Flows

3.1 Introduction to the Scenario Neutral (SN) framework

For those tasked with managing our water resources climate change presents complex logistical and adaptation challenges. Uncertainty regarding the exact magnitude and timing of future changes means these difficulties are particularly acute in cases where decisions regarding capital investment in long life infrastructure are required. Given its complexity no one prevailing approach to assessing climate impacts has emerged. Conventionally assessment has followed a 'top-down' (scenario-led; Figure 3.1) framework whereby models trained to simulate a given catchment or water supply system are run using an ensemble of climate projections, the latest generation of which (Couple Model Intercomparison Project Phase 5; CMIP5) underpin findings set out in the IPCC (Intergovernmental Panel on Climate Change) Fifth Assessment Report (Taylor *et al.*, 2012). Model projections relative to present day conditions are used to establish the hydrological response to future climate. Decisions are then made based on mitigating and/or adapting to projected impacts.

However this method has a number of limitations. Firstly, the resources required to undertake large-scale climate model experiments mean existing ensembles provide only a limited insight into what is a considerably uncertain future. Consequently, an over-reliance on model output may mean we fail to recognize and plan for important impacts which fall outside the limited trajectory of change they describe. Non-linearity in how catchments respond to altered climate forcing further heightens the risk of scenario-led approaches failing to highlight vulnerabilities across a wider range of possible impacts. Hence application of the scenario-led approach for risk-based planning decisions is vulnerable to over-confidence in particular climate outcomes. Importantly, from a management perspective this approach also makes it difficult to identify significant tipping points, critical thresholds and existing resilience or vulnerabilities within local systems, an understanding of which is necessary for devising robust and cost effective adaptation plans. To address some of these shortcomings a new Scenario Neutral (‘bottom-up’ or sensitivity testing) paradigm for impact assessment has emerged (Figure 3.1; Prudhomme *et al.*, 2010). Here sensitivity of the local system is examined based on how it responses to incremental alterations in climate iterated across an entire spectrum of possible changes. Which climate variables (e.g. temperature, precipitation) and associated parameters (e.g. precipitation intensity, seasonality) are altered is based on how the system or response indicator (e.g. flood peak, Q95) is known to be affected by climate variability. Based on how the indicator changes in accordance with the adjusted climate inputs response surfaces are constructed. Exposure to climate risk is established by mapping climate model projections onto the resultant surfaces (Kay *et al.*, 2014a, 2014c, 2014b; Prudhomme *et al.*, 2015, 2013a).

This represents a more systematic if model intensive approach to impact assessment which gives greater insight into the system’s vulnerability and resilience across a wider range of plausible changes. Furthermore, the response to individual climate scenarios can be established without requiring additional impact analysis. This highlights the framework's flexibility for integrating new climate data, thus allowing easy updating of management plans based on the latest available climate projections/information. For local decision makers the approach also allows identification of less/more sensitive systems, and highlights existing adaptive capacity as well as the presence of critical thresholds. Furthermore it facilitates easier interrogation of long-term management options, including cost-benefit assessment of prospective policy and engineering measures. Finally the framework facilitates assessing additional non-climatic drivers (e.g. population growth) alongside climate, and can be expanded beyond environmental indicators to related impacts (e.g. economic cost, ecological indicators, human health, etc.) (Brown *et al.*, 2012).

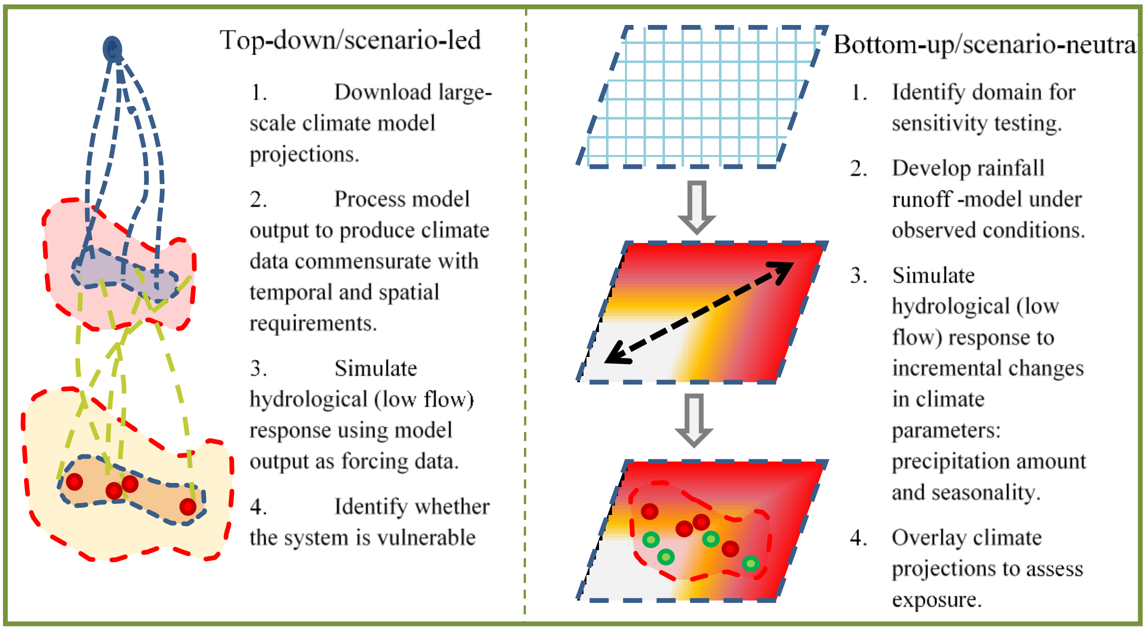

Figure 3.1 Contrasting 'top-down' and 'bottom-up approaches to climate impact assessment

3.2 Application of Scenario Neutral (SN) method to Q95 low flows

In this case the Scenario Neutral (SN) approach is being applied to identify catchments whose low flow regime is sensitive to climate change. The study is undertaken accordingly:

1. Apply scenario-neutral methodology to low flow case for Irish catchments
2. Develop (2-D) response surfaces based on changes in the annual temperature and precipitation cycle
3. Cluster response surfaces to identify more/less sensitive catchment types
4. Link catchment sensitivity to a series of hydrological signatures

5. Identify those physical characteristics which influence sensitivity
6. Assess climate vulnerability and risk exposure using the latest climate model projections
7. Classify ungauged and data sparse catchments into the identified sensitivity types
8. Examine the integration of the resultant response surfaces into decision making processes

Figure 3.2 outlines the methodology used to develop response surfaces. For this we examine how low flow indicators respond to incremental changes in the annual amount and seasonal distribution of precipitation. To examine responses across the sensitivity domain the intercept and amplitude of a single phase harmonic function - used to quantitatively describe the annual cycle at a monthly scale - are iteratively adjusted relative to a reference period (1976-2005) in 5% increments. Here the intercept is adjusted between -40% and +60% while the amplitude is increased by up to 120%.

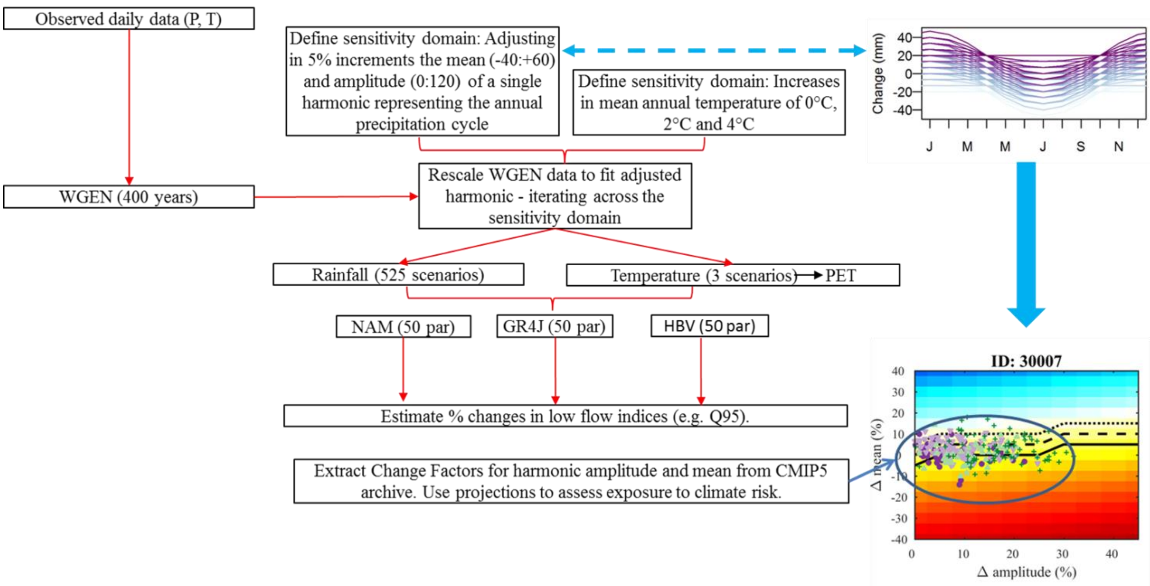

Figure 3.2 Schematic of methodology used to develop response surfaces for a sample of Irish catchments

For each increment the precipitation series is adjusted and input to three different hydrological models each trained to approximate the behaviour of a given catchment system. Model simulated changes in the selected low flow indices relative to a reference point (representing baseline conditions) quantify sensitivity to changes in precipitation and temperature forcing respectively. Once repeated for all increments the results are concatenated and used to construct the response surfaces. Exposure to climate risk is examined by mapping climate model projected changes in the harmonic parameters onto these surfaces. The methodology adopted allows both parametric and structural model uncertainty to be addressed. In addition, a weather generator is used to extend the observed precipitation series and to incorporate natural climate variability in hydrological simulations. To explore the impact of increased evaporation losses the process is repeated for three different temperature scenarios: +0°C, +2°C and +4°C (representing increases in mean annual temperatures). In the case of this study, temperature is used as a proxy for changes in catchment losses through evaporation.

3.3 The Sensitivity Domain

The present study adopts the sensitivity domain outlined by (Kay *et al.*, 2014a, 2014b; Prudhomme *et al.*, 2010, 2013b, 2013a) and employed to derive 2-D flood response surface for UK catchments. Herein the sensitivity domain requires investigating the low flow response to perturbations in the seasonality and mean annual amount of precipitation. For this the intercept and amplitude of a single phase harmonic function representing the baseline annual precipitation cycle are fitted to monthly mean values. The function used is defined as (equation 1):

$$\boldsymbol{X_t = X_0 + A\cos\left(\frac{2\pi}{12}(t - \Phi)\right)} \quad \textbf{(1)}$$

Here X_t is the fitted value for each calendar month, A and Φ represent the amplitude and phase respectively, and X_0 is the arithmetic mean. In this case the phase, denoting the month with the greatest mean precipitation is set to December ($\Phi = 12$). This corresponds with the median month for which the annual precipitation cycle peaks across the catchment sample. To traverse the domain, the amplitude and intercept parameters are iteratively adjusted relative to the reference period (1976-2005) in 5% increments. Changes in mean annual precipitation are reflected in alterations to the intercept, which is adjusted between -40% and +60%, while the amplitude, representing changes in seasonality is increased from 0% to 120%. For each of the 525 combined perturbations the weather generated series is adjusted and input to three rainfall-runoff models. This assessment is repeated for three scenarios representing an absolute increase in mean annual temperature of 0°C, 2°C and 4°C respectively. Adjustments to the WGEN weather generator temperature data are made by additively scaling the daily series. Potential Evapotranspiration (PET) is estimated from daily temperature in accordance with Oudin *et al.*, 2005 (equation 2).

$$\boldsymbol{PET = \frac{R_e}{\lambda_\rho}\frac{T_a + 5}{100} \; if \; T_a + 5 > 0} \quad \textbf{(2)}$$

$$\boldsymbol{PET = 0 \qquad\qquad otherwise}$$

Here PET is the rate of potential evapotranspiration (mm day^{-1}), R_e represents the extraterrestrial radiation (MJ m^{-2} day^{-1}), λ is the latent heat flux (MJ kg^{-1}), ρ is the density of water (kg m^{-3}) and T_a is the mean daily air temperature (C°) estimated from the long term average.

3.4 Rainfall Runoff Models Employed

To address the issue of structural uncertainty the study uses three different conceptual rainfall-runoff models: NAM, HBV and GR4J.

- NedborAfstromnings Model - **NAM**
- Hydrologiska Byråns Vattenbalansavdelning Model - **HBV**
- Génie Rural à 4 paramètres Journalier - **GR4J**

All models use precipitation and PET as input to simulate daily streamflow. The models used differ in their structure, number of calibration parameters and numeric representation of catchment stores, processes and routing routines. Model selection was based on whether the structures have: (i) previously been employed to model Irish hydroclimatological conditions; (ii) known performance for the catchment sample; (iii) computational efficiency; and (iv) dissimilar structures. A summary of each rainfall-runoff model is given below.

NAM (Madsen, 2000) is a lumped conceptual model with nine calibration parameters which simulates the transformation of precipitation to runoff by continuously updating the water content of three linked storage elements (surface storage, lower or root zone storage and a deeper groundwater store). Stores are depleted through evaporative losses and interflow. Overland flow is generated when the surface zone capacity is exceeded. A proportion of this is routed through infiltration to the root zone and the groundwater store respectively. Surface and interflow contributions are routed through two linear reservoirs, with baseflow being routed through a single linear reservoir.

GR4J (Perrin *et al.*, 2003) is catchment scale lumped conceptual model with four calibration parameters. Effective precipitation and soil moisture are derived from net precipitation (i.e. with evaporative losses accounted). Movement from the soil moisture zone along with effective precipitation are divided (10:90 ratio) between two routing channels. The first of which applies a single unit hydrograph; the second channel uses a unit hydrograph and nonlinear storage function. To simulate groundwater exchanges with deeper aquifers and/or adjoining watersheds a gain/loss function is applied to each routing channel.

HBV (Hydrologiska Byråns Vattenbalansavdelning; Seibert, 1996) includes 9 calibration parameters and simulates the rainfall-runoff process using three storage reservoirs: (i) soil moisture zone, (ii) upper subsurface zone, and (iii) lower subsurface reservoir. In addition to components which regulate snowmelt and soil moisture movements, HBV employs runoff response routines and a routing function. Within HBV recharge and evaporation are derived according to soil moisture volume in the upper zone. Outflow from the upper zone is related to activation of a quick flow pathway based on threshold exceedance. Total outflow is derived as the combination of three linear functions. A triangular weighting function is employed to route the outflows from each storage zone to the catchment outlet.

3.4.1 Uncertainty in model parameters: The GLUE method

Model parameter uncertainty is addressed using the Generalized Likelihood Uncertainty Estimation (GLUE) framework (Beven and Binley, 2014, 1992). This is a Monte Carlo (MC) approach to model calibration/validation and uncertainty estimation widely employed in hydrological and environmental modelling. For each rainfall-runoff model 10,000 simulations are conducted for the period 1970 - 2010 taking parameter sets sampled from uniform distributions using a Latin Hypercube scheme. Parameter sets are identified and weighted based on their performance over the calibration period. The sampled sets are also tested using an independent validation period. Three different efficiency measures are used for model evaluation. This includes the Nash Sutcliffe Efficiency criterion (NSE; equation 3) applied to the non-transformed, squared (NSE^2) and log (NSE^{log}) transformed series respectively. This ensures that performance across the flow regime including for variability in high (squared) and low flows (log transformed) determine the final parameter weightings.

$$\mathbf{NSE} = \sqrt{\frac{\sum_{i=1}^{N}\left(\widehat{Q_\iota} - Q_i\right)^2}{\sum_{i=1}^{N}\left(\widehat{Q_\iota} - \bar{Q}_i\right)^2}} \qquad \textbf{(3)}$$

In the above $\widehat{Q_i}$ and Q_i denote simulated and observed streamflow respectively; $\bar{Q}$ is the mean observed flow for the estimation period, i is the flow value for a given time step, and N is the number data points.

The efficiency measure is estimated by multiplying the individual NSE calibration values. Alongside the NSE criterion parameters sets are evaluated according to a volumetric based criterion. Here sets are omitted if they (over)underestimated flow volume by >15% estimated according to (PBIAS) equation 4:

$$\mathbf{PBIAS} = \frac{\sum_{\mathbf{i=1}}^{\mathbf{N}} \widehat{\mathbf{Q}_i} - \mathbf{Q}_i}{\sum_{\mathbf{i=1}}^{\mathbf{N}} \mathbf{Q}_i} \times \mathbf{100} \tag{4}$$

For each model the top 10% of performing sets ranked according to their individual weights are classified as behavioural and used to develop response surfaces. Herein individual model simulations are weighted based on their efficiency score rescaled so as to sum to unity across all behavioural parameter sets. Based on this the selected prediction quantiles at each time step can be derived using equation 5:

$$\boldsymbol{P}\big[\widehat{\boldsymbol{Z}}_{\boldsymbol{t}} < \boldsymbol{z}\big] = \sum_{\boldsymbol{i=1}}^{\boldsymbol{N}} \boldsymbol{RL}\big[\boldsymbol{f}(\boldsymbol{\theta_i})|\widehat{\boldsymbol{Z}}_{\boldsymbol{t,i}}, \boldsymbol{z}\big] \tag{5}$$

Where P is the selected quantile, θ_i is the *i*-th parameter set and N is the number of behavioural parameters. The value of the flow series at time step t by model $f(\theta_i)$ is represented by $\hat{Z}$. For each model the 50th percentile is considered the most likely estimate and adopted to calculate changes in low flow magnitudes across the sensitivity domain.

To ensure transferability between wet and dry conditions models are calibrated using the 6 (odd numbered) non-continuous wettest and driest years on record (Broderick *et al.*, 2016). Years are ranked wettest/driest according to the (1973-2010) catchment average precipitation series. For validation the 6 wettest and driest (even numbered) years respectively are used. To equalize model stores the years 1970–1973 are used as a warm-up period, the years up to 2010 are used for calibration and testing. By simulating the continuous series and adopting non-sequential 12 year periods for training/testing the internal dynamics and temporal stability of catchment stores are maintained.

3.5 Weather Generator (WG)

Weather Generators (WGs) produce climate data of unlimited length, which has the same statistical features (e.g. mean, variance) as the observed data but with a different sequencing of weather events. Their stochastic basis means WGs have the benefit of capturing natural variability in local scale conditions, which is critical for design considerations where high frequency variability is an issue (e.g. drought analysis). By altering their parameters using large scale weather predictors WGs can be adapted to downscale Global Climate Model (GCM) projections. For this study we employ the Weather Generator École de Technologie Supérieure (WeaGets) single-site stochastic weather generator developed by (Chen *et al.*, 2012). Numerically WeaGets is similar to the widely applied WG model (Richardson, 1981) but is altered to improve simulation of low-frequency climate variability (Chen *et al.*, 2010). WeaGets was selected based on its flexibility, parsimonious structure and concurrent simulation of precipitation and temperature - the latter of which is important when modelling systems that require the physical and temporal relationship between both variables to be maintained (e.g. water resource modelling). For this study the WG is trained to match the observed climate series and used to generate a 400 year series. This series is then rescaled - multiplicatively/additively in the case of precipitation/temperature - so as to represent iterative changes in the mean and amplitude of the annual precipitation and temperature cycle respectively. Using an extended low flow series allows greater confidence in the stationarity of the low flow regime under altered climate forcing. Initial work involved developing the model for Irish conditions and validating its performance under observed climate (Figure 3.3). For precipitation the model was found to perform best using a third order Markov chain for wet/dry day occurrence and two parameter Gamma distribution to simulate precipitation amount. The use of Fourier harmonics to smooth the temporal transition between parameters was found to improve performance (Chen *et al.*, 2010). Additional tests were conducted to determine the number and length of simulations required to capture the full range of internal variability.

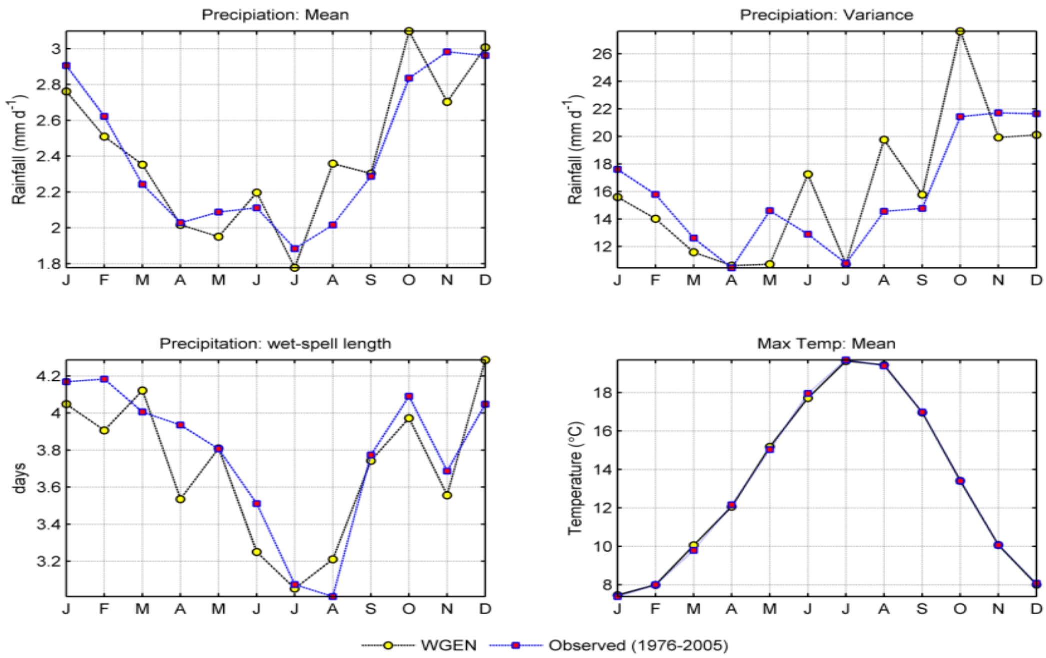

Figure 3.3 Weather generator performance in reproducing the statistical attributes of station scale temperature and precipitation estimated for the period 1976 - 2005

3.6 Low flow indicators

For this study the sensitivity of low flow response to changes in climate forcing is assessed for the daily flow exceeded 95% of the time on average (Q95; m^3/sec) This indicator was selected as the criterion of relevance for water management. Results are specific to this indicator and unlikely transferable to other parts of the flow regime.

3.7 Clustering catchment types

To identify catchments which have a similar response the individual 2-D surfaces for both rainfall-runoff models are concatenated and input to a *k*-means clustering procedure (Lloyd, 1982). Accordingly, the algorithm partitions p points of the $p \times m$ dimensional input matrix into *k* clusters for which each observation (2-D surface) is assigned to the cluster with the nearest centroid based on the Euclidean distance. As clusters are influenced by the initial position, 100 random initialization points are used. That seed point which minimizes the cost function is retained. The error function used is expressed as (equation 6):

$$\boldsymbol{J} = \sum_{\boldsymbol{j}=1}^{\boldsymbol{k}} \sum_{\boldsymbol{i}=1}^{\boldsymbol{n}} \left\| \boldsymbol{x}_{\boldsymbol{i}}^{(\boldsymbol{j})} - \boldsymbol{c}_{\boldsymbol{j}} \right\| \quad \textbf{(6)}$$

Where *k* and *n* represent the number of clusters and observations respectively; $x_i^{(j)}$ denotes the *i-th* member of the *j-th* cluster, the centroid of which is given by c_j. This algorithm is used in conjunction with the Calinski-Harabasz (CH) efficiency criterion (Calinski and Harabasz, 1974) to optimize the number of clusters. The criterion (equation 7) identifies a value for *k* which simultaneously minimizes/maximises the within/between cluster variance.

$$\boldsymbol{CH = \frac{SS_B}{SS_W} \times \frac{N-k}{k-1}} \quad \textbf{(7)}$$

SS_W and SS_B represent the within and between cluster sum of squares respectively, calculated using the squared Euclidean distance. Convergence to a local optimum is achieved when group membership is stable over successive iterations.

3.8 Classification Trees (CT) for ungauged catchments

Classification Trees (CT) are predictive models which use a set of decision rules inferred from features of the input data to determine group membership of the predictand. The algorithm reclusively partitions the input space into increasingly smaller regions until each is assigned a class label. Once terminated a hierarchical tree with root, decision and leaf nodes is returned. Here a CT is used to ascertain which physical attributes differentiate between typologies of catchment sensitivity identified using the *k*-mean clustered response surfaces. The PCDs and catchment clusters are used as inputs. Gini's impurity index (equation 8) is used as the split criterion.

$$\boldsymbol{GDI = 1 - \sum_i p^2(i)} \quad \textbf{(8)}$$

Here $p(i)$ is the observed probability of class i occurring at a given node. Once developed the tree structure encodes a set of decision rules that identify which PCDs predict the cluster membership of each catchment. The final classification tree is formed such that at least one path is assigned to each cluster and the features which differentiate catchments are hydrologically interpretable and physically meaningful. This allows regionalisation of the response surfaces and application of the SN approach to ungauged locations.

3.9 Datasets employed

3.9.1 Observed climate data

The study uses gridded (1×1 km) daily precipitation and temperature datasets developed from point scale observations by *Met Éireann* (Walsh, 2012). For each catchment the daily series for individual grid points situated within the catchment boundary are aerially averaged to derive a single precipitation and temperature series respectively. Daily PET required for model calibration is estimated from mean daily temperature according to equation 2 (Oudin *et al.*, 2005).

3.9.2 Catchment data

The catchments used (Table 3.1 and Table A1 (Appendix)) are selected on condition they: (i) provide good quality long-term data for hydrological model development and testing; (ii) have a flow regime which has not been significantly impacted by human activity; and (iii) provide a representative sample across a diversity of catchment types. In all 35 catchments (Figure 3.4) whose flow data variously cover the period 1973-2001 are included. The observed flow records are obtained from gauged locations administered by the Office of Public Works (OPW; http://waterlevel.ie/) and Environmental Protection Agency (EPA; http://www.epa.ie/hydronet/). Information on the physical characteristics (Physical Catchment Descriptors; PCDs) of the catchment sample used is taken from the OPW Flood Studies Update (FSU; Table 1; Mills *et al.*, 2014). Using PCDs in conjunction with the sensitivity testing methodology sheds light on which physical characteristics influence the catchments' low flow response to climate changes. Through regionalization the prototype response surfaces can thus be extended to ungauged or data sparse catchments. The PCDs variously provide information on the climatological, soil and morphometric properties of each catchment. A description of the PCDs available from the FSU is given in Table 3.1. As shown by Table 3.1, relative to a larger sample (206) the catchments used cover a diversity of hydroclimatological regimes and are representative of hydrological conditions across the country as a whole however, within this sample certain biases exist. In particular there is an underrepresentation of smaller upland catchments with a lower Baseflow Index (BFI) located along the coastal margins. Such biases have important implications as they add uncertainty to the extrapolation of catchment typologies to a wider population.

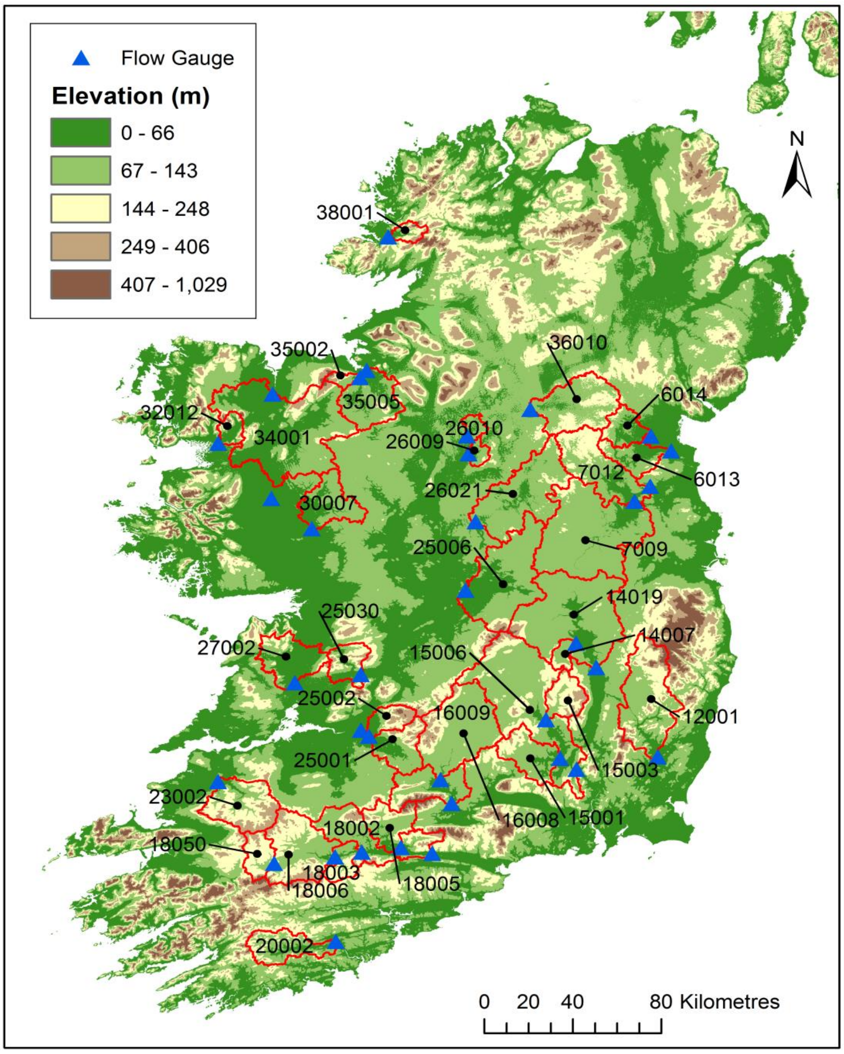

Figure 3.4 The location, boundaries and identification number of the catchment sample used to derive low flow response surfaces

Table 3.1 List of available Physical Catchment Descriptors (PCDs) derived for the Flood Studies Update (FSU). Also show is the range in values for 206 catchments included in the FSU and values for the 35 catchments used in this study.

PCD	Descriptors explained	Min (206)	Max (206)	Min (35)	Max (35)
ALLUV (Prop)	Proportional extent of floodplain alluvial deposit	0	0.11	0.01	0.1
AREA (km^2)	Catchment area (km^2)	5.46	7980.41	88.82	2460.27
ARTDRAIN (Prop)	Proportion of catchment area mapped as benefitting from arterial drainage schemes	0	0.37	0	0.28
ARTDRAIN 2 (Prop)	Proportion of river network length included in Arterial Drainage Schemes	0	0.85	0	0.78
BFIsoil (index)	Soil baseflow index (estimate of BFI derived from soils, geology and climate data)	0.26	0.91	0.28	0.83
DRAIND	Drainage density(km/km^2)	0.04	2.64	0.54	2.37

PCD	Descriptors explained	Min (206)	Max (206)	Min (35)	Max (35)
(km/km^2)					
FAI (Prop)	Flood Attenuation Index	0.01	0.52	0.06	0.27
FARL (index)	Flood attenuation by reservoirs and lakes	0.63	1	0.81	1
FLATWET (index)	PCD summarising proportion of time soils expected to be typically quite wet	0.54	0.73	0.54	0.73
FOREST (Prop)	Proportional extent of forest cover	0	0.56	0.24	0.35
MSL (km)	Mainstream length (km)	2.84	214.61	17.47	129.08
NETLEN (km)	Total length of river network above gauge (km)	2.94	6428.92	64.67	2669.46
PEAT (Prop)	Proportional extent of catchment area classified as peat bog	0	0.8	0	0.53
S1085 (m/km)	Slope of main stream excluding the bottom 10% and top 15% of its length (m/km)	0.1	31.16	0.2	13.26
SAAPE (mm)	Standard-period average annual potential evapotranspiration (mm)	448.28	562.64	459.6	532.6
SAAR (mm)	Standard period average annual precipitation (mm)	710.76	2464.73	814.07	1784.36
STMFRQ (no.)	Number of segments in river network above gauge	1	5490	35	3523
TAYSLO	Taylor-Schwartz measure of mainstream slope (m/km)	0.11	8.32	0.13	1.05

3.9.3 Climate model projections

Projected changes in the seasonality and mean annual amount of precipitation for each catchment are obtained from Global Climate Model (GCM) simulations which comprise the CMIP5 ensemble (Table A2). The present study uses monthly precipitation series from the CMIP archive which variously cover the period 1850-2100. Model projections are derived according to one of four different Representative Concentration Pathways (RCP2.6, RCP4.5, RCP6, and RCP8.5), each of which relates to a scenario of radiative forcing estimated for the year 2100 relative to pre-industrial values (+2.6, +4.5, +6.0, and +8.5 W/m^2). For each ensemble member monthly Change Factors (CFs) are estimated based on the ratio of mean monthly precipitation between the 1976-2005 baseline and three different 30 year horizons (2020s: 2010-2039; 2050s: 2040-2069; 2080s: 2070-2099). Changes in harmonic parameters derived from the ensemble CFs inform the domain used for sensitivity testing. In conjunction with the response surfaces these projections are also used to examine the exposure of individual catchments to climate risk.

3.10 Results

3.10.1 Rainfall-runoff model development

For the catchment sample rainfall-runoff model development is implemented using the GLUE procedure with behavioural parameter sets and their respective weightings estimated over the calibration period consisting of the six wettest/driest years on record. Evaluation over the calibration/validation period is based on the median simulation from each model using the NSE criterion (Table A1) applied to the non-transformed (NSE) and transformed (NSE^{log} and NSE^{2}) flow series respectively. Figure 3.5 indicates how each model reproduces a series of hydrological signatures estimated using the observed and median simulated flow series. Given the domain used for sensitivity testing indices relating to catchment memory and inter-seasonal variability are employed. Generally each model performs similarly over the calibration and validation period respectively. Model results show that differences between catchments are more significant than differences in performance between the individual model structures. Additional information on the model performance is given in Table A1.

Based on the NSE criterion the models perform to a high efficiency (>0.7). Such performance is common to all models and across both the calibration and validation period respectively. This is with the notable exception of catchment ID: 25001 (Mulkear) for which a relatively poor NSE scores (<0.6) are achieved. The highest (>0.95) NSE calibration/validation scores are returned for catchment ID 32012 by NAM and GR4J respectively. Generally GR4J performs better than NAM and HBV for the majority of catchments, particularly those with a lower Baseflow Index (BFI). Models generally show high skill in reproducing variations in the hydrological signatures between catchments. Each captures the Runoff Coefficient (RC), Baseflow Index, Annual Runoff and Coefficient of Variation. However all models consistently underestimate the Autocorrelation Coefficient of the observed mean monthly (Autocorrelation Coefficient) series for lags of 1, 3 and 6 months. It is noted that despite a relatively less skillful performance for a small number of catchments, their exclusion on this basis necessarily reduces the sample size available for clustering, and may mean limiting the diversity and geographical spread of those catchments which are included.

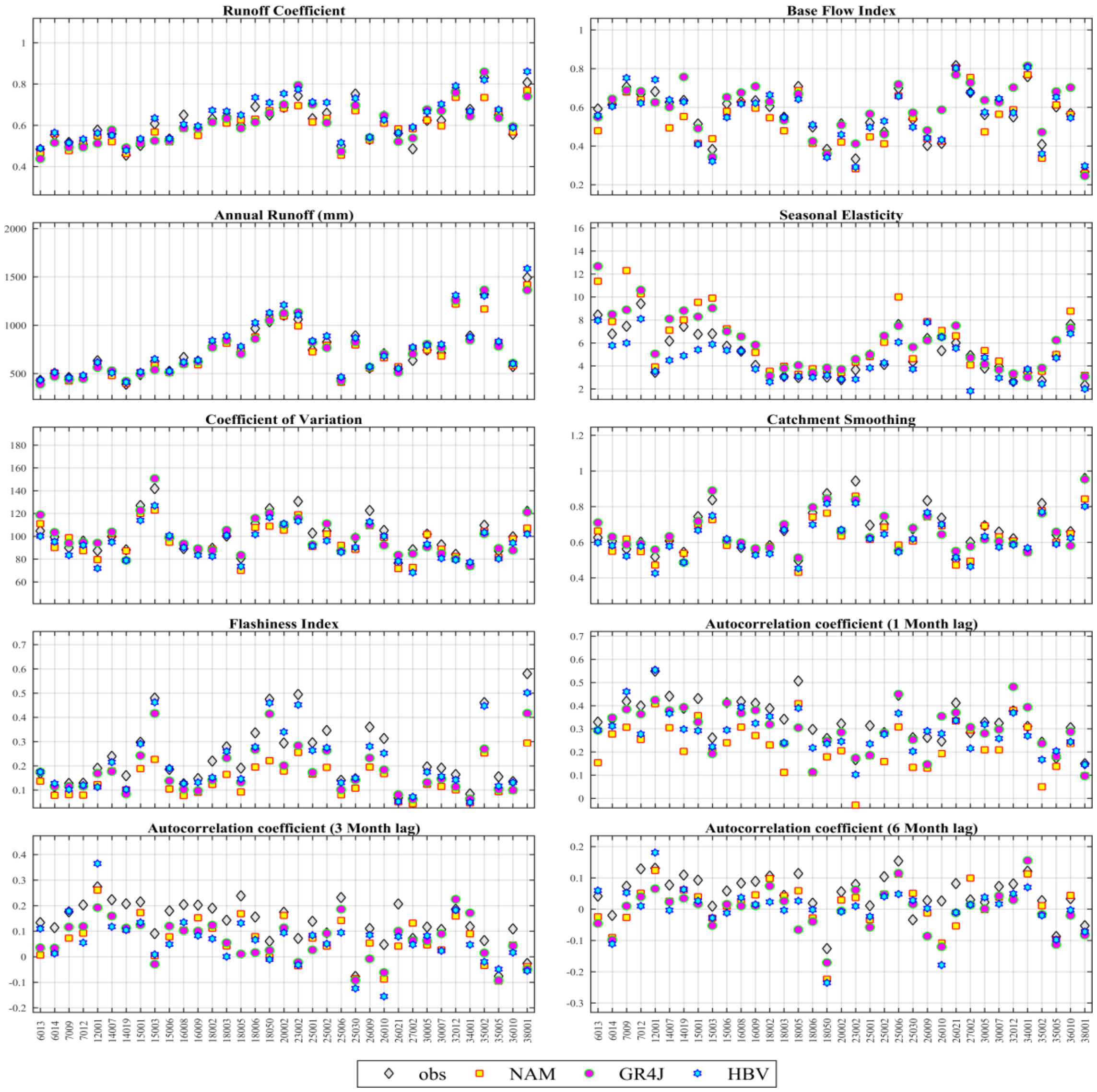

Figure 3.5 Observed and model simulated hydrological signatures estimated for each catchment using the period for which observed flow data is available

3.10.2 CMIP projected climate changes

The boxplots shown in Figure 3.6 illustrate changes in the harmonic mean (annual mean) and amplitude (seasonality) of the annual precipitation cycle projected by members of the CMIP5 multi-model ensemble for the combined 206 catchments. For each catchment and model projection relative (%) changes in both parameters are estimated by fitting the harmonic function (equation 1) to the associated monthly CFs calculated from the GCM grid point directly overlying each catchment centroid. Changes are estimated for three future time horizons (2010-2039: 2020s; 2040-2069: 2050s; 2070-2099: 2080s) and each RCP scenario. Based on the median ensemble estimate mean annual precipitation receipts are projected to increase slightly as the current century progresses however, this masks significant changes in the seasonal distribution. Projections largely suggest an increase in the amplitude of the annual cycle commensurate with the occurrence of wetter winters and drier summers.

Figure 3.6 highlights the degree of uncertainty associated with precipitation wherein changes in the annual amount spans a sign change irrespective of the horizon and RCP considered. By the end of the century mean annual precipitation is projected to decrease/increase by up to 20% relative to 1976-2005. Changes in the seasonality are also uncertain however, the signal does notably strengthen over each successive time horizon for the more GHG (greenhouse gas) intensive RCP6 and RCP8.5 scenarios. Also depicted in Figure 3.6 are changes in mean annual temperature projected for the 206 catchments by the CMIP5 ensemble for each horizon and RCP. With the exception of RCP8.5 for the 2080s temperature (for which the median ensemble estimate is +2.7°C) increases are largely within +2°C (relative to 1976-2005).

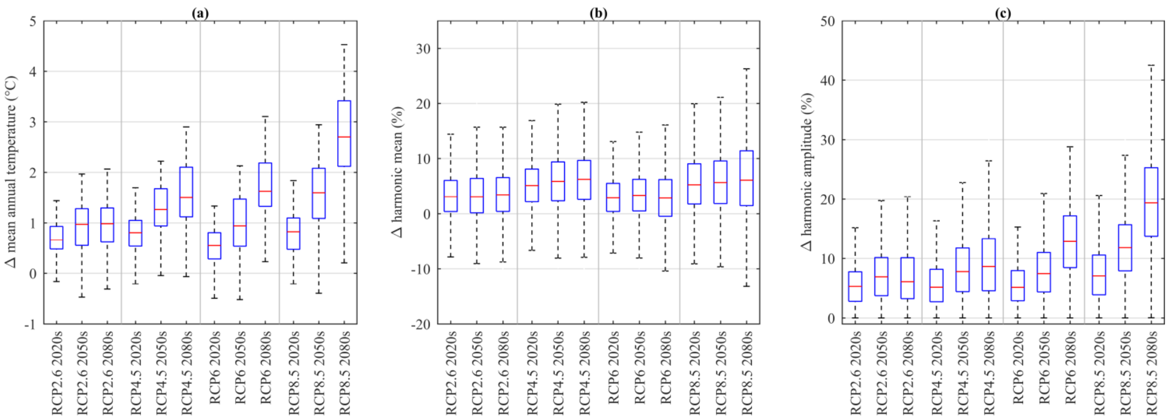

Figure 3.6 Boxplots showing percent changes in the mean annual amount (harmonic mean) and seasonality (harmonic amplitude) of the precipitation cycle described using a single phase harmonic function (equation 1). Plots are developed using GCM simulations from the CMIP5 archive stored at a monthly resolution for all 206 catchments (FSU). Changes are examined for three future time horizons (2010-2039; 2040-2069 and 2070-2099) relative to the 1976-2005 reference and for four different RCP scenarios. Also shown are absolute changes in mean annual temperature for all catchments projected by the CMIP5 ensemble (°C; a).

3.10.3 A typology of catchment sensitivity

Figure 3.7, 3.8 and 3.9 display 2-D response surfaces developed for 35 catchments using the median GLUE simulation from NAM, GR4J and HBV respectively. Surfaces relate to relative (%) changes in the Q95 indicator estimated for the sensitivity domain outlined above. For plotting purposes the range for harmonic mean (-40% to +40%) and amplitude (0% to +50%) changes are constrained. Overlain on each plot are the percentage changes in the harmonic parameters projected for the 2080s under each

RCP scenario for all members of the CMIP5 ensemble. Response surfaces relate to the scenario of a +2°C increase in mean annual temperature (relative to 1976-2005).

Response surfaces relating to the earlier 30-year horizons (2020s and 2050s) and covering all temperature scenarios (0°C, +2°C, +4°C) are shown in Figure A1-A24.

Figures 3.7, 3.8 and 3.9 also show a proposed 10%, 20%, and 30% allowance on current Q95 levels which would provide additional capacity for the realisation of future climate change. As illustrated in these Figures a reduction in abstractions is required to maintain Q95 at a set percentage above current rates. This additional volume would offset future decreases in Q95 resulting from climate change alone. Various mitigation and adaptation measures are available to water managers to increase current low flows; this includes for example: (i) reducing user demand, (ii) investing in supply infrastructure (e.g. increased reservoir capacity, reduced leakages, etc.), (iii) setting more conservative abstraction limits - particularly with respect to Q95, (iv) developing new sources of supply, and (v) implementing earlier drought (user supply and abstraction) restrictions. In future planning resource managers must calculate the additional capacity (on current Q95) which such measures may provide. Once estimated the reduction in exposure to future risk such measures may then provide can be established using the response surfaces and climate allowances (10%, 20%, and 30%) highlighted.

Generally Q95 is shown to increase/decrease incrementally in-line with iterative changes in the mean and amplitude respectively, reflecting their individual and combined effects on the catchment water balance and low flow processes. However, while the pattern of response is largely consistent across the sample, individually catchments display differing degrees and magnitudes of sensitivity, with some showing large % increases/decreases in Q95 for relatively small perturbations in the mean and amplitude of the precipitation cycle. In some cases decreases in Q95 are more pronounced for changes in amplitude as opposed to mean amount, with some catchments being relatively insensitive to an increasingly seasonal cycle. This particularly applies in the case of response surfaces developed using NAM. In contrast all catchments are to some degree responsive to changes in mean annual receipts, with Q95 responding to increases/decreases to precipitation amounts and the annual water balance. Catchments which are more sensitive (relatively) to changes in mean precipitation - as opposed to its seasonal distribution - exhibit a greater rate of change along the *y*-axis (e.g. Figure 3.7; catchment ID: 7012). In contrast those with a greater degree of variation along the *x*-axis are more responsive to increases in seasonal amplitude (e.g. Figure 3.7; catchment ID: 34001). Differences in the magnitude and pattern of the response surface reflect the contrasting ability of catchments to dampen or amplify seasonal/annual scale precipitation changes. It also highlights the role which localised rainfall-runoff and storage processes play in influencing the low flow response and ultimately the catchment's innate resilience/vulnerability to changes in climate as defined by the sensitivity domain.

Figure 3.10 highlights the extent to which increases in temperature/PET influence the Q95 flow response for seven catchments used as a case study. Here it is shown that, as mean annual temperature is increased from 0°C, to 2°C and 4°C respectively (relative to 1976-2005) Q95 decreases. Figure 3.10 also highlights the extent to which lower allowance thresholds (e.g. 10%) are surpassed as temperature is increased. This underlines the importance of considering future changes in temperature alongside precipitation in infrastructure design and water supply planning decisions. Used alongside the CMIP5 simulations the response surfaces (Figures 3.7-3.9) highlight the contrasting exposure of individual catchments to projected climate. Here changes in the seasonality and mean annual amount of precipitation, as projected for the period 2070-2099 and for all RCPs by the CMIP5 ensemble members are plotted over the response surface for each catchment. In some instances it is shown that a reduction in abstractions to increase Q95 by 30% on current levels would be insufficient to avoid future climate change impacting low flows. This is notably the case with catchment ID: 18050 (Figure 3.7) for which a large proportion of the GCM projections lie outside this allowance. In contrast for catchment ID: 14019 (Figure 3.7) most simulations are within the 30% allowance threshold.

Figure 3.7 to 3.9 also demonstrate the influence which structural differences in the rainfall-runoff models have on the resultant response surfaces. In the majority of cases all models produce surfaces which, on a catchment-by-catchment basis have a similar pattern of response however, the magnitude of change in Q95 in some cases differs noticeably. In comparison with GR4J and HBV, NAM is shown to be relatively less sensitive to increases in seasonality. Such differences reflect the influence of the model structure and in particular the representation of longer term stores within the system on the simulation of low flows under more strenuous climate conditions. Structural uncertainties have important implications for how response surfaces are used for water management and infrastructural development. In this context the results highlight the importance of addressing this aspect of uncertainty in future low flow assessments.

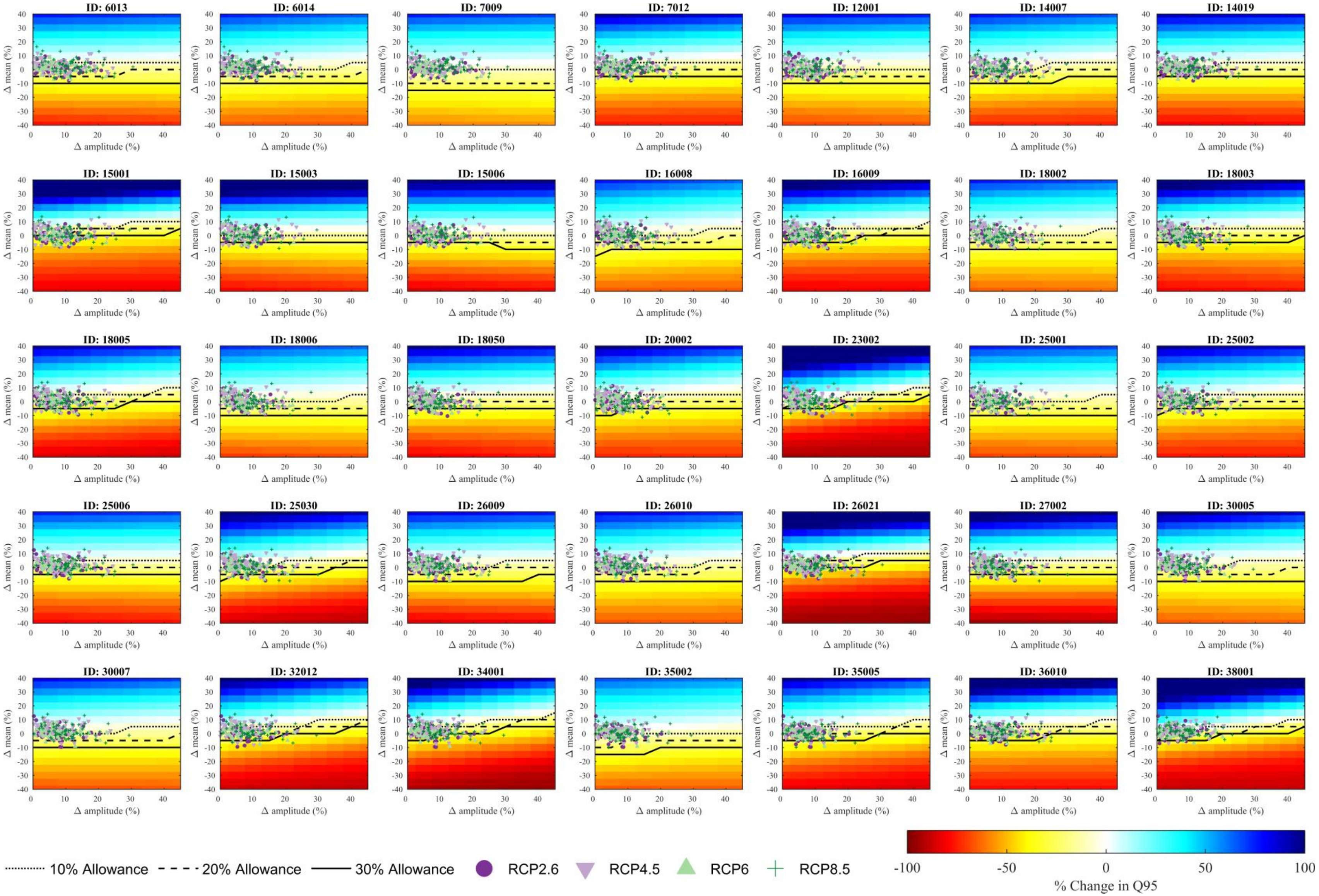

Figure 3.7 Response surfaces showing changes (%) in the magnitude of the Q95 low flow indicator for incremental changes (5%) in harmonic parameters representing the mean amount (-40% to +40%; x-axis) and seasonality (0% to 50%; y-axis) of the annual precipitation cycle. Surfaces are developed for each of the 35 catchments using the median NAM simulation. Overlain on each plot are changes (%) in the harmonic mean and amplitude projected for the 2080s under all 4 RCPs by each member of the CMIP5 ensemble. Surfaces relate to +2^{0} C increase in mean annual temperature to 1976-2005.

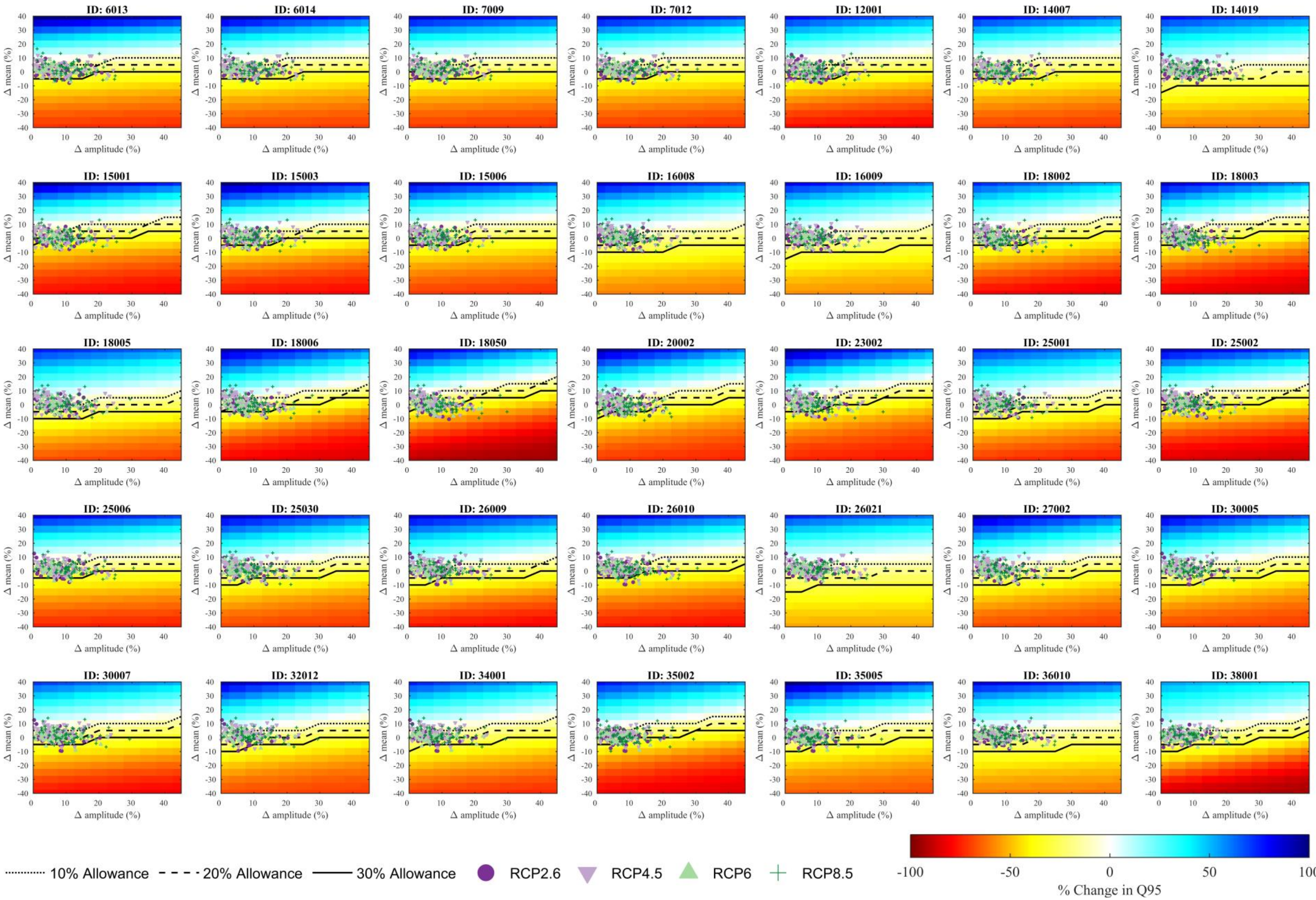

Figure 3.8 Response surfaces showing changes (%) in the magnitude of the Q95 low flow indicator for incremental changes (5%) in harmonic parameters representing the mean amount (-40% to +40%; x-axis) and seasonality (0% to 50%; y-axis) of the annual precipitation cycle. Surfaces are developed for each of the 35 catchments using the median GR4J simulation. Overlain on each plot are changes (%) in the harmonic mean and amplitude projected for the 2080s under all 4 RCPs by each member of the CMIP5 ensemble. Surfaces relate to +2^{0} C increase in mean annual temperature to 1976-2005.

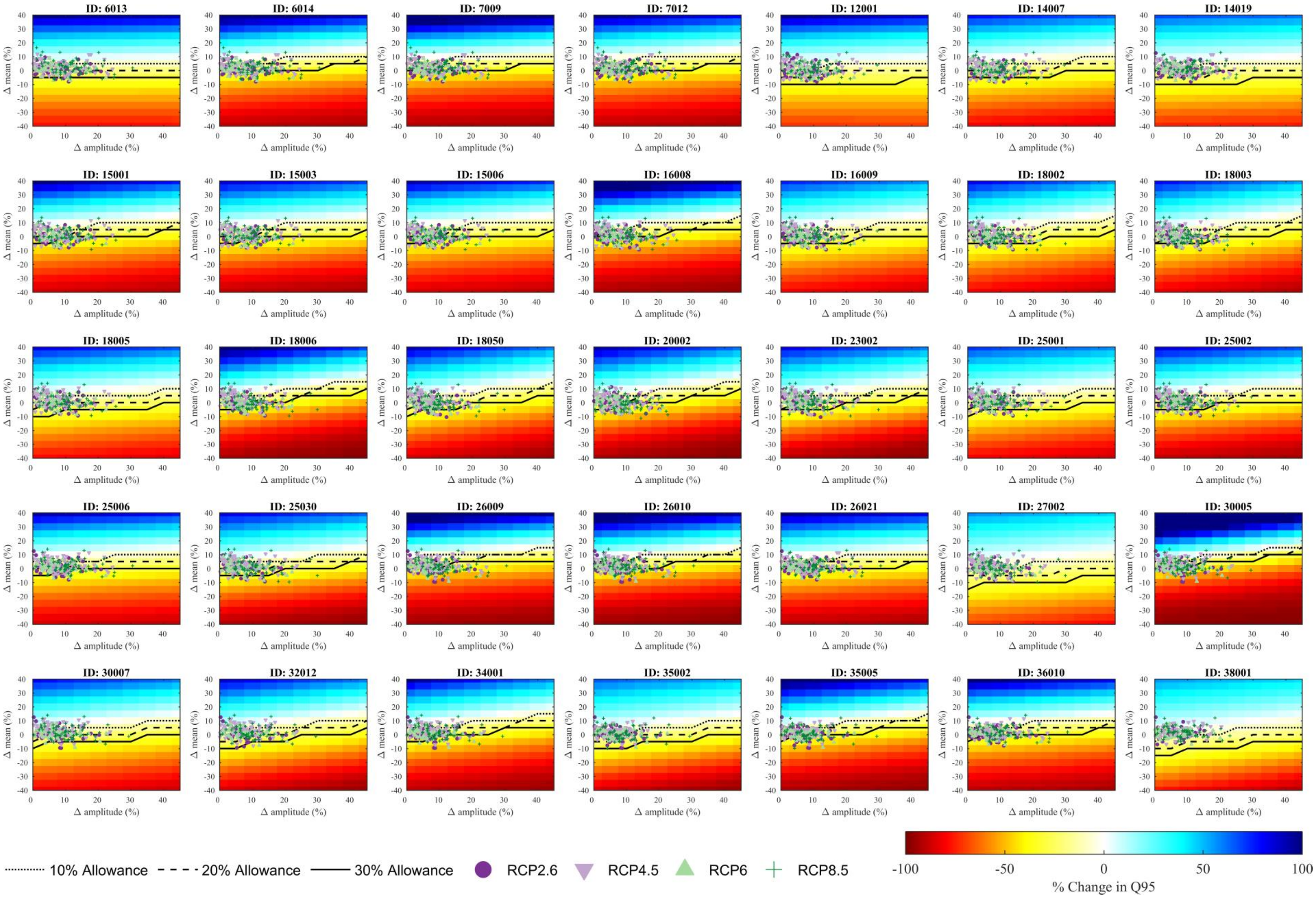

Figure 3.9 Response surfaces showing changes (%) in the magnitude of the Q95 low flow indicator for incremental changes (5%) in harmonic parameters representing the mean amount (-40% to +40%; x-axis) and seasonality (0% to 50%; y-axis) of the annual precipitation cycle. Surfaces are developed for each of the 35 catchments using the median HBV simulation. Overlain on each plot are changes (%) in the harmonic mean and amplitude projected for the 2080s under all 4 RCPs by each member of the CMIP5 ensemble. Surfaces relate to +2⁰ C increase in mean annual temperature to 1976-2005.

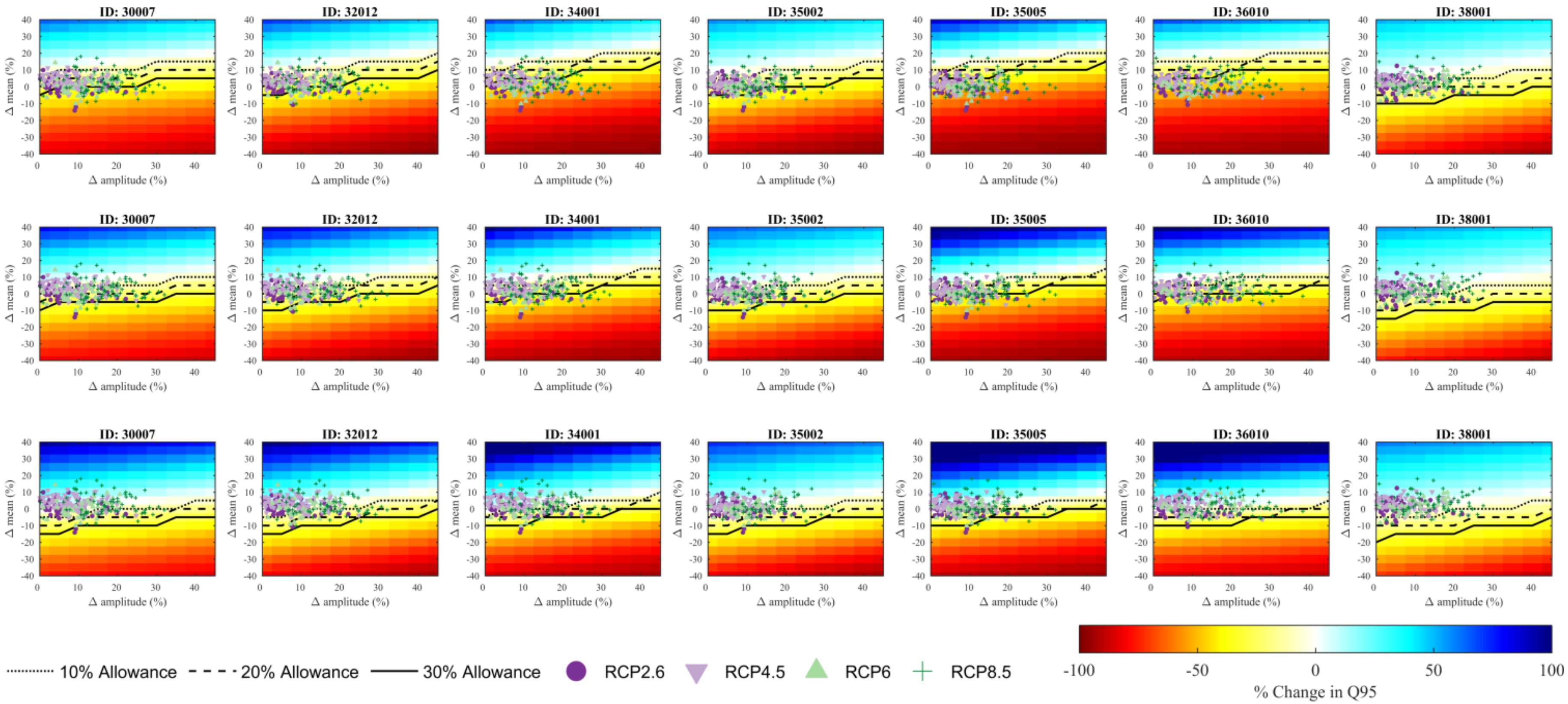

Figure 3.10. Response surfaces showing changes (%) in the magnitude of the QAS low flow indicator for incremental changes (5%) in harmonic parameters representing the mean amount (-40% to +40%; x-axis) and seasonality (0% to 50%; y-axis) of the annual precipitation cycle. Surfaces are developed using the median HBV simulation. Overlain on each plot are changes (%) in the harmonic mean and amplitude projected for the 2080s under all 4 RCPs by each member of the CMIP5 ensemble. Surfaces relate to a +4°C (top row), +2°C (middle row) and +0° (bottom row) increase in mean annual temperature.

3.10.4 Response surface typologies

Individual response surfaces derived using the median simulation from each rainfall-runoff model and for temperature scenarios of +0°C, +2°C and +4°C are grouped according to (*dis*)similarities in their Q95 response across using a *k*-means clustering algorithm. The program is used in conjunction with the CH evaluation criterion to identify the optimal number of clusters. Based on this criterion 5 clusters are returned ranging in size from 4 to 8 catchments (Table 3.2). The centroid for each cluster is estimated as the arithmetic average of the individual grid points from the response surfaces of each cluster member and hydrological model. Figure 3.11 shows each cluster centroid and the location of its catchment members.

Table 3.2 Mean gradient (*y* and *x*-axis respectively) and slope of the +2°C centroid response surface for each rainfall-runoff model. Also shown is the identification (ID) number of catchments assigned to each cluster.

		Mean Gradient						Mean Slope (°)		
		Harmonic mean (y axis)			Harmonic Amplitude (x axis)					
Cluster	Catchment members	GR4J	NAM	HBV	GR4J	NAM	HBV	GR4J	NAM	HBV
(a)	6013, 12001, 14007, 14019, 18005, 25001, 25006, 27002	1.89	2.03	2.00	0.29	0.13	0.23	58.73	62.32	61.99
(b)	18002, 18003, 18006, 18050, 20002, 25002, 30007, 35002	1.83	1.95	1.93	0.44	0.18	0.47	57.65	60.56	60.65
(c)	23002, 32012, 34001, 38001	1.69	2.69	1.91	0.43	0.58	0.48	56.15	62.49	60.83
(d)	15001, 15003, 15006, 16009, 25030, 26021, 36010	1.90	2.97	2.17	0.30	0.30	0.34	57.66	65.88	62.58
(e)	6014, 7009, 7012, 16008, 26009, 26010, 30005, 35005	1.95	1.93	2.70	0.32	0.17	0.45	58.43	60.50	63.26

Differences between centroids based on the mean rate of change (surface gradient) in Q95 as a function of changes along the *x* (horizontal) and *y* (vertical) axis respectively are shown in Table 3.2. This quantifies the degree of sensitivity to change in each harmonic parameter independently, without explicitly considering their interactive effects. Also listed is the mean slope for each centroid calculated as the change in Q95 per unit distance along the path of steepest ascent/descent from a grid point to one of its eight nearest neighbours. This quantifies the rate of change across the surface in the both *x* and *y* directions simultaneously and is indicative of the overall sensitivity.

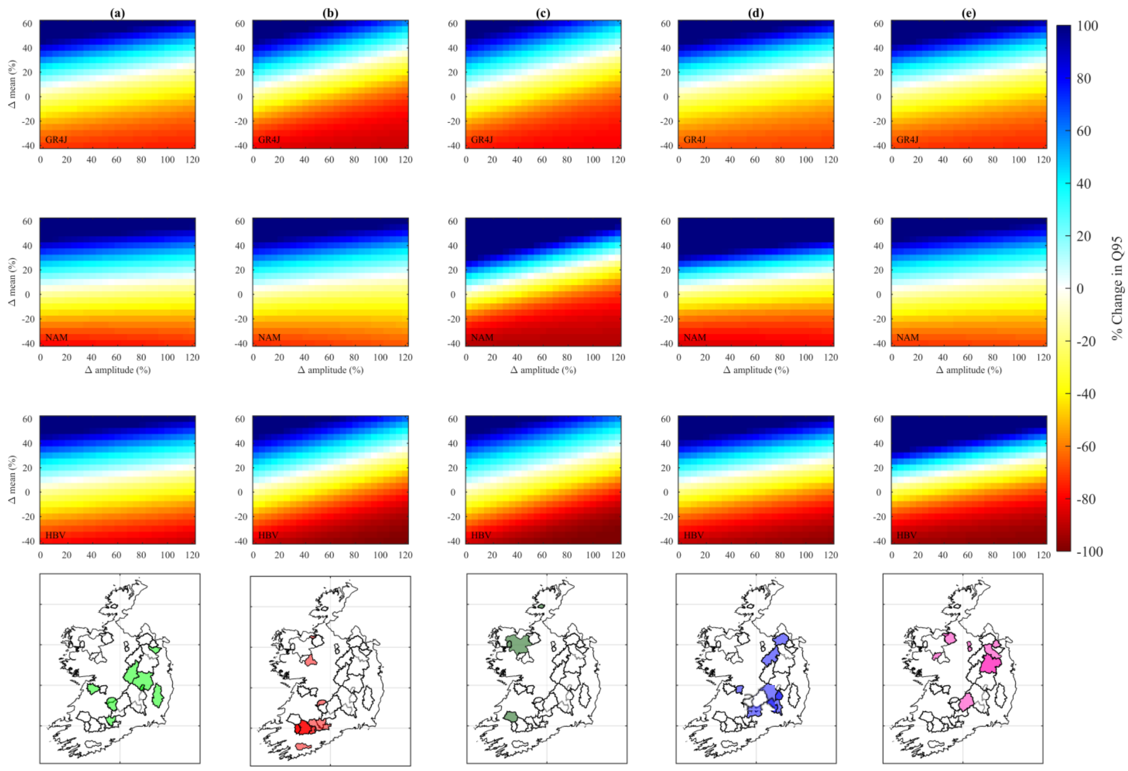

Figure 3.11. The centroid of five clusters for each rainfall runoff model (GR4J, HBV and NAM) showing the composite response surface relating to a 2°C temperature increase. Response surfaces show change (%) in Q95 for percent changes n the mean amount (-40% to +60%; x-axis) and seasonality (0% to 120%; y-axis) of the annual precipitation cycle. For plotting purposes the range is constrained between -100% and +100%.

According to the mean gradient along the *y*-axis the centroid for cluster (d) is most sensitive to changes in annual mean precipitation, albeit that a degree of uncertainty between models is evident. In comparison the greatest proportional decreases in Q95 relating changes in amplitude (seasonality) are associated with catchments in clusters (b) and (c). Similarly a degree of differentiation between each is evident dependent on the choice of rainfall-runoff. Here NAM is associated with a clearer differentiation between clusters, with cluster (c) being most strongly affected by a more seasonal precipitation cycle. Cluster (a) is highlighted as the least sensitive to changes in seasonal amplitude. When changes in amplitude and mean amount are considered together - based on the mean slope across the centroid surfaces - cluster (d) or (b) is the most or least sensitive. This reflects the heightened sensitivity of cluster (d) to changes in mean annual precipitation. As highlighted by Figure 3.11 there is a geographical pattern in the composition of cluster members. This is most evident in the difference between clusters (c) and (d) and reflects a general east-west gradient across the country. Generally catchments from cluster (a), (d) and (e) are situated on the east coast and midlands region. Catchments from clusters (b) and (c) are located along the furthermost south/north-western perimeter of the catchment sample and in upland areas.

3.10.5 Interpretation of catchment clusters

In interpreting results there are a number of broad features which differentiate between sensitivity types. In general, by changing the interaction of longer duration and more slowly responding storage and baseflow releases, alterations to the mean and amplitude (in particular) of the precipitation cycle are likely to have a greater impact on catchments which have a 'shorter hydrological memory' (i.e. predominantly upland type systems with an impermeable geology and thin peaty soils). Conversely, as they possess greater storage capacity catchments with a 'longer hydrological memory' (i.e. lowland type systems with permeable geology providing abundant long-term storage) and greater long term reserves have a low flow regime which is less sensitive to the impacts of inter-annual and inter-seasonal precipitation changes.

As highlighted, when considering changes in the mean and amplitude together catchments from cluster (d) are classified as being the most sensitive. However they are generally more sensitive to increases in mean annual precipitation as opposed to the seasonal amplitude (Table 3.2). This highlights that, due to increases in winter precipitation these catchments are better able to offset - through the availability of greater storage and/or more favourable antecedent conditions (e.g. higher soil moisture) - the corresponding decreases in summer low flows likely to result from an increasingly seasonal (i.e. wetter winters and drier summers) precipitation cycle. In contrast, as they respond more linearly to decreases in summer precipitation, and are more impacted by inter-seasonal storage dynamics, systems characterised as runoff-dominated have a low flow regime which is more sensitive to drier summers (i.e.

increased amplitude). Despite increased winter precipitation these catchments do not possess the storage capacity to offset preceding summer reductions. It is shown that, despite an increase of up to ~20% in total annual precipitation, catchments in cluster (b) and (c) indicate a pronounced decrease in Q95 under an amplified seasonal cycle (>60%). While the same trend is evident in clusters (a), (d) and (e), owing to the greater natural storage they possess the impact on Q95 (under the same conditions) is much reduced.

It is noted that catchments from cluster (b) and (c) which are most sensitive to increases in seasonal amplitude are associated with high Runoff Coefficient (RC) - varying between 0.62 (catchment ID: 30007) and 0.81 (catchment ID: 38001). In contrast catchments from clusters (a), (d) and (e) tend to have a lower RC (0.45 (catchment ID: 14019) - 0.65 (catchment ID: 35005)). This is with the exception of catchment ID: 25030, which has a coefficient value of 0.75. The RC is calculated as the ratio of annual precipitation to runoff and is related to catchment losses through actual evaporation moderated by soil moisture storage dynamics. Catchments with a lower RC also tend to be those with the lowest precipitation receipts. This indicates that, in dry catchments increased summer soil moisture and storage deficits influence recharge capacity during wetter seasons, leading to reduced sensitivity to an increasingly seasonal precipitation cycle. The importance of the annual water balance with respect to catchment sensitivity is also highlighted by differences in mean annual runoff (mm/yr^{-1}). Catchments in clusters (b) and (c) (ranging from 711-1491 to mm/yr^{-1}) generally have greater annual runoff than catchments in clusters (a), (d) and (e) (ranging from 389-798 to mm/yr^{-1}). Differences in runoff underline that catchments more sensitive to changes in seasonal amplitude are also those which are more linearly responsive to changes in the inter-seasonal distribution of precipitation and less affected by storage and evaporative effects. The significance of this is also highlighted by differences in seasonal elasticity, which provides a measure of streamflow sensitivity to climate fluctuations on seasonal timescales.

The Baseflow Index (BFI), which provides a measure of long-term baseflow to the catchment outflow, is a valuable descriptor of the hydrological regime. It quantifies the lagged contribution to total outflow and is linked to storage effects. Although the BFI does not provide as clear a distinction between clusters as the RC, it gives an insight into the physical attributes which influence the climate sensitivity of low flows. Clusters (a) and (c) which, with respect to sensitivity to seasonal amplitude sit at opposite ends of the spectrum have a mean BFI of ~0.65 and ~0.47, which categorize them (in relative terms) as groundwater and runoff type systems respectively. The BFI for cluster (a) indicates that these catchments have a 'longer memory'. This is with the notable exception of the Moy (catchment ID: 34001), which despite being classified as relatively sensitive to seasonal changes has a high BFI.

3.10.6 Discriminant analysis

The climatology (variability, seasonality, frequency/magnitude of extremes, etc.) and physical catchment characteristics (e.g. area, slope, geology, soil cover, land-use type, etc.) combine to influence hydrological processes at different spatio-temporal scales and ultimately determine the sensitivity or natural resilience of the low flow regime to changes in climate. Thus, establishing a connection between membership of each sensitivity type (or cluster) and the physical catchment attributes (i.e. PCDs) enables extrapolation of the classification to ungauged or poorly observed catchments which do not possess the requisite flow data to undertake detailed hydrological modelling. The physical descriptors highlighted in Table 1 are used with a recursive partitioning algorithm to identify which descriptors are associated with each cluster. Figure 3.12 shows the results of the discriminant analysis presented as a decision tree. It indicates that clusters can be distinguished according to four predictors, listed in order of significance: ALLUV, SAAR, and SAAPE. The level of importance is calculated by summing changes in risk which result from splits on the selected predictors. This value is divided by the number of connection nodes

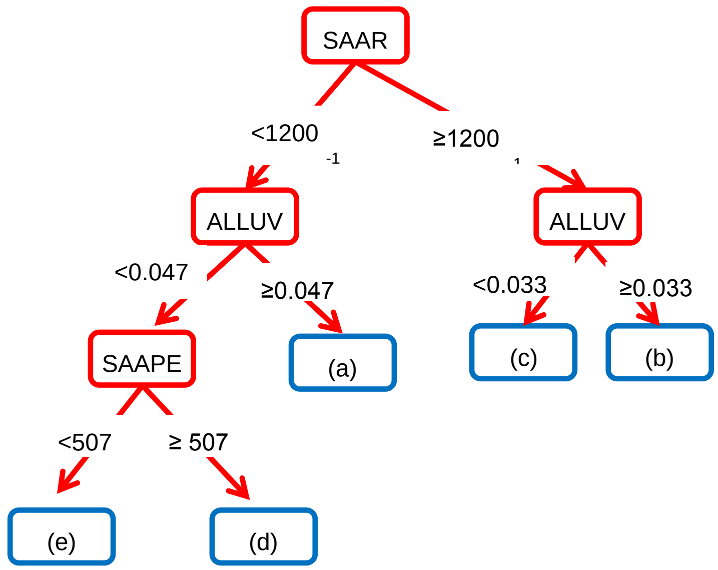

Figure 3.12 Decision tree used to classify catchments into cluster types.

The foremost distinction between classes is related to differences in annual precipitation. Herein catchments with greater precipitation (clusters (c), and (b)) are designated as more sensitive to changes in seasonal amplitude. Drier catchments are classified in clusters (a), (d) and (e). ALLUV indicates the proportion or extent of floodplain alluvial deposits and is indicative of poorly draining soil. For wetter catchments (>1200mm/yr^{-1}) this predictor distinguishes between cluster (c) and (b). For drier catchments it also distinguishes between clusters (e)/(d) and cluster (a). A final split is made between clusters (e) and (d) wherein the latter experiences greater loss in the annual water balance due to potential evapotranspiration (SAAPE). Although SAAR acts as the root node ALLUV is a more informative predictor of cluster membership. This is related to its position along two branch nodes of the decision tree.

The classification tree outlined in Figure 3.12 is applied in a predictive context to classify all (206) catchments into one of the five sensitivity types (Figure 3.11) based on their PCDs. Figure 3.13 shows the location and class membership of each catchment. The spatial pattern evident in Figure 3.11 using the reduced sample (35 catchments) is largely reproduced. Generally the pattern follows longitudinal bands across the country, with catchments classified as sensitivity type (b) and (c) being located in the south-west and west. Conversely catchments classified as sensitivity type (a), (d) and (e) are situated in the midlands and east. An elevational divide is also apparent, with catchments sensitive to a more pronounced seasonal cycle generally being located in upland areas. The south-west to north/north-east divide in annual precipitation across the country is highlighted as important for determining sensitivity. The importance of precipitation is reiterated by the differentiation between upland (wetter) and lowland (drier) catchments. Typically catchments from sensitivity type (b) and (c) are situated in upland and/or more westerly areas with greater precipitation.

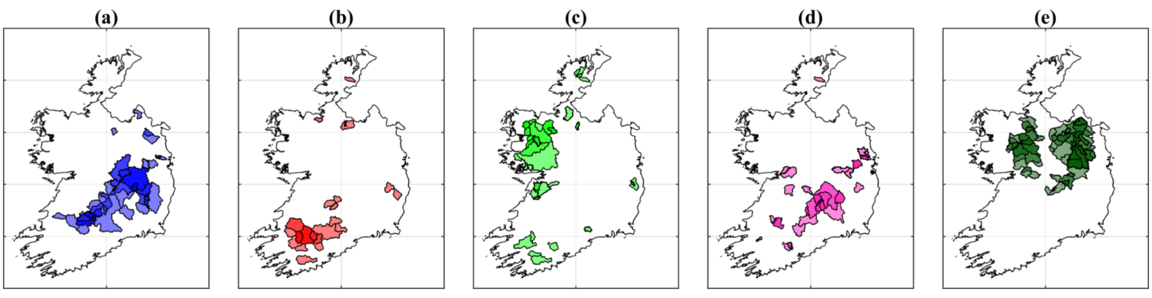

Figure 3.13 Classification of (206) catchments from the FSU into one of five different sensitivity types according to their climatological and physical

Catchments identified as sensitivity type (a), (d) and (e) are indicative of more slowly responding drier catchments in the midlands and east. Catchments belonging to types (e) and (d) are differentiated based on evaporative exposures, with those in the midlands (d) experiencing the greatest losses. It is noted that the predictors used to differentiate sensitivity type are correlated with several other physical attributes including elevation, coastal location, topography, land-use and soil type - which are not included in the set of FSU physical descriptors or captured more clearly by the catchment sample. The classification scheme also indicates a general distinction between runoff (sensitivity type (b) and (c)) and groundwater type (sensitivity type (a), (d) and (e)) catchments across the country. The hydroclimatological processes associated with each influence the degree to which individual catchments can dampen the climate change signal (particularly seasonal amplitude) with respect to its effects on the low flow regime. Table A3 lists group membership for each of the 206 catchments.

3.10.7 Catchment exposure to projected climate changes

Figure 3.14 shows the exposure of all 206 catchments to a plausible range of future climate changes projected by the CMIP5 ensemble. Catchments are grouped into each of the five identified sensitivity types (type (a) to type (e)) according to the classification rules outlined in Figure 3.12. The number of CMIP5 ensemble simulations (given as a percentage of the total number of ensemble members) which exceed climate change allowances of 0% to -40% relative to baseline (1976-2005) conditions is calculated using the corresponding centroid response surface for each cluster/sensitivity type (Figure 3.11). In this respect the centroid response surface from clusters identified within the smaller catchment sample (35) are assumed representative of catchments which share the same physical characteristics within the larger set of (206) FSU catchments. Thresholds indicate whether a reduction in abstractions (ranging in 5% increments between 0 and -40%) in order to increase low flows (Q95) above current levels would offset decreases in Q95 arising from future changes in climate - as specified by the domain used for sensitivity testing. Results illustrate the degree to which climate risk exposure differs for the same threshold across the five sensitivity types. Figure 3.14 relates to a 2°C increase, Figure A.25 and A26 (Appendix) show exposure for increases of 0°C and 4°C respectively.

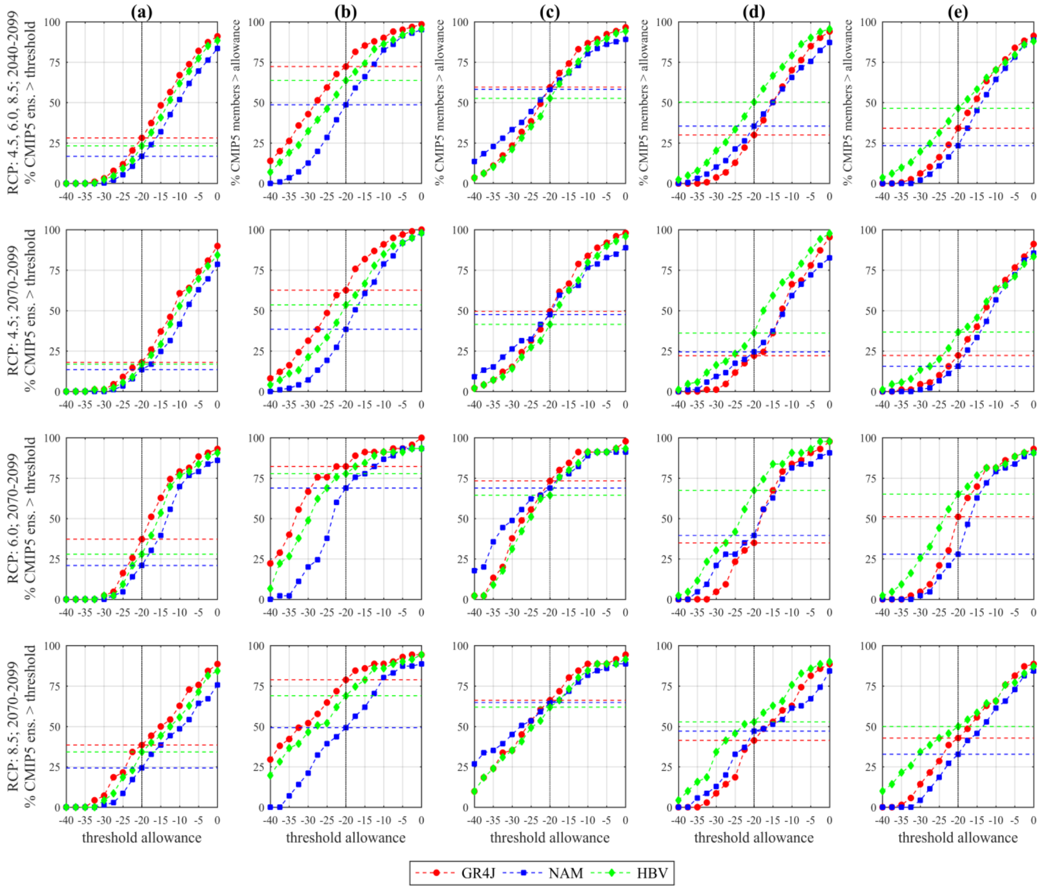

Figure 3.14. Percent of CMIP5 projections (y-axis) which exceed climate change allowances of 0% - 40% (relative to baseline period 1976-2005; x-axis) calculated for each catchment type (a-e) and rainfall-runoff model. Thresholds relate to a temperature scenario of +2°C relative to baseline conditions. Climate risk exposure based on the CMIP5 ensemble is calculated using projections for all 206 catchments and the corresponding centroid relating to their sensitivity type (Figure 3.11). Plots show the exposure of each type to projected climate and the adequacy of different adaptive thresholds. The 20% reduction allowance is emphasised using the black line. Combined threshold calculated for RCP4.5, RCP6 and RCP8.5 over the period 2040-2069 and 2070-2099 are shown in the upped row. The second, third and fourth row show thresholds for the period 2070-2099 relating to RCP4.5, RCP6 and RCP8.5 respectively.

Figure 3.14 (upper row) quantifies exposure when model projected changes for all emission scenarios (RCP 2.6, 6.0, 4.5, and 8.5) and mid-late century time slices (i.e. 2040-2069 and 2070-2099) are investigated. Plots emphasize a theoretical allowance of 20% as a potential threshold for adaptation planning. This is shown to offset decreases in Q95 in ~25 to 75% of the CMIP5 ensemble dependent on the rainfall-runoff model and catchment type considered. Generally a reduction in abstractions to increase current Q95 by 20% for catchment type (b) and (c) would be insufficient to reduce these sites exposure to significant risk. In this case >50% of ensemble members indicate a decrease in low flows despite adaptation steps to increase current Q95. This is in contrast to type (a) wherein an increase of 20% would reduce exposure significantly. In this case, ~20-25% of the CMIP5 ensemble suggests decreases in

Q95. As highlighted by type (b), adoption of a 25-35% allowance may be necessary to provide an equivalent level of protection against future risk (as measured by the % of the ensemble members accommodated).

Differences in the degree of exposure between types generally reflect the ranking of cluster centroids with respect to their sensitivity (Table 3.2). Irrespective of the time period and emission scenario considered, plots indicate that type (b) and (c) are generally the most exposed. This is due to both types being more sensitive to an increasingly seasonal precipitation cycle (i.e. wetter winters and drier summers). The exposure of these catchment types is underlined by the strengthening of the climate change signal with respect to this aspect of the precipitation cycle over each successive time horizon and RCP (Figure 3.6). Conversely due to their natural capacity to offset an increasingly seasonal regime - through greater storage capacity - types (a), (d) and (e) are relatively less exposed to more pronounced changes in seasonality.

Figure 3.14 highlights the degree to which uncertainty in the hydrological model structure leads to differences in the exposure of individual catchment types. There is a general concordance between models for catchment types (a) and (c). This agreement is due to the similarity of the centroid response surface for individual models - as shown in Figure 3.11. In contrast for types (b) and (e) there is greater uncertainty in catchment exposure across exceedance thresholds. As is highlighted by Figure 3.11, in both cases NAM is associated with a lesser exposure. In contrast GR4J and HBV are more sensitive, particularly to seasonality, and thus suggest greater exposure to decreases in low flows. According to Figure 3.14 there is an up to ~25% difference in exposure dependent on model type. However, it is noted that although models disagree regarding the exact exposure level for individual catchment types, there is a general agreement as to the relative exposure between types, wherein type (a) or (b) is shown to be the most or least exposed based on the 20% exceedance threshold.

Figure A25 and A26 reflect the relative differences shown in Figure 3.14 between models and catchment types regarding exposure to future climate. The influence of greater losses through evaporation as underlined by the differences between A25 and A26 wherein the latter, relating to an increase of 4°C relative to 1976-2005, shows greater exposure under the CMIP5 ensemble. Differences between models are most pronounced for a temperature scenario of +4°C. In this case exposure is least for NAM and most pronounced for HBV/GR4J dependent on catchment type.

The initial modelling outlay required to develop response surfaces may be extensive however, once complete resource managers can easily estimate climate change impacts for many alternate scenarios without the need to conduct additional hydrological modelling. Herein the impact of climate changes on the projected flow indicator (e.g. Q95) can be quickly read from the response surfaces based on changes in parameters along the *x* and *y* axis (e.g. intercept and amplitude of the annual precipitation cycle). Hence once the next generation of climate model projections comes on-line, exposure to climate risk can be revised using the same approach adopted in this study for the CMIP5 ensemble.

3.11 Conclusion

Despite the advantages of using the 'scenario-neutral' approach for impact and adaptation planning, the general framework has a number of limitations, which must be highlighted. Firstly, despite the catchment sample used providing good coverage of hydroclimatological conditions across the island there is a general under-representation of smaller and more responsive (i.e. 'flashy') type systems located in upland areas and along coastal margins. Similarly there is an absence of urban environments or catchments with a heavily modified (e.g. artificial impoundments, large urban extent) flow regime. The number of catchments in the sample has implications for study robustness particularly given the influence that a larger and more diverse catchment sample may have on the clustering and discriminant analysis. It is possible that a larger sample may allow a more detailed assessment and clearer identification of more distinct catchment/sensitivity types. There is also opportunity to improve the transference of results to ungauged or data sparse catchments wherein inferences regarding their sensitivity are made based on their shared physical characteristics. It is important to note that response surfaces are restricted to examining precipitation changes along two dimensions. It is possible that changes in additional aspects of the precipitation cycle (e.g. persistence of dry periods) are also likely to influence future Q95 flows. In particular, the use of a single harmonic function means that the combination of wetter springs and drier autumns (and vice versa) is poorly sampled. Future research should examine sensitivity of other low flow thresholds, together with other aspects of change in precipitation. As a result the study provides only one component in a more complex picture of Q95 low flow sensitivity.

However, given their limitations (e.g. spatio-temporal resolution, parameterizations) we have more confidence in the monthly or annual precipitation and temperature changes projected by the Global Climate Models used to develop the CMIP5 ensemble. While GCMs can more reliably simulate changes in slowly responding and spatially homogenous elements of the climate regime (e.g. seasonal cycle), their resolution limits their capability to resolve finer scale processes related to extremes. Consequently, the study focuses on assessing sensitivity to those components of the climate (e.g. seasonality) best captured by the current generation of models. In addition, it is assumed that the hydrological models used provide a reliable simulation of low flow behaviour under climate conditions which diverge greatly from the observed period used for model calibration. The study underlines the influence which structural differences in model formulation can have when examining catchment responses across the same sensitivity domain. This is best demonstrated by differences in sensitivity between NAM and GR4J/HBV. In this case GR4J/HBV suggests greater reductions in current abstractions are required to offset future climate impacts than those indicated by NAM. This is particularly the case when assessing exposure to increased seasonality. Such differences underline the importance of addressing structural model uncertainty, and highlight that model choice has important implications for the robustness and costing of adaptation plans. It is therefore imperative that managers consider hydrological model uncertainty when considering climate change allowances for a given catchment type, emission scenario and future horizon. The hydrological models employed here are widely used in the water industry and academic literature, future work could explore the sensitivity of low flows to additional model structures.

The study highlights that, dependent on the local climate and physical conditions Q95 flows are differently affected by climate change. Consequently adaptation should be tailored to address local vulnerabilities on a catchment by catchment basis. The results provide an ideal grounding for developing more strategic adaptation plans. In cases where natural resilience is greater relative to the types of changes assessed, unnecessary and costly low-flow mitigation measures may be minimised. For example catchment types (a), (d) and (e) are generally located in the midlands and east and are characterised as drier, low lying, and possess greater natural storage to offset reduced summer precipitation. Such sites are less affected by inter-seasonal variations in precipitation than changes in annual mean. In contrast, in cases of heightened sensitivity and/or greater exposure additional attention can be given to increasing resilience to future changes. Catchment type (b) and (c) are situated in wetter areas of the country - particularly along the western seaboard and uplands. They are associated with poor storage capacity and have a shorter catchment ‘memory’, being more linearly driven by shorter term variations in precipitation. These catchments are more vulnerable to an increasingly seasonal precipitation regime.

Results highlight the significant influence which temperature increases are likely to have on low flows. The majority of CMIP5 ensemble members suggest increases of ~2°C (relative to 1976-2005). Hence the study focuses on this as a threshold to assess sensitivity to precipitation changes. However, despite temperature increases beyond this being relatively less likely, the sensitivity of low flows to this driver should be carefully considered, particularly if the next generation of climate projections indicate that increases should be revised upwards.

The study illustrates the valuable insights which the scenario-neutral framework can provide into the climate sensitivity of Q95 low flows in individual and regionalized catchment types. By assessing the suitability of adaptation measures with respect to the spread of uncertainty in the CMIP5 ensemble it is shown that adaptation measures will need to be tailored to address the natural resilience or heightened vulnerability of catchments on a case by case basis.

References

Beh, E.H.Y., Maier, H.R., Dandy, G.C. 2015. Adaptive, multi-objective optimal sequencing approach for urban water supply augmentation under deep uncertainty. Water Resources Research, 51, 1529-1551.

Beven, K., Binley, A., 1992. The future of distributed models: model calibration and uncertainty prediction. Hydrological Processes, 6(3), 279-298.

Beven, K., Binley, A., 2014. GLUE: 20 years on. Hydrological Processes 28, 5897-5918. https://doi.org/10.1002/hyp.10082

BMU (2008) German Strategy for Adaptation to Climate Change. Federal Ministry for the Environment, Nature Conservation and Nuclear Safety, Berlin.

Broderick, C., Matthews, T., Wilby, R.L., Bastola, S., Murphy, C., 2016. Transferability of hydrological models and ensemble averaging methods between contrasting climatic periods. Water Resources Research 52, 8343-8373. https://doi.org/10.1002/2016WR018850

Brown, C., Ghile, Y., Laverty, M., Li, K., 2012. Decision scaling: Linking bottom-up vulnerability analysis with climate projections in the water sector. Water Resources Research 48. https://doi.org/10.1029/2011WR011212

Burton, I., Lim, B., Spanger-Siegfried, E., Malone, E., Huq, S. (2005) Adaptation policy frameworks for climate change. Cambridge: Cambridge University Press.

Calinski, T., Harabasz, J., 1974. A dendrite method for cluster analysis. Communication Stategy - Theory Methods 3, 1-27. https://doi.org/10.1080/03610927408827101

Chen, J., Brissette, F.P., Leconte, R., 2010. A daily stochastic weather generator for preserving low-frequency of climate variability. Journal of Hydrolology 388, 480-490. https://doi.org/10.1016/j.jhydrol.2010.05.032

Downing, T.E., Butterfield, R.E., Edmonds, B., Knox, J.W., Moss, S., Piper, B.S., Weatherhead, E.K. (and the CCDeW project team) (2003) Climate change and the demand for water research report. Oxford: Stockholm Environment Institute.

European Commission (2009) Common implementation strategy for the Water Framework Directive (2000/60/EC), Guidance document No. 24 River Basin Management in a changing climate. Technical report - 2009 - 040.

Gustard A., Bullock A., Dixon J.M. (1992) Low flow estimation in the United Kingdom, Report number 108, Institute of Hydrology, Wallingford, Oxfordshire, OX12 8BB, UK.

Hall, J., Lempert, R., Keller, K., Hackbarth, A., Mijere, C., McInerney, D. (2012). Robust climate policies under uncertainty: A comparison of Robust Decision Making and Info-Gap Methods. Risk Analysis, 32(10), 1657-1672.

IPCC (2014) Climate Change 2014: Impacts, Adaptation and Vulnerability, Part A: Global and Sectoral Aspects. Contributions of Working Group II the Fifth Assessment Report of the Intergovernmental Panel on Climate Change. [Field, C.B., V.R. Barros, D.J. Dokken, K.J. Mach, M.D. Mastrandrea, T.E. Bilir, M. Chatterjee, K.L. Ebi, Y.O. Estrada, R.C. Genova, B. Girma, E.S. Kissel, A.N. Levy,S. MacCracken, P.R. Mastrandrea, and L.L. White (eds.)]. Cambridge University Press, Cambridge, United Kingdom and New York, NY, USA, 1132 pp.

Jacob D., Petersen J., Eggert B., et al. (2014) EURO-CORDEX: new high-resolution climate change projections for European impact research. Regional Environmental Change, 14(2), 563-578.

Kay, A.L., Crooks, S.M., Davies, H.N., Prudhomme, C., Reynard, N.S., 2014a. Probabilistic impacts of climate change on flood frequency using response surfaces I: England and Wales Regional Environmental Change 14, 1215-1227. https://doi.org/10.1007/s10113-013-0563-y

Kay, A.L., Crooks, S.M., Davies, H.N., Reynard, N.S., 2014b. Probabilistic impacts of climate change on flood frequency using response surfaces II: Scotland. Regional Environmental Change 14, 1243-1255. https://doi.org/10.1007/s10113-013-0564-x

Kay, A.L., Crooks, S.M., Reynard, N.S., 2014c. Using response surfaces to estimate impacts of climate change on flood peaks: assessment of uncertainty. Hydrological Processes 28, 5273-5287. https://doi.org/10.1002/hyp.10000

Korteling, B., Dessai, S., Kapelan, Z. (2012). Using Information-Gap Decision Theory for Water Resources Planning Under Severe Uncertainty. Water Resources Management, 27(4), 1149-1172.

Kwadijk, J., Haasnoot, M., Mulder, J., Hoogvliet, M., Jeuken, A., van der Krogt, R., van Oostrom, N., Schelfhout, H., van Velzen, E., van Waveren, H., de Wit, M. (2010). Using adaptation tipping points to prepare for climate change and sea level rise: a case study in the Netherlands. Wiley Interdisciplinary Reviews: Climate Change, 1(5), 729-740.

Lloyd, S. 1982. Least squares quantization in PCM. IEEE Transactions on Information Theory 28, 129-137.

Madsen H. (2000), Automatic calibration of a conceptual rainfall-runoff model using multiple objectives, Journal of Hydrology, 235(3), 276-288.

Matrosov, E., Woods, A., Harou, J. (2013). Robust Decision Making and Info-Gap Decision Theory for water resource system planning. Journal of Hydrology, 494, 43-58.

McKay M., Beckman R., Conover W. (1979) A comparison of three methods for selecting values of input variables in the analysis of output from a computer code, Technometrics, 21(2), 239-245.

Mills, P., Nicholson, O., Reed, D., 2014. Flood Studies Update Technical Research Report, Volume IV Physical Catchment Descriptors. Office of Public Works.

Murphy C., Harrigan S., Hall J., Wilby R.L. (2013) Climate-driven trends in mean and high flows from a network of reference stations in Ireland. Hydrological Sciences Journal, 58(4).

Nielsen, S.A., Hansen, E., 1973. Numerical Simulation of the Rainfall-Runoff Process on a Daily Basis. Hydrolgical Resource 4, 171-190.

Oudin L., et al. (2005) Which potential evapotranspiration input for a lumped rainfall-runoff model? Part 2 - Towards a simple and efficient potential evapotranspiration model for rainfall-runoff modelling. Journal of Hydrology, 303(1-4). 290-306.

Perrin C., Michel C., Andréassian V. (2003) Improvement of a parsimonious model for streamflow simulation, Journal of Hydrology, 279(1-4), 275-289.

Poff, N., Brown, C., Grantham, T., Matthews, J., Palmer, M., Spence, C., Wilby, R., Haasnoot, M., Mendoza, G., Dominique, K., Baeza, A. (2015). Sustainable water management under future uncertainty with eco-engineering decision scaling. Nature Climate Change, 6(1), 25-34.

Prudhomme C., Wilby R.L., Crooks S., Kay A.L., Reynard N.S. (2010) Scenario-neutral approach to climate change impact studies: Application to flood risk. Journal of Hydrology, 390(3-4) 198-209.

Prudhomme, C., Crooks, S., Kay, A.L., Reynard, N., 2013a. Climate change and river flooding: part 1 classifying the sensitivity of British catchments. Climate Change 119, 933-948. https://doi.org/10.1007/s10584-013-0748-x

Prudhomme, C., Kay, A.L., Crooks, S., Reynard, N., 2013b. Climate change and river flooding: Part 2 sensitivity characterisation for British catchments and example vulnerability assessments. Climate Change 119, 949-964. https://doi.org/10.1007/s10584-013-0726-3

Prudhomme, C., Sauquet, E., Watts, G., 2015. Low Flow Response Surfaces for Drought Decision Support: A Case Study from the UK. Journal Extreme Events 02, 1550005. https://doi.org/10.1142/S2345737615500050

Ranger, N., Reeder, T., Lowe, J. (2013). Addressing 'deep' uncertainty over long-term climate in major infrastructure projects: four innovations of the Thames Estuary 2100 Project. EURO Journal on Decision Processes, 1(3-4), 233-262.

Ray, P., Brown, C., Brown, C. (2015). Confronting Climate Uncertainty in Water Resources Planning and Project Design. Washington: World Bank Publications.

Richardson, C.W., 1981. Stochastic simulation of daily precipitation, temperature, and solar radiation. Water Resources Research 17, 182-190. https://doi.org/10.1029/WR017i001p00182

Seibert J. (1996) HBV Light, User's Manual, Department of Hydrology, Uppsala University, Institute of Earth Science, Uppsala, Sweden.

Taylor, K.E., Stouffer, R.J., Meehl, G.A., 2012. An Overview of CMIP5 and the Experiment Design. Bulletin of the American Meteorological Society 93, 485-498. https://doi.org/10.1175/BAMS-D-11-00094.1

Von Christierson, B., Wade, S., Counsell, C., Arnell, N., Charlton, M., Prudhomme, C., Hannaford, J., Lawson, R., Tattersall, C., Fenn, C., Bell, A. (2013) Climate change approaches in water resource planning - overview of new methods. Report number SC090017/R3, Bristol: Environment Agency.

Walker, W., Haasnoot, M., Kwakkel, J. (2013). Adapt or Perish: A Review of Planning Approaches for Adaptation under Deep Uncertainty. Sustainability, 5(3), 955-979.

Walsh S (2012), Long term rainfall averages for Ireland, in National Hydrology Seminar 2012, Office of Public Works, Tullamore, Ireland.

Weaver, C., Lempert, R., Brown, C., Hall, J., Revell, D., Sarewitz, D. (2012). Improving the contribution of climate model information to decision making: the value and demands of robust decision frameworks. Wiley Interdisciplinary Reviews: Climate Change, 4(1), 39-60.

Wilby, R. and Murphy, C. (in press) Planning for Climate Change Hazards.

Wilby, R., Dessai, S. (2010). Robust adaptation to climate change. Weather, 65(7), 180-185.

Woodward, M., Kapelan, Z., Gouldby, B. (2013). Adaptive Flood Risk Management Under Climate Change Uncertainty Using Real Options and Optimization. Risk Analysis, 34(1), 75-92.

Yates, D., Miller, K., Wilby, R., Kaatz, L. (2015). Decision-centric adaptation appraisal for water management across Colorado's Continental Divide. Climate Risk Management, 10, 35-50.

Zebisch, M., Grothmann, T., Schröter, D., Hasse, C., Fritsch, U., Cramer, W., 2005. Climate change in Germany. Vulnerability and adaptation of climate sensitive sectors/Klimawandel in Deutschland-Vulnerabilität und Anpassungsstrategien klimasensitiver Systeme. Federal Environmental Agency Germany/Umweltbundesamt, Dessau, Report, 201, 41-253.

Appendix

Table A1 Physical attributes of the catchment sample used for low flow sensitivity testing. Also listed are the NSE efficiency score for the median simulations from the GLUE procedure estimated for the calibration and validation period for each rainfall-runoff model

ID	Catchment	River Name	AREA	SAAR	FARL	FOREST	PEAT	ALLUV	FLATWET	SAAPE	FAI	BFIsoil	NETLEN	STMFRQ	DRAIND	MSL	S1085	TAYSLO	ARTDRAIN	ARTDRAIN2	Mean Elevation	Cal: NAM		NSE GR4J	HBV	Val: NAM	NSE GR4J	HBV
6013	Glyde & Dee	Dee	309.1	873.1	0.971	0.024	0	0.052	0.6	506.4	0.16	0.617	345.4	275	1.1	54	2.6	0.205	0.1688	0.782	83.9	0.85		0.9	0.87	0.86	0.87	0.87
6014	Glyde & Dee	Glyde	270.4	927.5	0.927	0.044	0.001	0.045	0.62	498.8	0.12	0.634	234.1	235	0.9	34.4	2.8	0.192	0.1302	0.6586	84.5	0.9		0.93	0.94	0.9	0.91	0.93
7009	Boyne	Boyne	1658.2	868.6	0.986	0.043	0.07	0.037	0.6	506.6	0.22	0.713	1398	1152	0.8	81	0.6	0.173	0.2673	0.728	84.8	0.86		0.91	0.9	0.83	0.9	0.88
7012	Boyne	Boyne	2460.3	890.1	0.965	0.04	0.051	0.035	0.61	504	0.2	0.678	2145.7	1773	0.9	93.7	0.7	0.172	0.2124	0.6059	91	0.89		0.92	0.91	0.85	0.9	0.88
12001	Slaney	Slaney	1030.8	1167.3	0.999	0.114	0.07	0.048	0.54	521.7	0.1	0.716	1101	1302	1.1	89.3	2.1	0.345	0	0	160.6	0.73		0.78	0.75	0.69	0.79	0.75
14007	Barrow	Stradbally	118.6	814.1	1	0.094	0	0.098	0.57	508.2	0.11	0.642	64.7	35	0.5	20.5	3.9	0.665	0	0	134.9	0.78		0.86	0.86	0.77	0.86	0.84
14019	Barrow	Barrow	1697.3	861.5	1	0.099	0.126	0.053	0.58	510.3	0.26	0.624	995.4	794	0.6	83.7	0.7	0.163	0.003	0	93.9	0.87		0.85	0.86	0.82	0.79	0.8
15001	Nore	Kings	444.3	935.2	1	0.06	0.004	0.055	0.58	523.1	0.17	0.514	490.7	561	1.1	44.9	3.6	1.046	0	0	118.4	0.78		0.9	0.88	0.74	0.86	0.84
15003	Nore	Dinin	299.2	933.9	0.997	0.172	0	0.03	0.57	508.1	0.08	0.381	327.5	317	1.1	34.8	3.9	0.886	0	0	208.3	0.72		0.82	0.8	0.68	0.78	0.77
15006	Nore	Nore	2418.3	941.9	0.999	0.106	0.023	0.045	0.58	513.4	0.17	0.633	2196.7	1956	0.9	117.4	0.9	0.212	0	0.0021	136.6	0.87		0.91	0.91	0.86	0.91	0.91
16008	Suir	Suir	1090.3	1029.6	0.999	0.084	0.047	0.046	0.59	516	0.22	0.635	1074.9	1195	1	68.6	0.9	0.249	0	0	138	0.9		0.9	0.94	0.89	0.88	0.92
16009	Suir	Suir	1582.7	1078.6	0.998	0.096	0.053	0.047	0.59	518.1	0.22	0.631	1585.2	1810	1	85.4	1	0.224	0	0	139.4	0.9		0.91	0.92	0.89	0.9	0.92
18002	Blackwater	Blackwater	2333.7	1200.4	0.999	0.145	0.053	0.042	0.62	515.7	0.12	0.622	2237	2040	1	129.1	1.3	0.192	0	0	165.6	0.84		0.87	0.88	0.83	0.88	0.89
18003	Blackwater	Blackwater	1256.7	1299	0.999	0.122	0.062	0.041	0.63	508.7	0.11	0.461	1274.8	1168	1	89.9	1.7	0.233	0	0	181.1	0.82		0.9	0.91	0.8	0.88	0.89
18005	Blackwater	Funshion	378.5	1190.4	1	0.082	0.049	0.029	0.61	524.3	0.1	0.707	370.8	380	1	53.3	2.5	0.377	0.0001	0	158.3	0.77		0.8	0.8	0.76	0.76	0.79
18006	Blackwater	Blackwater	1054.8	1331.6	0.999	0.125	0.074	0.043	0.63	507.8	0.11	0.501	1090.7	1004	1	75.5	1.9	0.269	0	0	187.8	0.81		0.9	0.93	0.77	0.85	0.89
18050	Blackwater	Blackwater	248.8	1469.4	0.999	0.121	0.184	0.035	0.64	505.6	0.12	0.406	296.4	261	1.2	36.9	3.2	0.533	0	0	210.7	0.72		0.83	0.83	0.74	0.87	0.85
20002	Bandon	Bandon	423.7	1668.9	0.987	0.112	0.079	0.045	0.67	517.9	0.1	0.526	506.4	663	1.2	58.2	2.1	0.33	0.0005	0.0058	124.3	0.8		0.88	0.88	0.69	0.81	0.78
23002	Feale	Feale	646.8	1345	1	0.262	0.236	0.038	0.63	513.6	0.06	0.312	718.6	861	1.1	50.5	4.3	0.685	0.001	0.0019	195.8	0.78		0.89	0.87	0.81	0.9	0.88
25001	Mulkear	Mulkear	647.6	1166.2	0.999	0.201	0.065	0.072	0.59	522.3	0.24	0.519	888.3	1030	1.4	53.2	4.1	0.376	0.0845	0.0458	152.5	0.58		0.68	0.58	0.58	0.67	0.57
25002	Mulkear	Newport	221.6	1300	0.999	0.334	0.114	0.066	0.59	516.5	0.15	0.542	314	376	1.4	40.9	6.9	0.822	0.084	0.0499	188.9	0.72		0.83	0.84	0.67	0.77	0.78
25006	Brosna	Brosna	1162.8	932	0.955	0.075	0.101	0.06	0.63	495.1	0.25	0.708	846.2	629	0.7	67.3	0.8	0.16	0.2802	0.5109	88.4	0.81		0.86	0.9	0.81	0.86	0.89
25030	Graney	Graney	280	1183.8	0.85	0.358	0.162	0.04	0.61	522.6	0.15	0.542	341.5	351	1.2	37.3	3.9	0.261	0	0	136	0.79		0.88	0.89	0.74	0.81	0.82
26009	Rinn	Black	98.2	1018.8	0.936	0.061	0.156	0.016	0.68	467.5	0.17	0.538	94.3	68	1	17.5	3	0.392	0	0	90	0.86		0.91	0.93	0.82	0.9	0.9
26010	Cloone	Cloone	94.5	1064.3	0.937	0.104	0.034	0.067	0.69	468	0.18	0.578	128	132	1.4	20.5	1.9	0.211	0	0	82	0.76		0.83	0.78	0.76	0.81	0.76
2602	Inny	Inny	1098.	945.3	0.80	0.07	0.07	0.02	0.66	485.	0.1	0.82	817	607	0.7	90.2	0.2	0.13	0.166	0.633	89.7	0.7		0.7	0.8	0.7	0.7	0.8

ID	Catchment	River Name	AREA	SAAR	FARL	FOREST	PEAT	ALLUV	FLATWET	SAAPE	FAI	BFIsoil	NETLEN	STMFRQ	DRAIND	MSL	S1085	TAYSLO	ARTDRAIN	ARTDRAIN2	Mean Elevation	Cal: NAM		NSE GR4J	HBV	Val: NAM	NSE GR4J	HBV
1			8		7	4	5	2		7	9	8						4	2	9		9		8	4	2	5	1
27002	Fergus	Fergus	564.3	1336.4	0.835	0.12	0.038	0.014	0.62	532.6	0.07	0.697	303.1	391	0.5	40.4	1.2	0.17	0	0	70.1	0.93		0.91	0.93	0.87	0.88	0.88
30005	Robe	Robe	237.8	1172.5	0.985	0.04	0.142	0.015	0.71	459.6	0.27	0.564	224.3	256	0.9	44.8	1	0.182	0.1725	0.6873	61.2	0.89		0.93	0.8	0.87	0.91	0.77
30007	Clare	Clare	469.9	1115.1	0.989	0.041	0.192	0.022	0.7	461.4	0.14	0.646	380.6	302	0.8	50.3	1.1	0.227	0.1168	0.6865	75	0.9		0.88	0.92	0.91	0.89	0.93
32012	Lee	Newport	146.2	1784.4	0.843	0.251	0.529	0.024	0.72	471.2	0.14	0.595	278.7	483	1.9	31.4	4.1	0.224	0	0	133.4	0.96		0.89	0.96	0.94	0.88	0.94
34001	Moy	Moy	1974.8	1322.7	0.825	0.094	0.315	0.023	0.73	461.5	0.2	0.776	2669.5	3523	1.4	88.9	0.7	0.174	0.136	0.3359	81.2	0.67		0.79	0.81	0.66	0.76	0.79
35002	Owenmore	Owenbeg	88.8	1380.6	0.986	0.34	0.246	0.036	0.72	465	0.18	0.422	151	289	1.7	25.7	13.3	0.724	0	0	183.2	0.92		0.94	0.94	0.91	0.91	0.93
35005	Owenmore	Ballyasdare	639.7	1198.3	0.898	0.14	0.114	0.029	0.71	462.7	0.21	0.609	836.1	1226	1.3	41	1.2	0.144	0	0	99.7	0.92		0.92	0.93	0.92	0.92	0.93
36010	Erne	Annalee	771.7	967.6	0.861	0.034	0.005	0.033	0.66	481.9	0.12	0.632	775.5	741	1	64.3	1.6	0.187	0.0001	0	123.5	0.65		0.76	0.78	0.66	0.77	0.79
38001	Owenea	Owenea	111.2	1753.2	0.922	0.217	0.344	0.031	0.7	498.1	0.12	0.285	263.7	576	2.4	25.7	6	0.661	0	0	184.9	0.89		0.93	0.94	0.86	0.9	0.9

Table A2 Global Climate Model simulations obtained from CMIP5 archive

Modelling group	Model	RCP 4.5	RCP 2.6	RCP 6	RCP 8.5
Commonwealth Scientific and Industrial Research Organization (CSIRO) and Bureau of Meteorology (BOM), Australia (CSIRO-BOM)	ACCESS1-0	1	0	0	1
	ACCESS1.3	1	0	0	1
Beijing Climate Center, China Meteorological Administration (BCC)	bcc-csm1-1	1	1	1	1
	bcc-csm1-1-m	1	1	1	1
College of Global Change and Earth System Science, Beijing Normal University (BNU)	BNU-ESM	1	1	0	1
Canadian Centre for Climate Modelling and Analysis (CCCma)	CanESM2	5	5	0	5
University of Miami – RSMAS	CCSM4	6	6	6	5
Community Earth System Model Contributors	CESM1-CAM5	3	3	3	3
	CESM1-WACCM	3	3	0	3
Centro Euro-Mediterraneo per I Cambiamenti Climatici (CMCC)	CMCC-CM	1	0	0	1
	CMCC-CMS	1	0	0	1
Commonwealth Scientific and Industrial Research Organization in collaboration with Queensland Climate Change Centre of Excellence (CSIRO-QCCCE)	CSIRO-Mk3-6-0	10	10	10	10
EC-EARTH consortium	EC-EARTH	1	1	0	1
LASG, Institute of Atmospheric Physics, Chinese Academy of Sciences and CESS, Tsinghua University	FGOALS_g2	1	1	0	1
NOAA Geophysical Fluid Dynamics Laboratory (NOAA GFDL)	GFDL-CM3	1	1	1	1
	GFDL-ESM2G	1	1	1	1
	GFDL-ESM2M	1	1	1	1
NASA Goddard Institute for Space Studies (NASA GISS)	GISS-E2-H	15	3	3	3
	GISS-E2-H-CC	1	0	0	0
	GISS-E2-R	16	2	2	2
	GISS-E2-R-CC	1	0	0	0
Met Office Hadley Centre (additional HadGEM2-ES realizations contributed by Instituto Nacional de Pesquisas Espaciais) (MOHC)	HadCM3	10	0	0	0
	HadGEM2-CC	1	0	0	3
	HadGEM2-ES	4	4	4	4
Institute for Numerical Mathematics (INM)	inmcm4	1	0	0	1
Institut Pierre-Simon Laplace (IPSL)	IPSL-CM5A-LR	4	4	1	4
	IPSL-CM5A-MR	1	1	1	1
	IPSL-CM5B-LR	1	0	0	1
Atmosphere and Ocean Research Institute (The University of Tokyo), National Institute for Environmental Studies, and Japan Agency for Marine-Earth Science and Technology (MIROC)	MIROC5	3	3	3	3
	MIROC4h	3	0	0	0
Japan Agency for Marine-Earth Science and Technology, Atmosphere and Ocean Research Institute (The University of Tokyo), and National Institute for Environmental Studies (MIROC)	MIROC-ESM	1	1	1	1
	MIROC-ESM-CHEM	1	1	1	1
Max Planck Institute for Meteorology (MPI-M)	MPI-ESM-LR	3	3	0	3
	MPI-ESM-MR	3	1	0	1
Meteorological Research Institute (MRI)	MRI-CGCM3	1	1	1	1
Norwegian Climate Centre (NCC)	NorESM1-M	1	1	1	1
	NorESM1-ME	1	1	1	1

Table A3 Group membership for each of the 206 catchments included in the FSU. Catchments are classified according to their physical attributes using the decision rules specified in Figure 3.12

Catchment Type	Catchment ID
(a)	14029, 14018, 16011, 14034, 14019, 25011, 25006, 15012, 12001, 24008, 24001, 24082, 25001, 15004, 25021, 15001, 24013, 25003, 18004, 6013, 25029, 25016, 16003, 24004, 24002, 9001, 25005, 23001, 7003, 25022, 14013, 6026, 3051, 25027, 14007, 8008, 26010, 25044, 16005, 6033, 24022, 8007
(b)	18002, 18003, 18006, 18048, 23002, 20002, 36027, 22006, 16007, 22003, 18050, 16012, 25002, 19031, 12013, 10028, 25038, 19016, 1041, 25158, 35002, 20006, 23012, 36021
(c)	30061, 34001, 34003, 30031, 27002, 22071, 34010, 35011, 10002, 34029, 39009, 19015, 19014, 28001, 27003, 34007, 32012, 27070, 34011, 29071, 30001, 34009, 18016, 31072, 38001, 34018, 16013, 33070, 39008
(d)	15006, 15002, 16009, 16008, 16002, 15005, 18005, 24012, 29011, 18001, 15003, 24011, 25030, 14004, 24030, 16004, 8011, 14011, 25025, 11001, 16001, 29004, 9010, 8003, 16006, 19020, 19046, 13002, 8009
(e)	7012, 7009, 7041, 36019, 7005, 26007, 26021, 26005, 30012, 14006, 36010, 7010, 30004, 26002, 35005, 26108, 26012, 36016, 30007, 7007, 14005, 15007, 36011, 34005, 35001, 7002, 7011, 26008, 29007

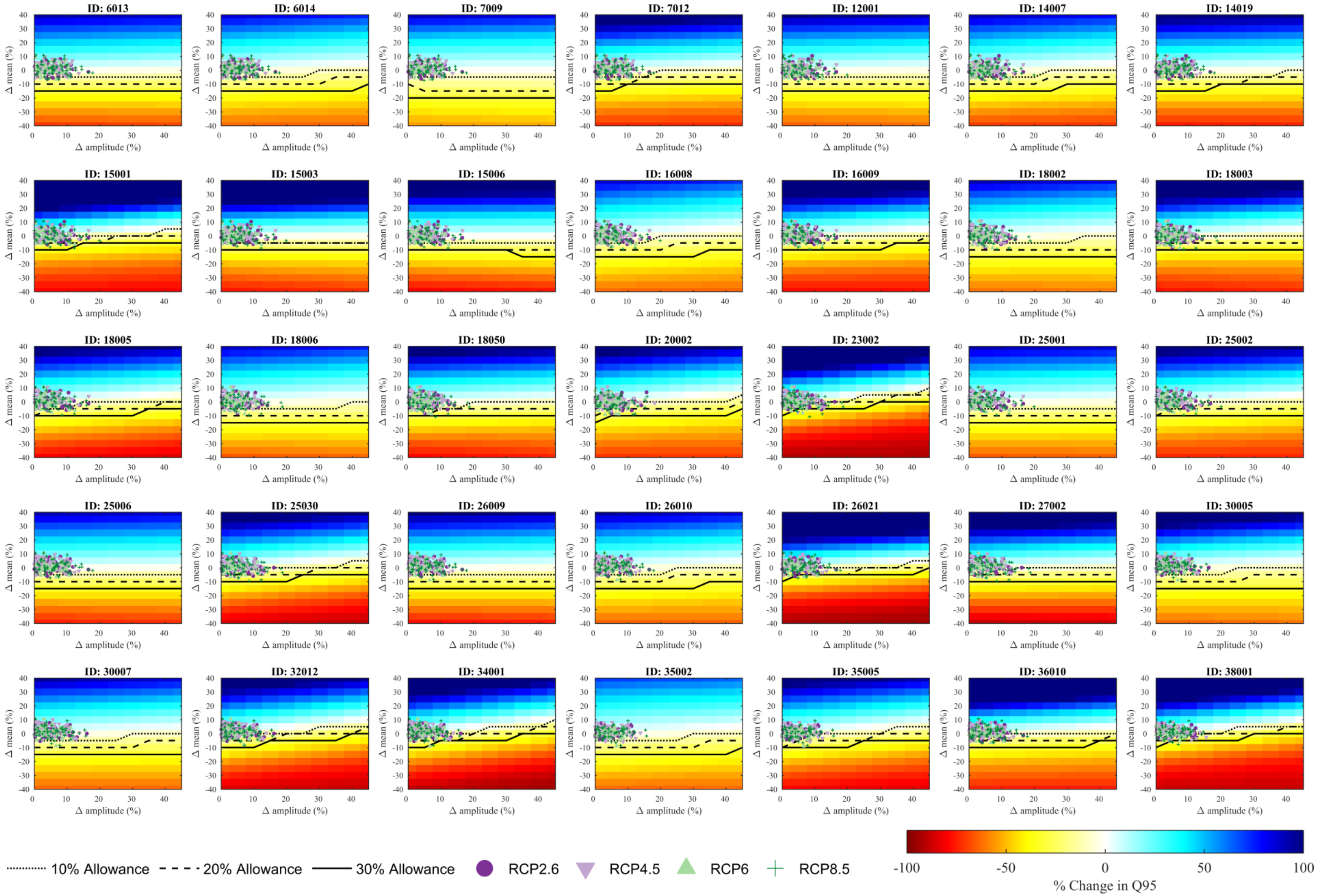

Figure A1 Response surfaces showing changes (%) in the magnitude of the Q95 low flow indicator for incremental changes (5%) in harmonic parameters representing the mean amount (-40% to +40%; x-axis) and seasonality (0% to 50%; y-axis) of the annual precipitation cycle. Surfaces are developed for each of the 35 catchments using the median NAM simulation. Overlain on each plot are changes (%) in the harmonic mean and amplitude projected for the 2010-2039 under all 4 RCPs by each member of the CMIP5 ensemble. Surfaces relate to +0^0 C increase in mean annual temperature to 1976-2005.

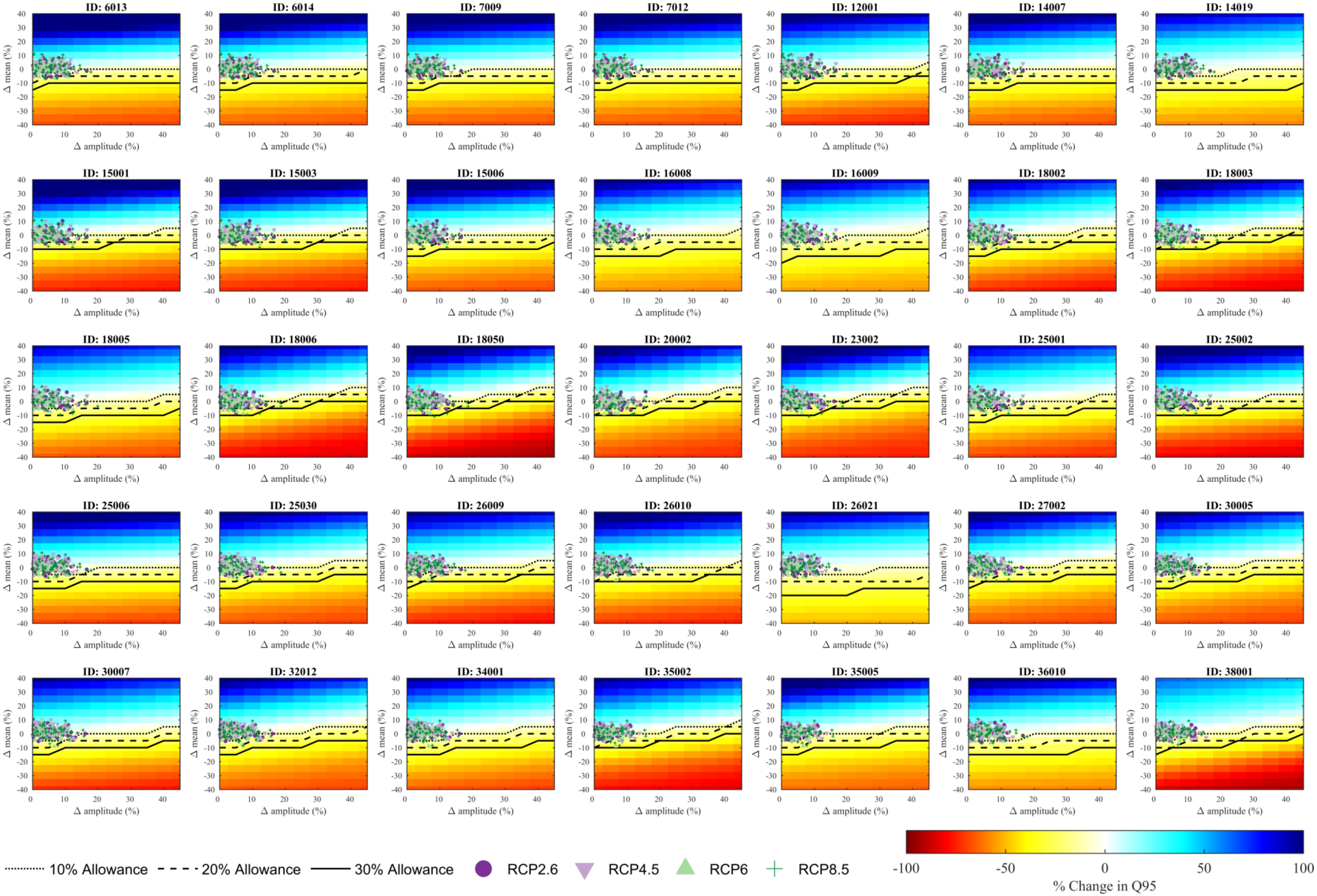

Figure A2 Response surfaces showing changes (%) in the magnitude of the Q95 low flow indicator for incremental changes (5%) in harmonic parameters representing the mean amount (-40% to +40%; x-axis) and seasonality (0% to 50%; y-axis) of the annual precipitation cycle. Surfaces are developed for each of the 35 catchments using the median GR4J simulation. Overlain on each plot are changes (%) in the harmonic mean and amplitude projected for the 2010-2039 under all 4 RCPs by each member of the CMIP5 ensemble. Surfaces relate to +0^0 C increase in mean annual temperature to 1976-2005.

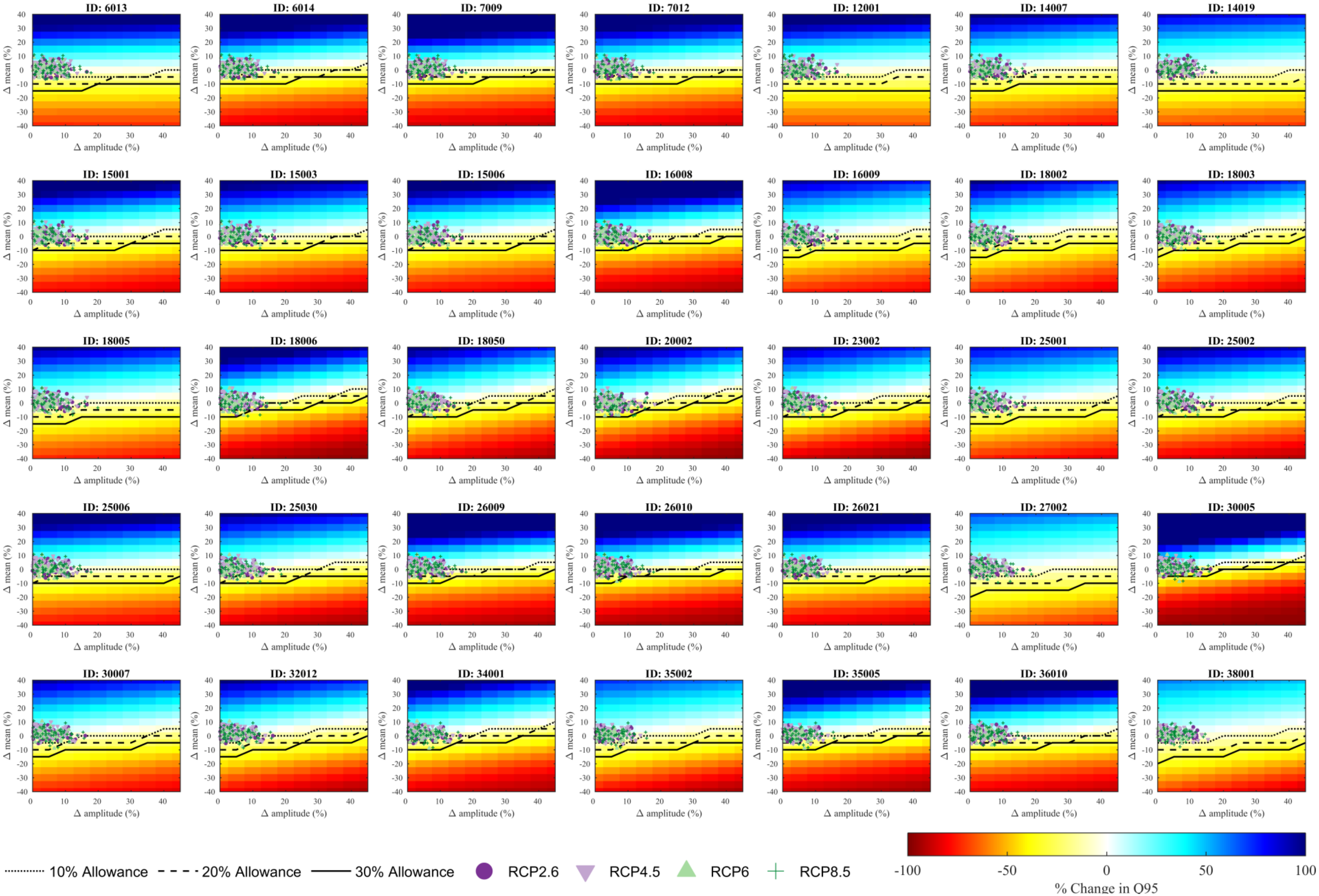

Figure A3 Response surfaces showing changes (%) in the magnitude of the Q95 low flow indicator for incremental changes (5%) in harmonic parameters representing the mean amount (-40% to +40%; x-axis) and seasonality (0% to 50%; y-axis) of the annual precipitation cycle. Surfaces are developed for each of the 35 catchments using the median HBV simulation. Overlain on each plot are changes (%) in the harmonic mean and amplitude projected for the 2010-2039 under all 4 RCPs by each member of the CMIP5 ensemble. Surfaces relate to +0^{0} C increase in mean annual temperature to 1976-2005.

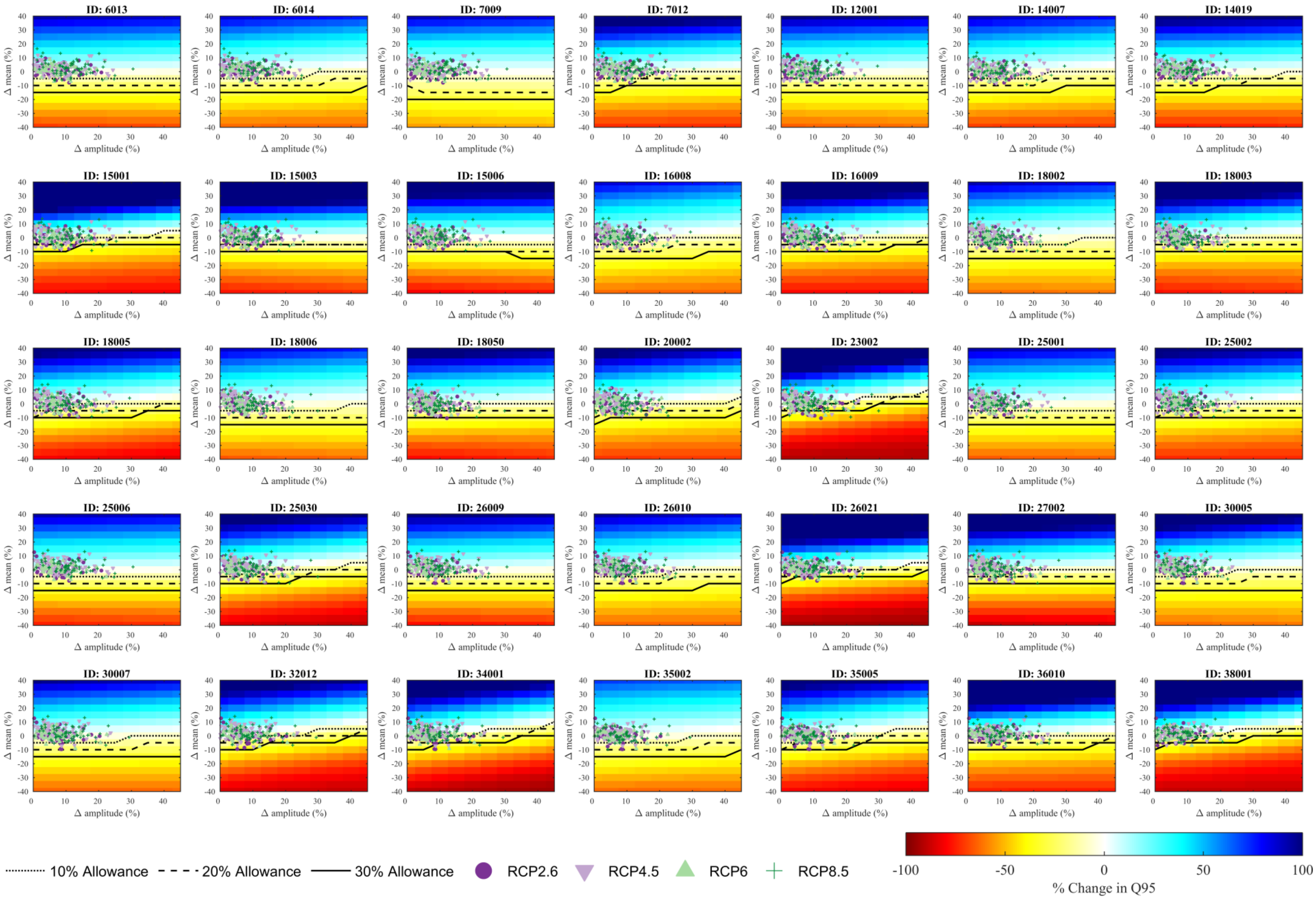

Figure A4 Response surfaces showing changes (%) in the magnitude of the Q95 low flow indicator for incremental changes (5%) in harmonic parameters representing the mean amount (-40% to +40%; x-axis) and seasonality (0% to 50%; y-axis) of the annual precipitation cycle. Surfaces are developed for each of the 35 catchments using the median NAM simulation. Overlain on each plot are changes (%) in the harmonic mean and amplitude projected for the 2040-2069 under all 4 RCPs by each member of the CMIP5 ensemble. Surfaces relate to +0^0 C increase in mean annual temperature to 1976-2005.

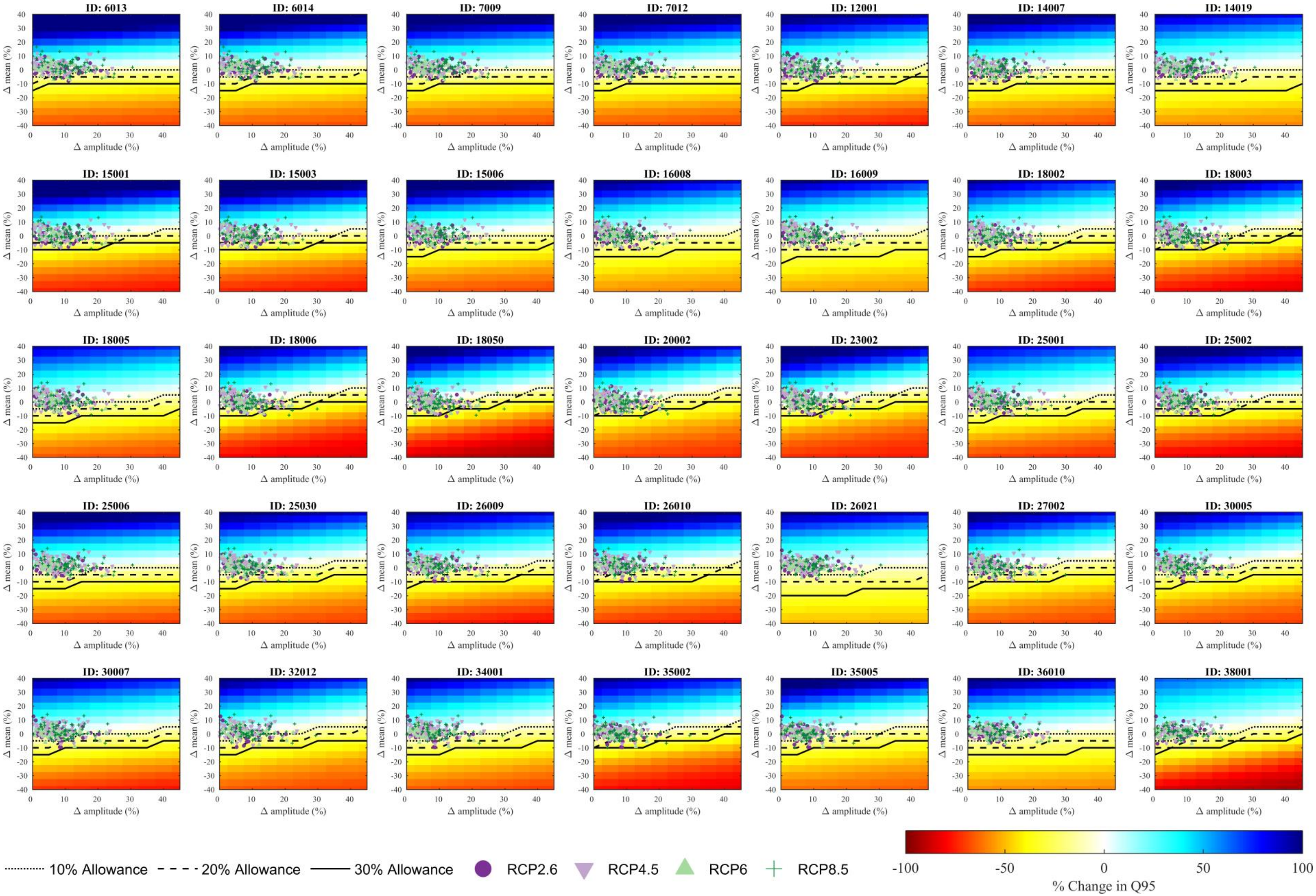

Figure A5 Response surfaces showing changes (%) in the magnitude of the Q95 low flow indicator for incremental changes (5%) in harmonic parameters representing the mean amount (-40% to +40%; x-axis) and seasonality (0% to 50%; y-axis) of the annual precipitation cycle. Surfaces are developed for each of the 35 catchments using the median GR4J simulation. Overlain on each plot are changes (%) in the harmonic mean and amplitude projected for the 2040-2069 under all 4 RCPs by each member of the CMIP5 ensemble. Surfaces relate to +0^{0} C increase in mean annual temperature to 1976-2005.

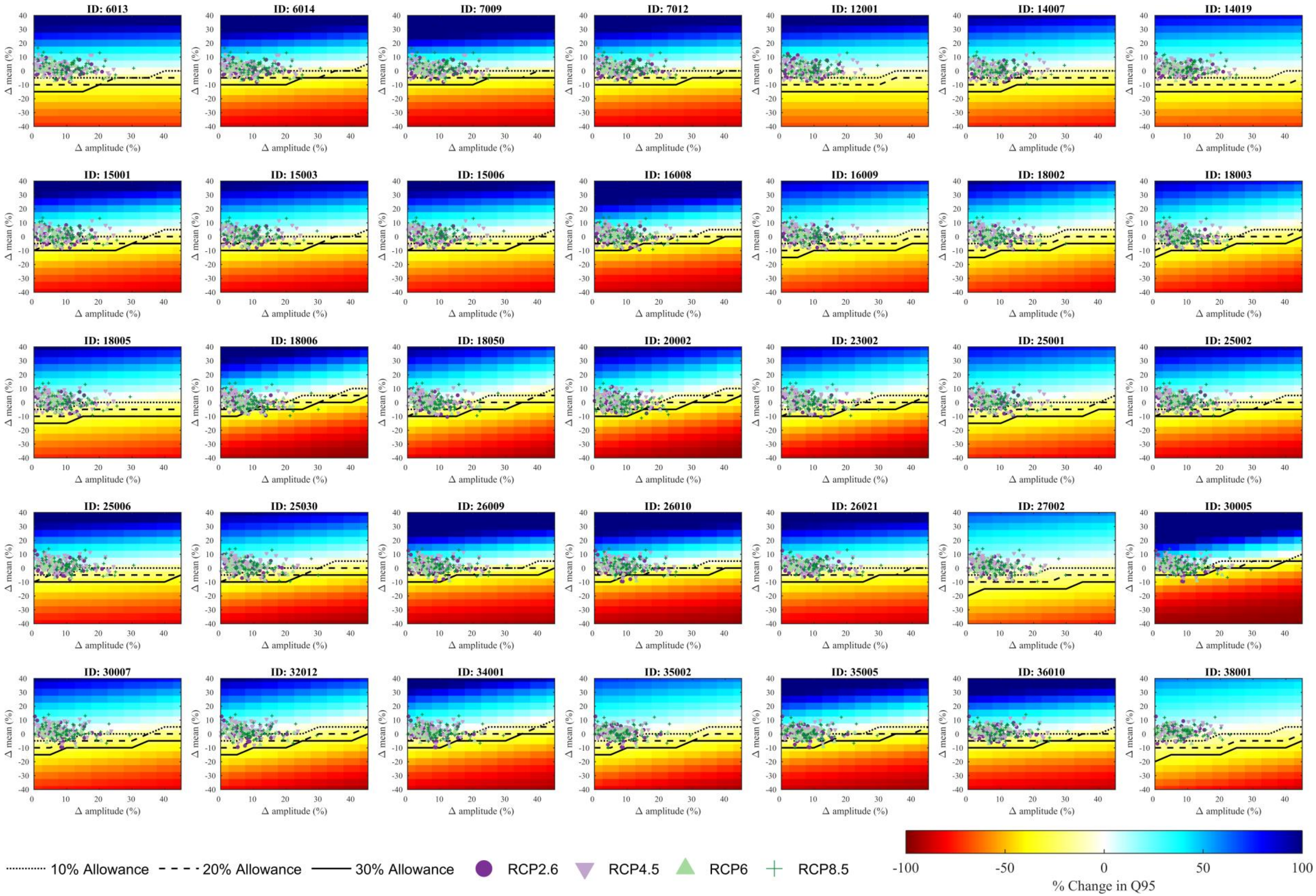

Figure A6 Response surfaces showing changes (%) in the magnitude of the Q95 low flow indicator for incremental changes (5%) in harmonic parameters representing the mean amount (-40% to +40%; x-axis) and seasonality (0% to 50%; y-axis) of the annual precipitation cycle. Surfaces are developed for each of the 35 catchments using the median HBV simulation. Overlain on each plot are changes (%) in the harmonic mean and amplitude projected for the 2040-2069 under all 4 RCPs by each member of the CMIP5 ensemble. Surfaces relate to +0^{0} C increase in mean annual temperature to 1976-2005.

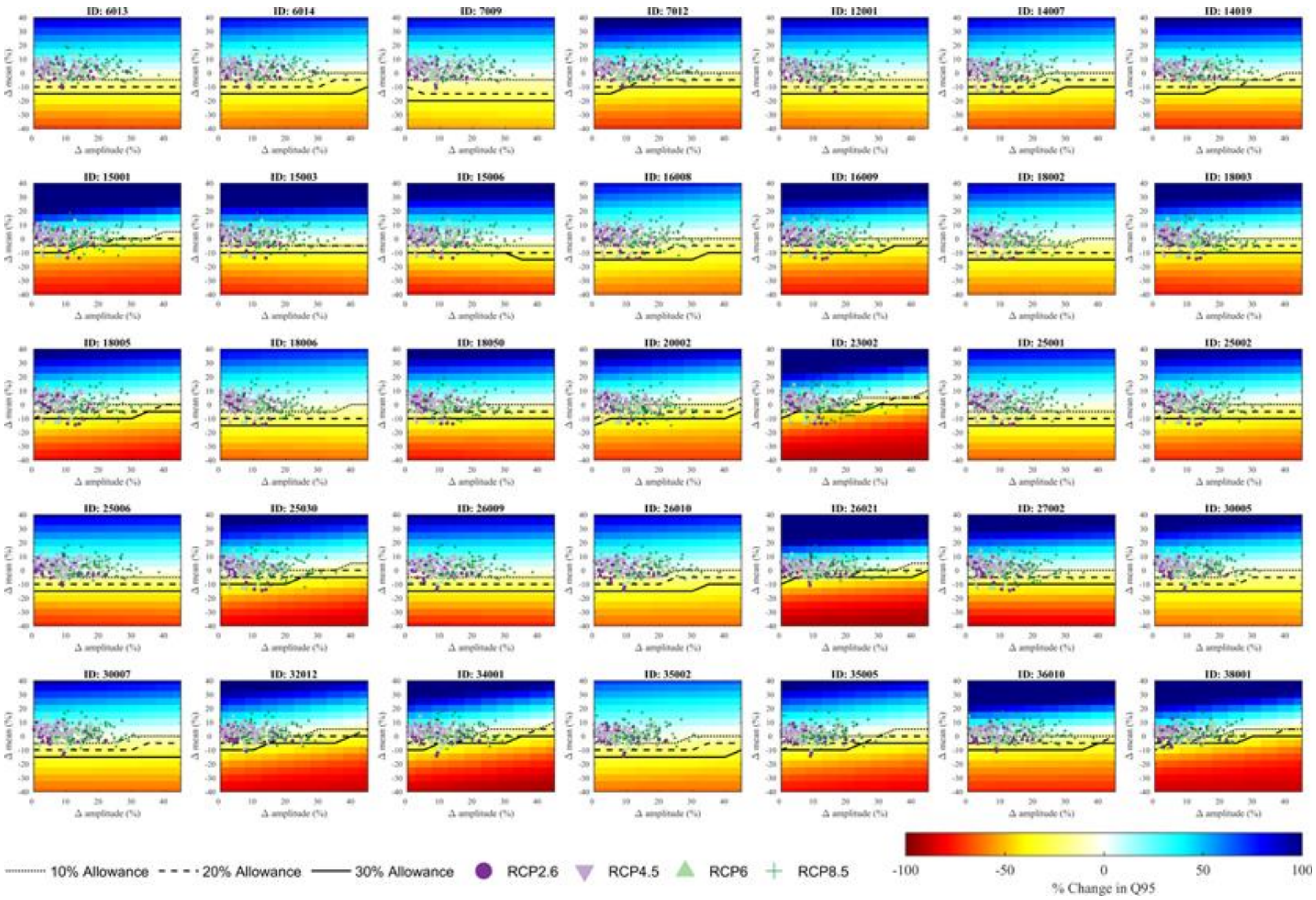

Figure A7 Response surfaces showing changes (%) in the magnitude of the Q95 low flow indicator for incremental changes (5%) in harmonic parameters representing the mean amount (-40% to +40%; *x*-axis) and seasonality (0% to 50%; *y*-axis) of the annual precipitation cycle. Surfaces are developed for each of the 47 catchments using the median NAM simulation. Overlain on each plot are changes (%) in the harmonic mean and amplitude projected for the period 2070-2099 under all 4 RCPs by each member of the CMIP5 ensemble. Surfaces relate to a +0°C increase in mean annual temperature relative to 1976-2005.

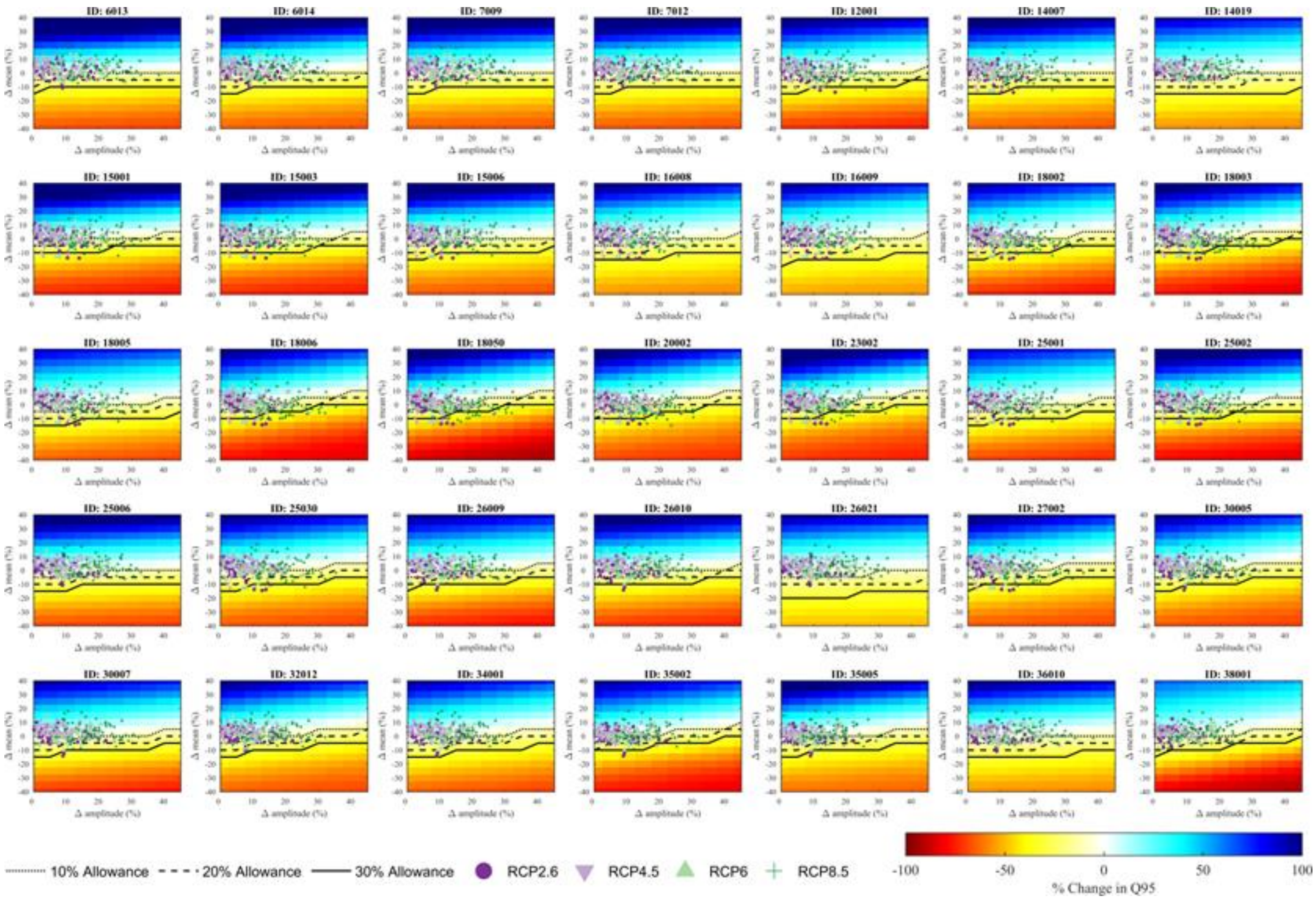

Figure A8 Response surfaces showing changes (%) in the magnitude of the Q95 low flow indicator for incremental changes (5%) in harmonic parameters representing the mean amount (-40% to +40%; *x*-axis) and seasonality (0% to 50%; *y*-axis) of the annual precipitation cycle. Surfaces are developed for each of the 47 catchments using the median GR4J simulation. Overlain on each plot are changes (%) in the harmonic mean and amplitude projected for the period 2070-2099 under all 4 RCPs by each member of the CMIP5 ensemble. Surfaces relate to a +0°C increase in mean annual temperature relative to 1976-2005.

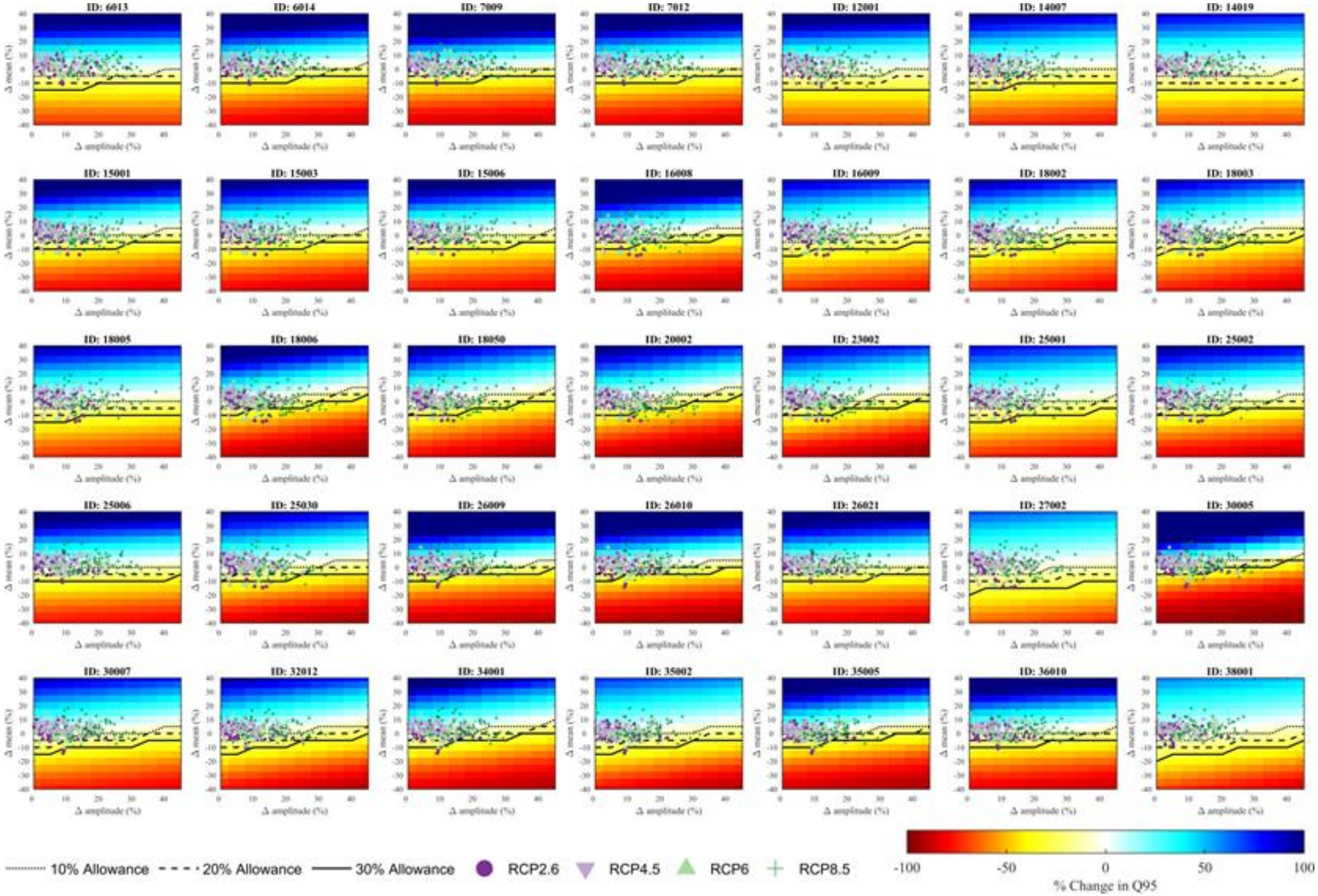

Figure A9 Response surfaces showing changes (%) in the magnitude of the Q95 low flow indicator for incremental changes (5%) in harmonic parameters representing the mean amount (-40% to +40%; *x*-axis) and seasonality (0% to 50%; *y*-axis) of the annual precipitation cycle. Surfaces are developed for each of the 47 catchments using the median HBV simulation. Overlain on each plot are changes (%) in the harmonic mean and amplitude projected for the period 2070-2099 under all 4 RCPs by each member of the CMIP5 ensemble. Surfaces relate to a +0°C increase in mean annual temperature relative to 1976-2005.

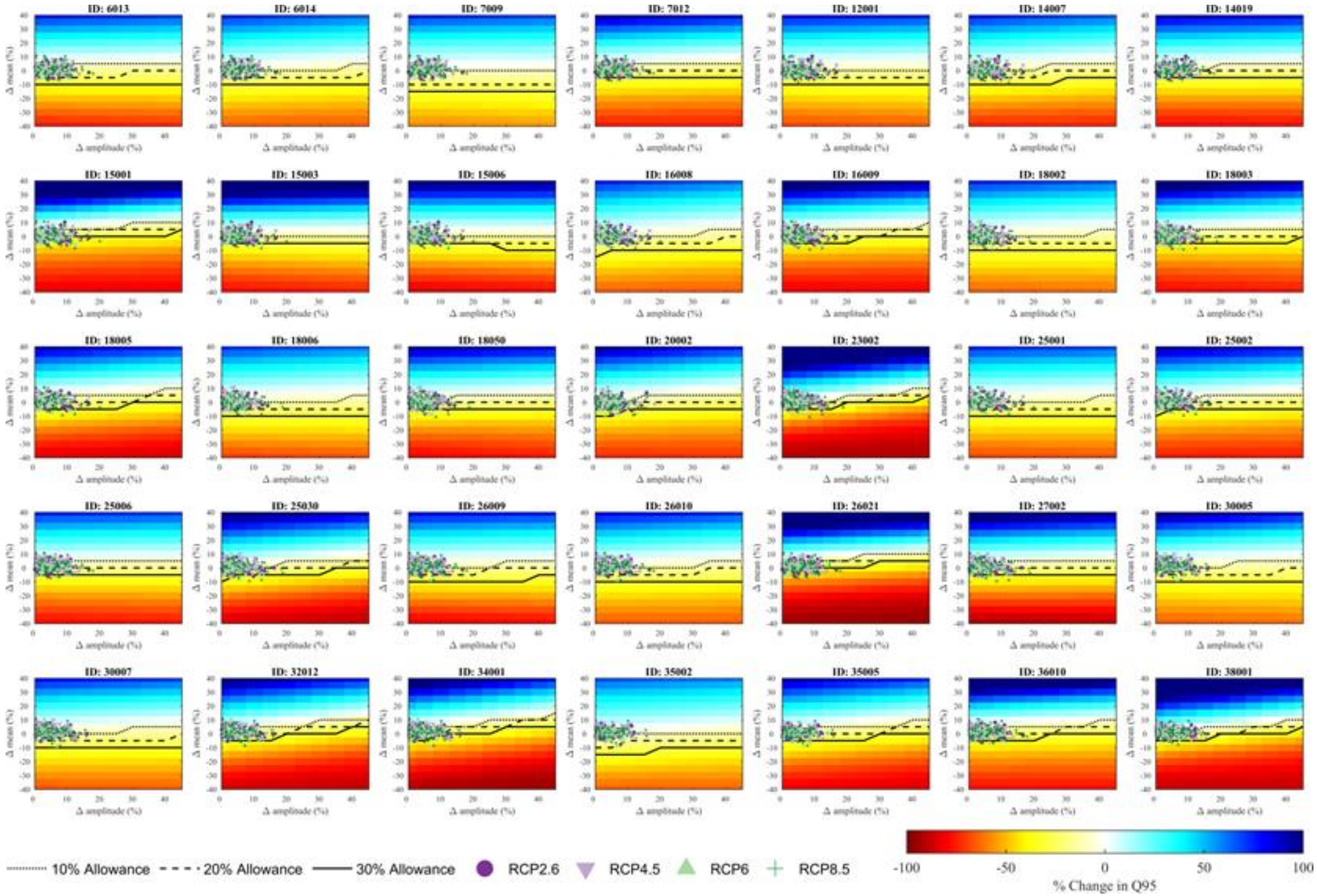

Figure A10 Response surfaces showing changes (%) in the magnitude of the Q95 low flow indicator for incremental changes (5%) in harmonic parameters representing the mean amount (-40% to +40%; *x*-axis) and seasonality (0% to 50%; *y*-axis) of the annual precipitation cycle. Surfaces are developed for each of the 35 catchments using the median NAM simulation. Overlain on each plot are changes (%) in the harmonic mean and amplitude projected for the period 2010-2039 under all 4 RCPs by each member of the CMIP5 ensemble. Surfaces relate to a +2°C increase in mean annual temperature relative to 1976-2005.

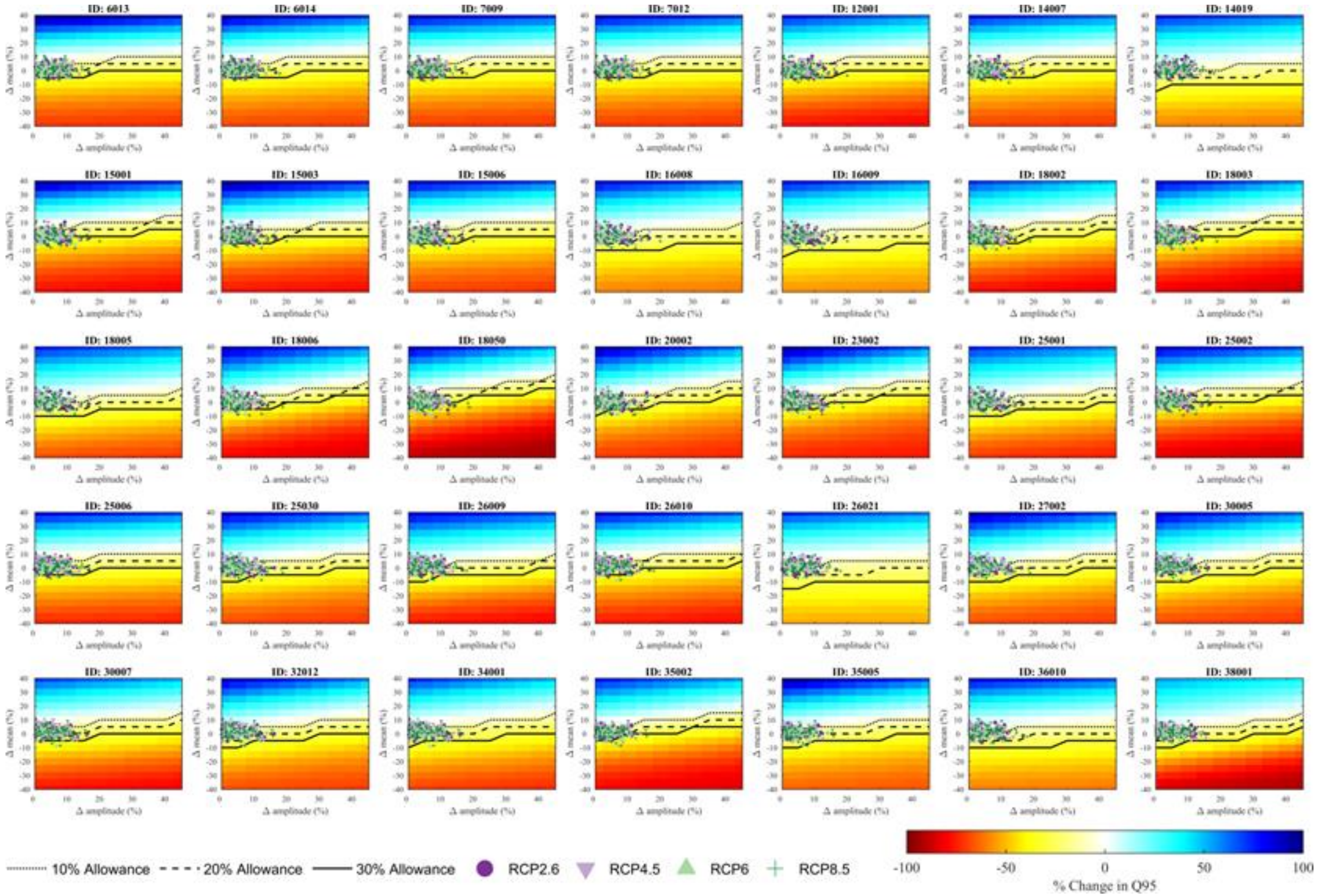

Figure A11 Response surfaces showing changes (%) in the magnitude of the Q95 low flow indicator for incremental changes (5%) in harmonic parameters representing the mean amount (-40% to +40%; *x*-axis) and seasonality (0% to 50%; *y*-axis) of the annual precipitation cycle. Surfaces are developed for each of the 35 catchments using the median GR4J simulation. Overlain on each plot are changes (%) in the harmonic mean and amplitude projected for the period 2010-2039 under all 4 RCPs by each member of the CMIP5 ensemble. Surfaces relate to a +2°C increase in mean annual temperature relative to 1976-2005.

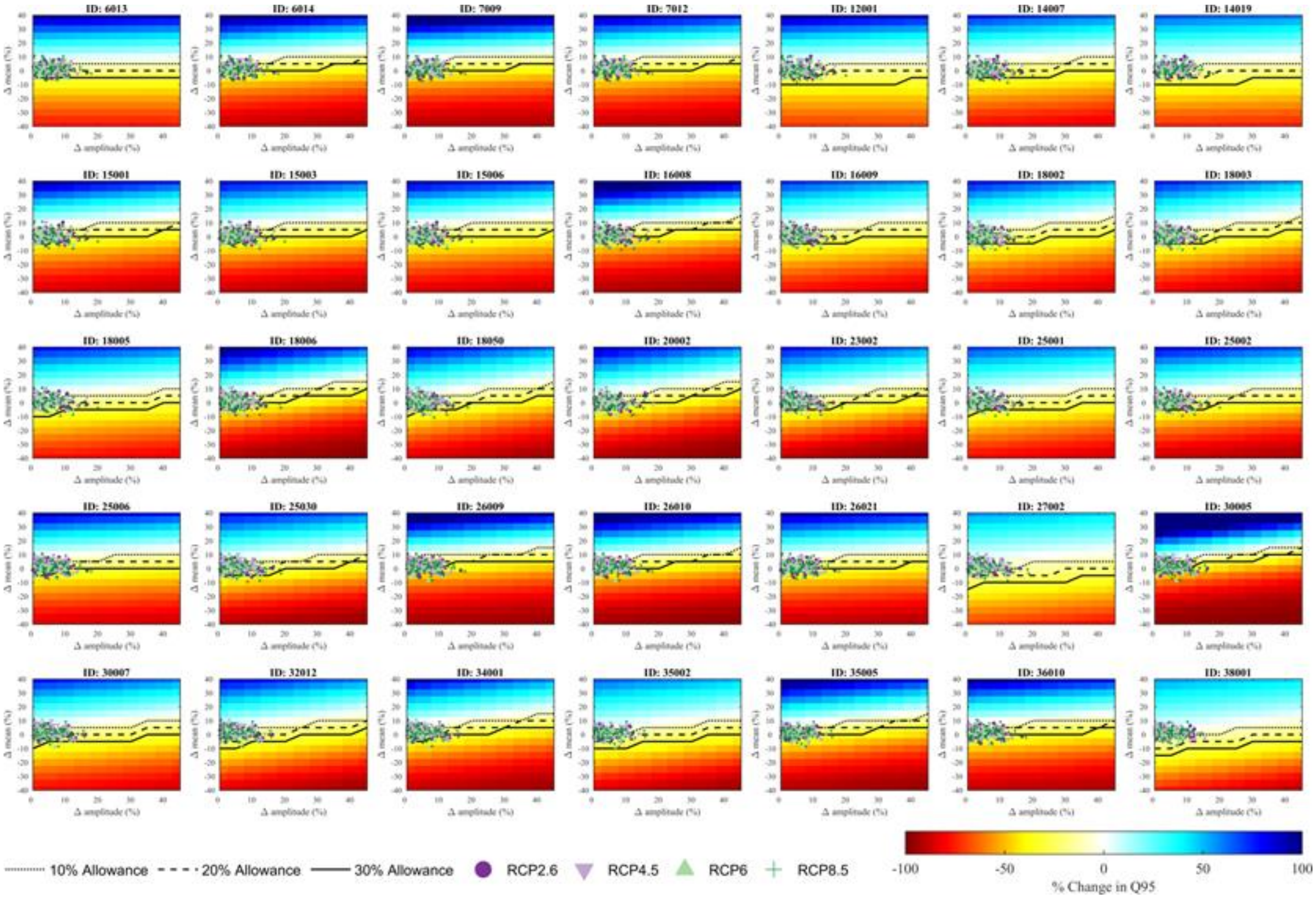

Figure A12.Response surfaces showing changes (%) in the magnitude of the Q95 low flow indicator for incremental changes (5%) in harmonic parameters representing the mean amount (-40% to +40%; *x*-axis) and seasonality (0% to 50%; *y*-axis) of the annual precipitation cycle. Surfaces are developed for each of the 35 catchments using the median HBV simulation. Overlain on each plot are changes (%) in the harmonic mean and amplitude projected for the period 2010-2039 under all 4 RCPs by each member of the CMIP5 ensemble. Surfaces relate to a +2°C increase in mean annual temperature relative to 1976-2005.

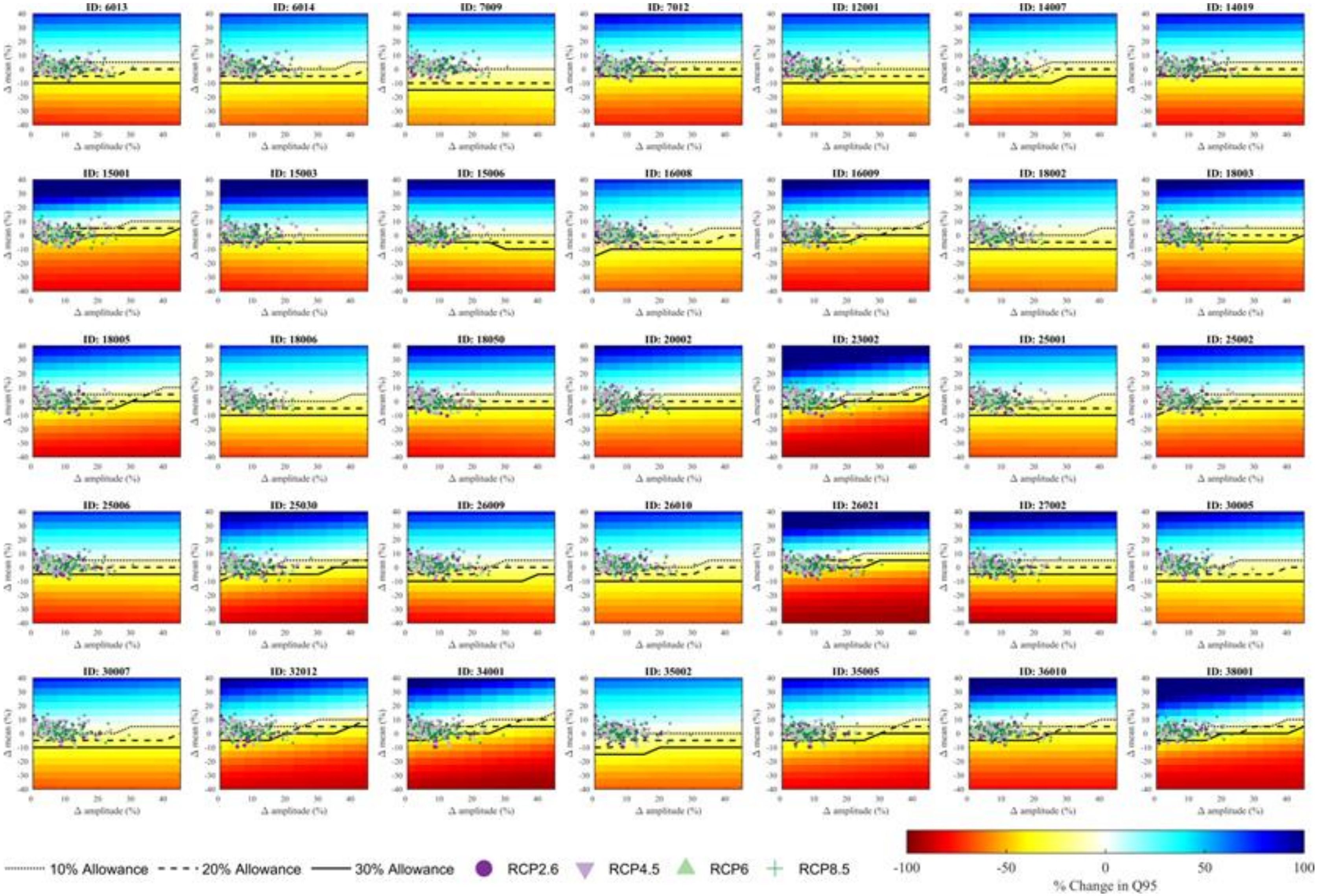

Figure A13 Response surfaces showing changes (%) in the magnitude of the Q95 low flow indicator for incremental changes (5%) in harmonic parameters representing the mean amount (-40% to +40%; *x*-axis) and seasonality (0% to 50%; *y*-axis) of the annual precipitation cycle. Surfaces are developed for each of the 35 catchments using the median NAM simulation. Overlain on each plot are changes (%) in the harmonic mean and amplitude projected for the period 2040-2069 under all 4 RCPs by each member of the CMIP5 ensemble. Surfaces relate to a +2°C increase in mean annual temperature relative to 1976-2005.

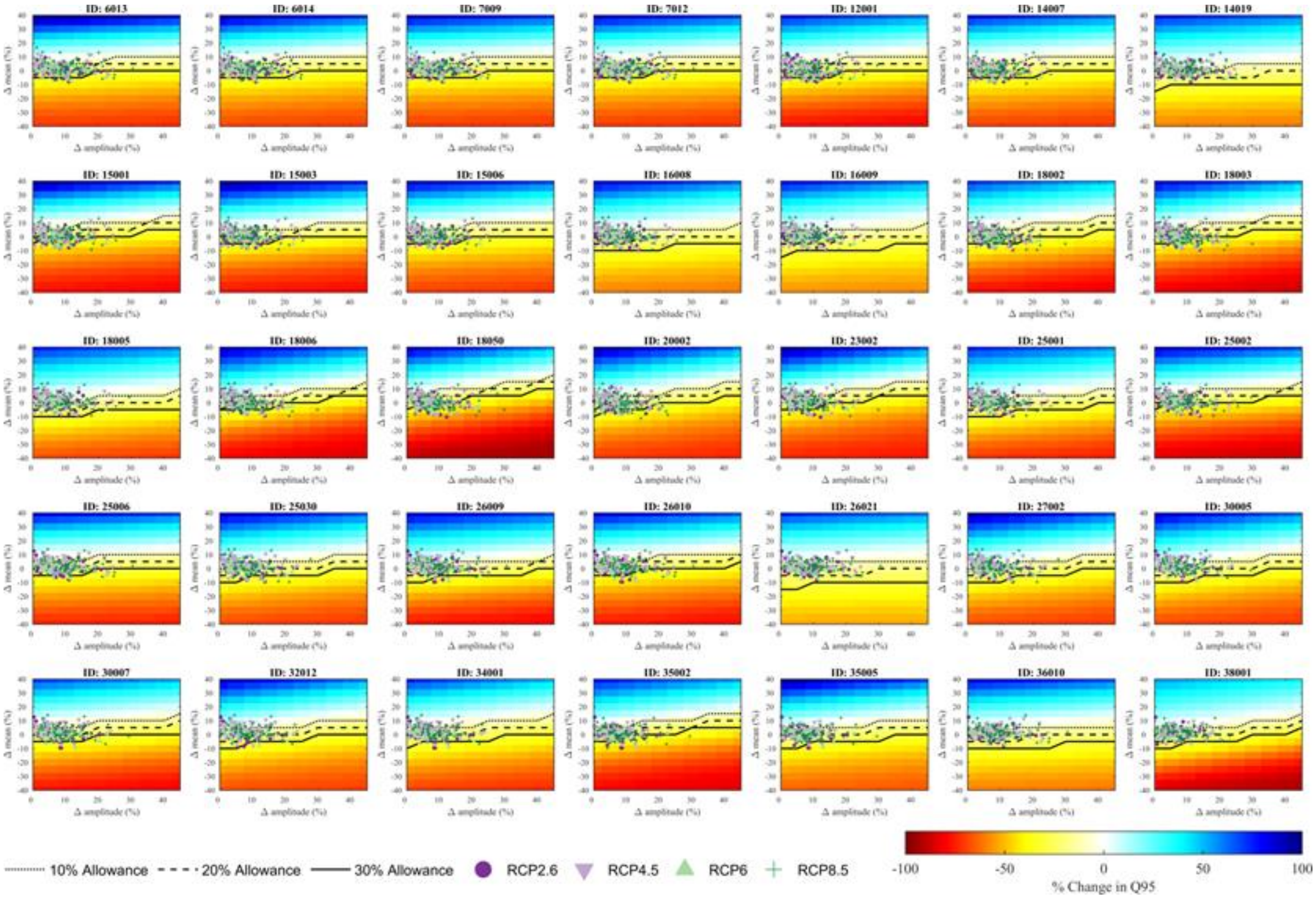

Figure A14 Response surfaces showing changes (%) in the magnitude of the Q95 low flow indicator for incremental changes (5%) in harmonic parameters representing the mean amount (-40% to +40%; *x*-axis) and seasonality (0% to 50%; *y*-axis) of the annual precipitation cycle. Surfaces are developed for each of the 35 catchments using the median GR4J simulation. Overlain on each plot are changes (%) in the harmonic mean and amplitude projected for the period 2040-2069 under all 4 RCPs by each member of the CMIP5 ensemble. Surfaces relate to a +2°C increase in mean annual temperature relative to 1976-2005.

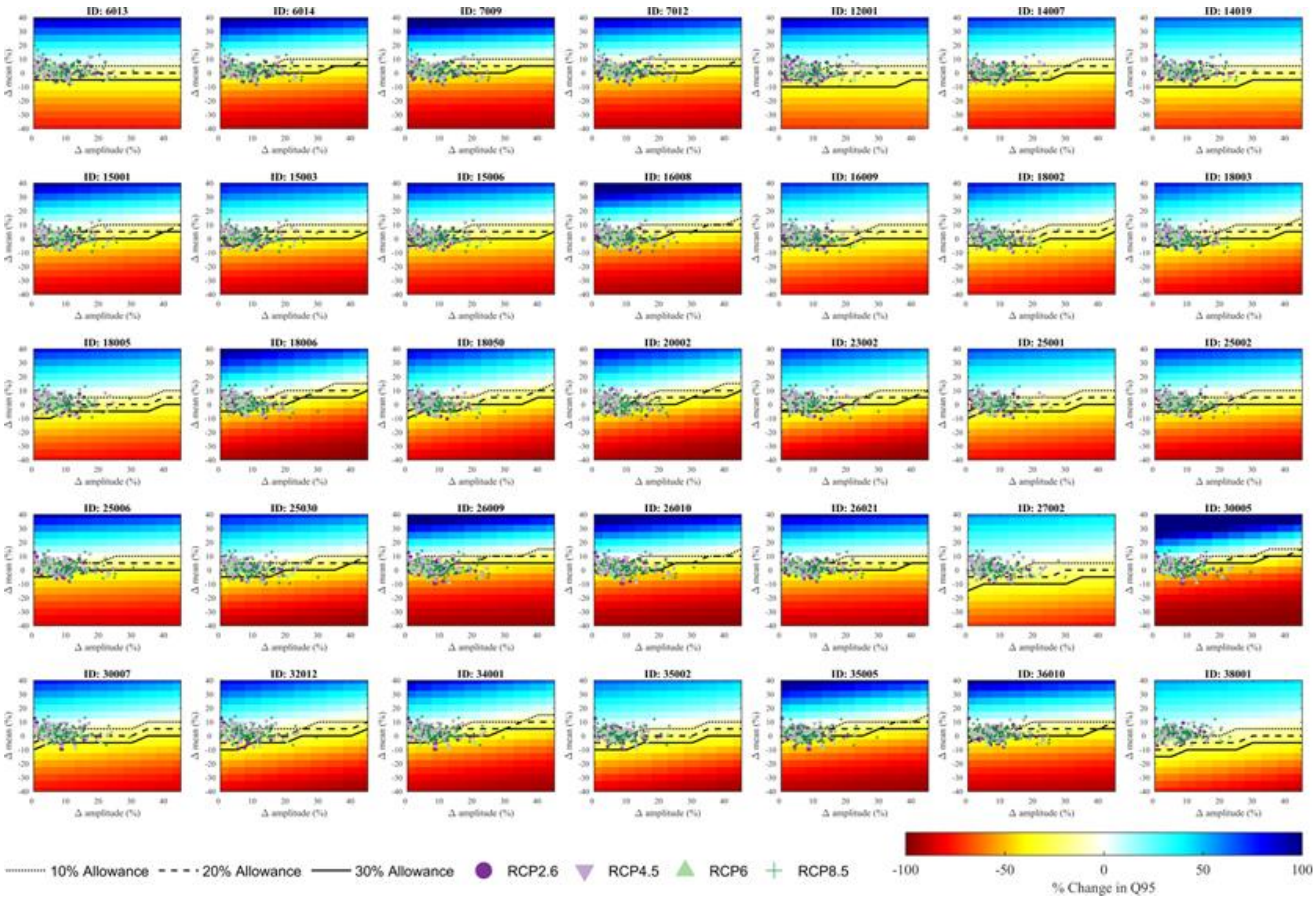

Figure A15 Response surfaces showing changes (%) in the magnitude of the Q95 low flow indicator for incremental changes (5%) in harmonic parameters representing the mean amount (-40% to +40%; *x*-axis) and seasonality (0% to 50%; *y*-axis) of the annual precipitation cycle. Surfaces are developed for each of the 35 catchments using the median HBV simulation. Overlain on each plot are changes (%) in the harmonic mean and amplitude projected for the period 2040-2069 under all 4 RCPs by each member of the CMIP5 ensemble. Surfaces relate to a +2°C increase in mean annual temperature relative to 1976-2005.

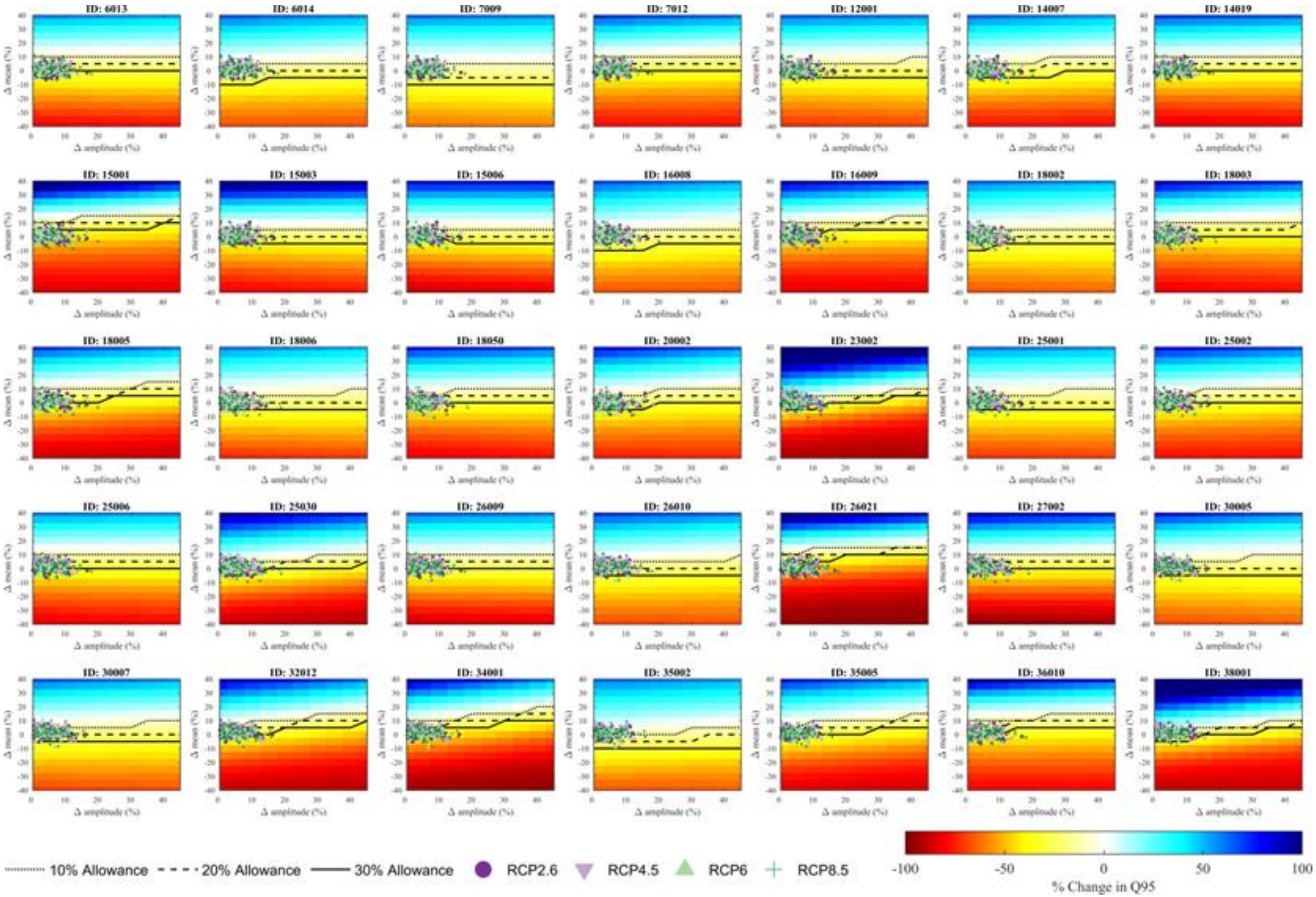

Figure A16 Response surfaces showing changes (%) in the magnitude of the Q95 low flow indicator for incremental changes (5%) in harmonic parameters representing the mean amount (-40% to +40%; x-axis) and seasonality (0% to 50%; y-axis) of the annual precipitation cycle. Surfaces are developed for each of the 35 catchments using the median NAM simulation. Overlain on each plot are changes (%) in the harmonic mean and amplitude projected for the period 2010-2039 under all 4 RCPs by each member of the CMIP5 ensemble. Surfaces relate to a +4°C increase in mean annual temperature relative to 1976-2005.

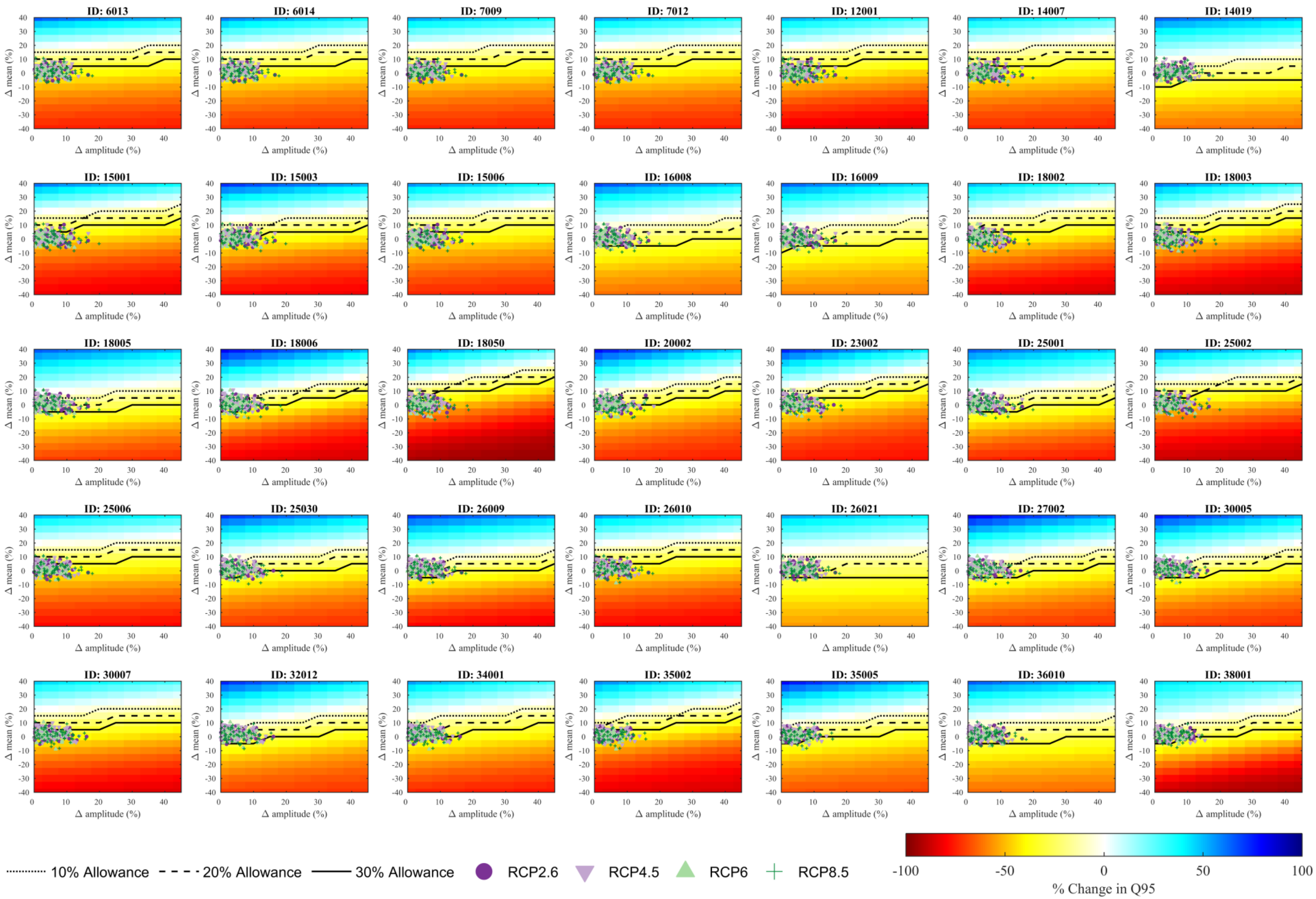

Figure A17 Response surfaces showing changes (%) in the magnitude of the Q95 low flow indicator for incremental changes (5%) in harmonic parameters representing the mean amount (-40% to +40%; x-axis) and seasonality (0% to 50%; y-axis) of the annual precipitation cycle. Surfaces are developed for each of the 35 catchments using the median GR4J simulation. Overlain on each plot are changes (%) in the harmonic mean and amplitude projected for the period 2010-2039 under all 4 RCPs by each member of the CMIP5 ensemble. Surfaces relate to a +4°C increase in mean annual temperature relative to 1976-2005.

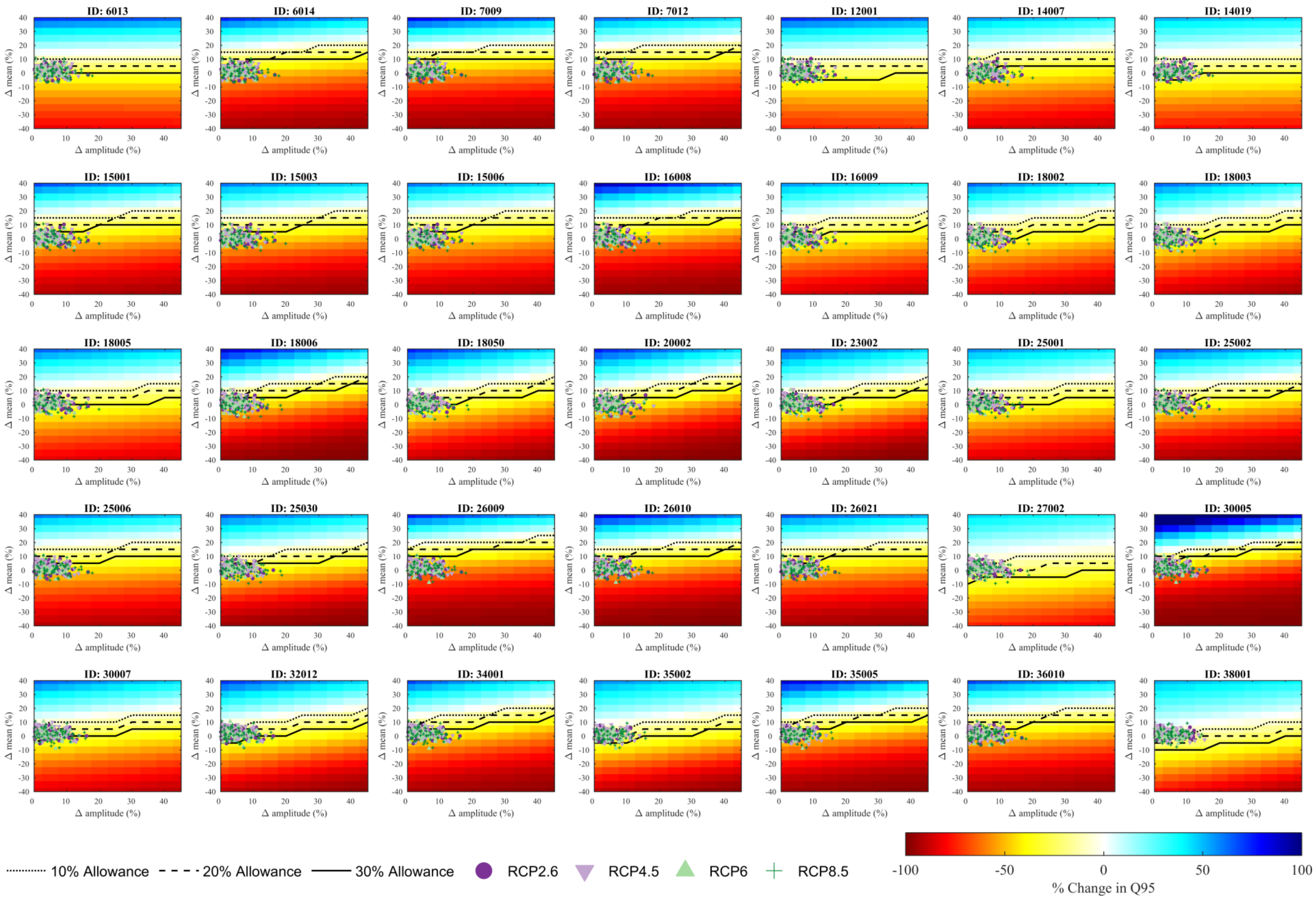

Figure A18 Response surfaces showing changes (%) in the magnitude of the Q95 low flow indicator for incremental changes (5%) in harmonic parameters representing the mean amount (-40% to +40%; x-axis) and seasonality (0% to 50%; y-axis) of the annual precipitation cycle. Surfaces are developed for each of the 35 catchments using the median HBV simulation. Overlain on each plot are changes (%) in the harmonic mean and amplitude projected for the period 2010-2039 under all 4 RCPs by each member of the CMIP5 ensemble. Surfaces relate to a +4°C increase in mean annual temperature relative to 1976-2005.

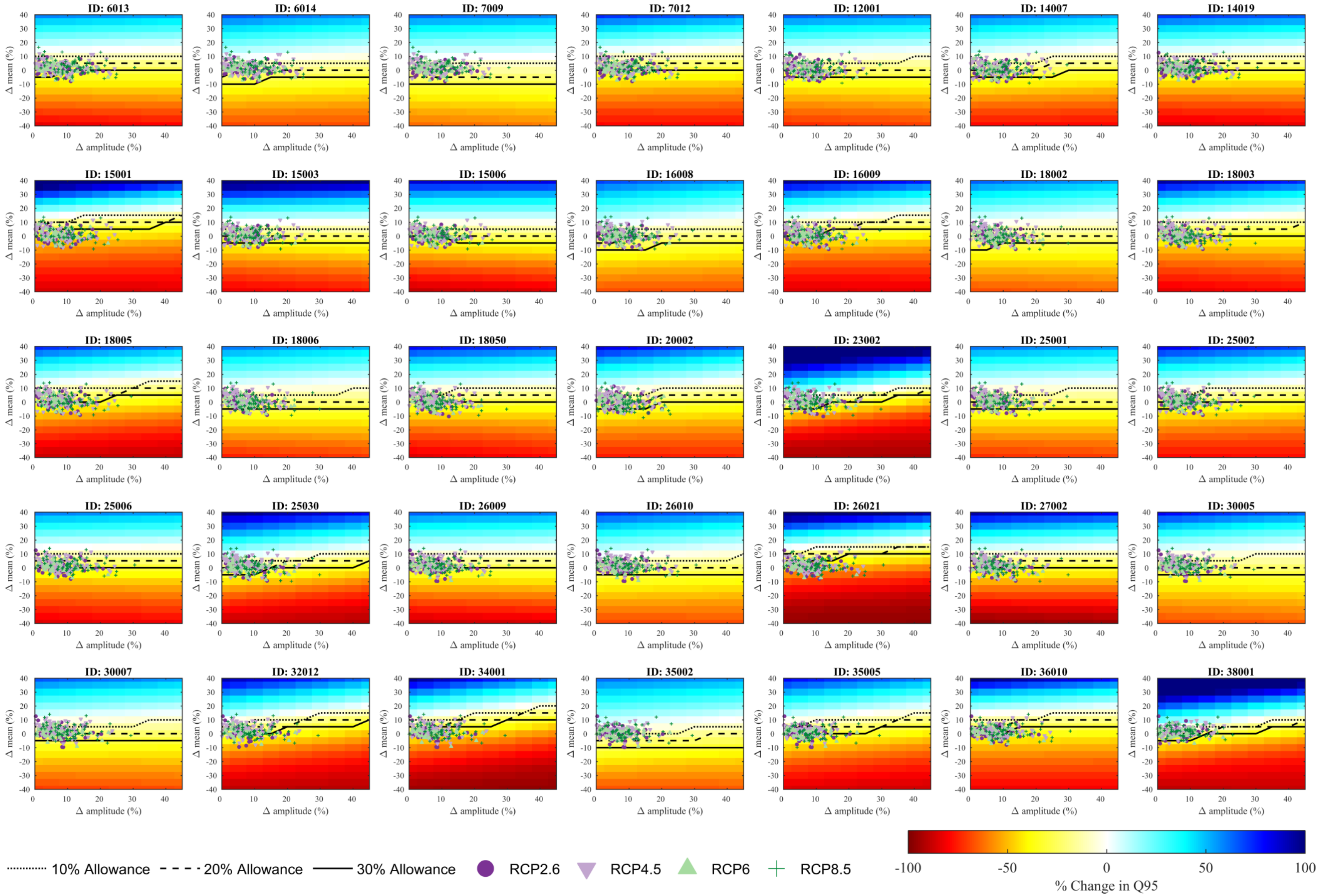

Figure A19 Response surfaces showing changes (%) in the magnitude of the Q95 low flow indicator for incremental changes (5%) in harmonic parameters representing the mean amount (-40% to +40%; *x*-axis) and seasonality (0% to 50%; *y*-axis) of the annual precipitation cycle. Surfaces are developed for each of the 47 catchments using the median NAM simulation. Overlain on each plot are changes (%) in the harmonic mean and amplitude projected for the period 2040-2069 under all 4 RCPs by each member of the CMIP5 ensemble. Surfaces relate to a +2°C increase in mean annual temperature relative to 1976-2005.

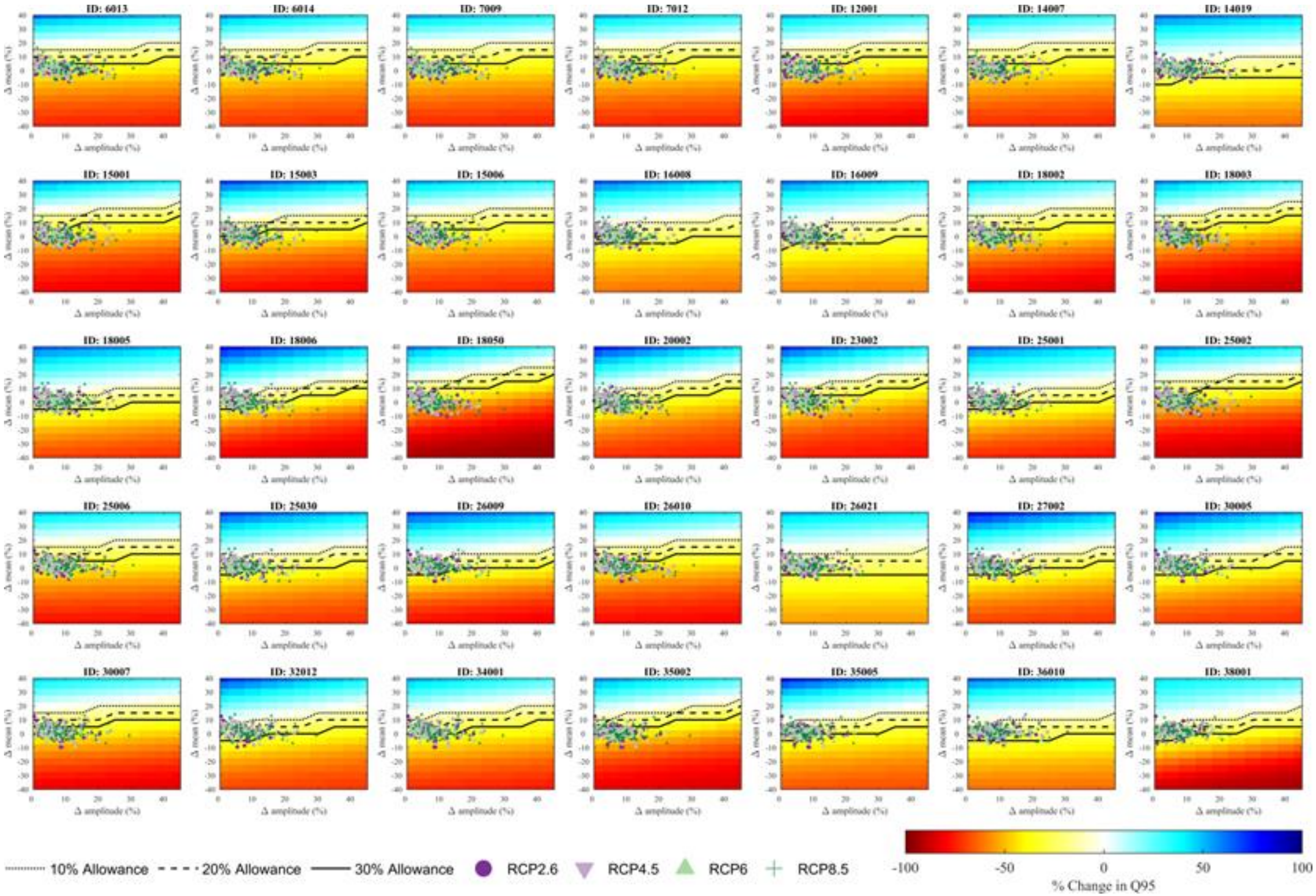

Figure A20 Response surfaces showing changes (%) in the magnitude of the Q95 low flow indicator for incremental changes (5%) in harmonic parameters representing the mean amount (-40% to +40%; *x*-axis) and seasonality (0% to 50%; *y*-axis) of the annual precipitation cycle. Surfaces are developed for each of the 47 catchments using the median GR4J simulation. Overlain on each plot are changes (%) in the harmonic mean and amplitude projected for the period 2040-2069 under all 4 RCPs by each member of the CMIP5 ensemble. Surfaces relate to a +2°C increase in mean annual temperature relative to 1976-2005.

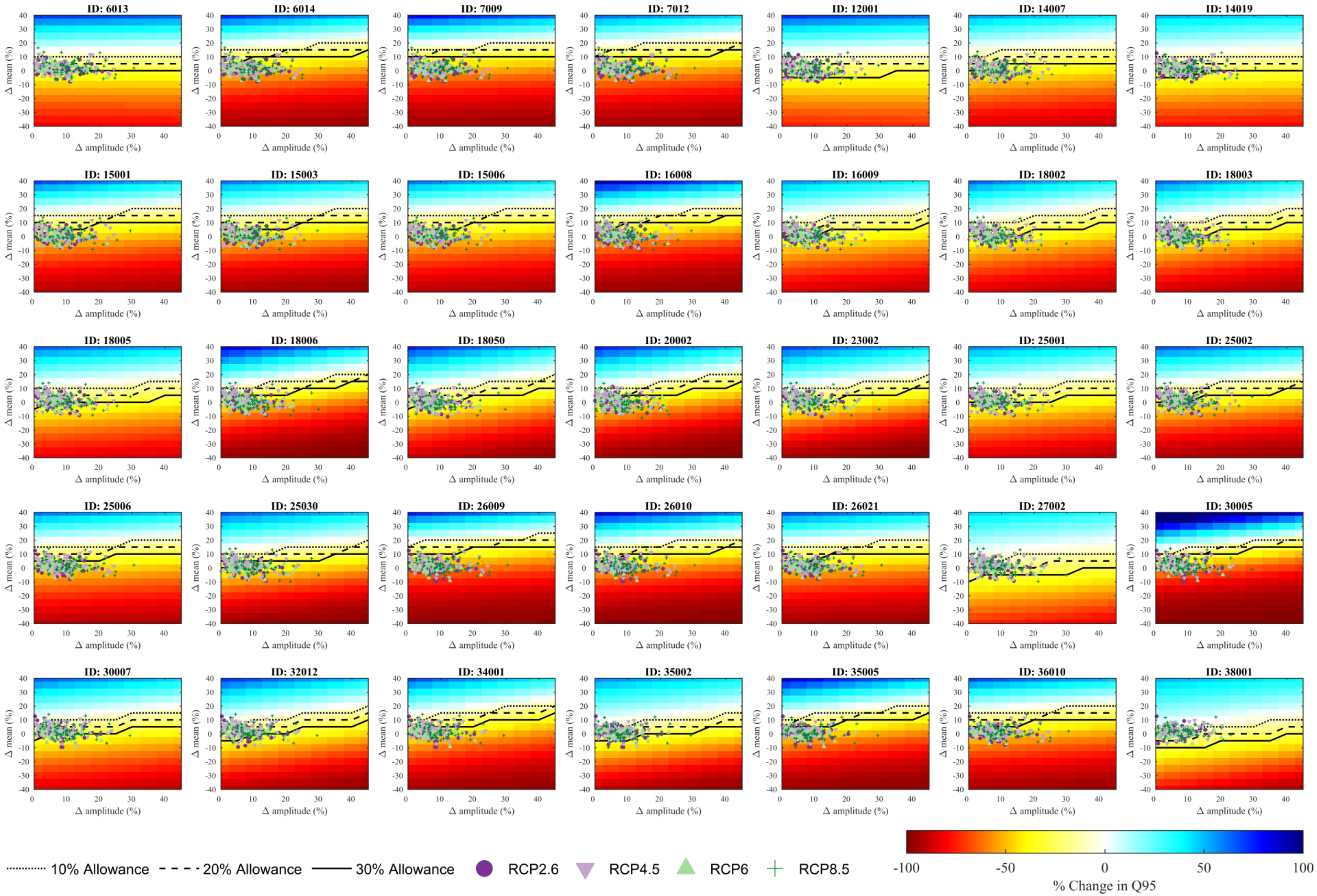

Figure A21 Response surfaces showing changes (%) in the magnitude of the Q95 low flow indicator for incremental changes (5%) in harmonic parameters representing the mean amount (-40% to +40%; *x*-axis) and seasonality (0% to 50%; *y*-axis) of the annual precipitation cycle. Surfaces are developed for each of the 47 catchments using the median HBV simulation. Overlain on each plot are changes (%) in the harmonic mean and amplitude projected for the period 2040-2069 under all 4 RCPs by each member of the CMIP5 ensemble. Surfaces relate to a +2°C increase in mean annual temperature relative to 1976-2005.

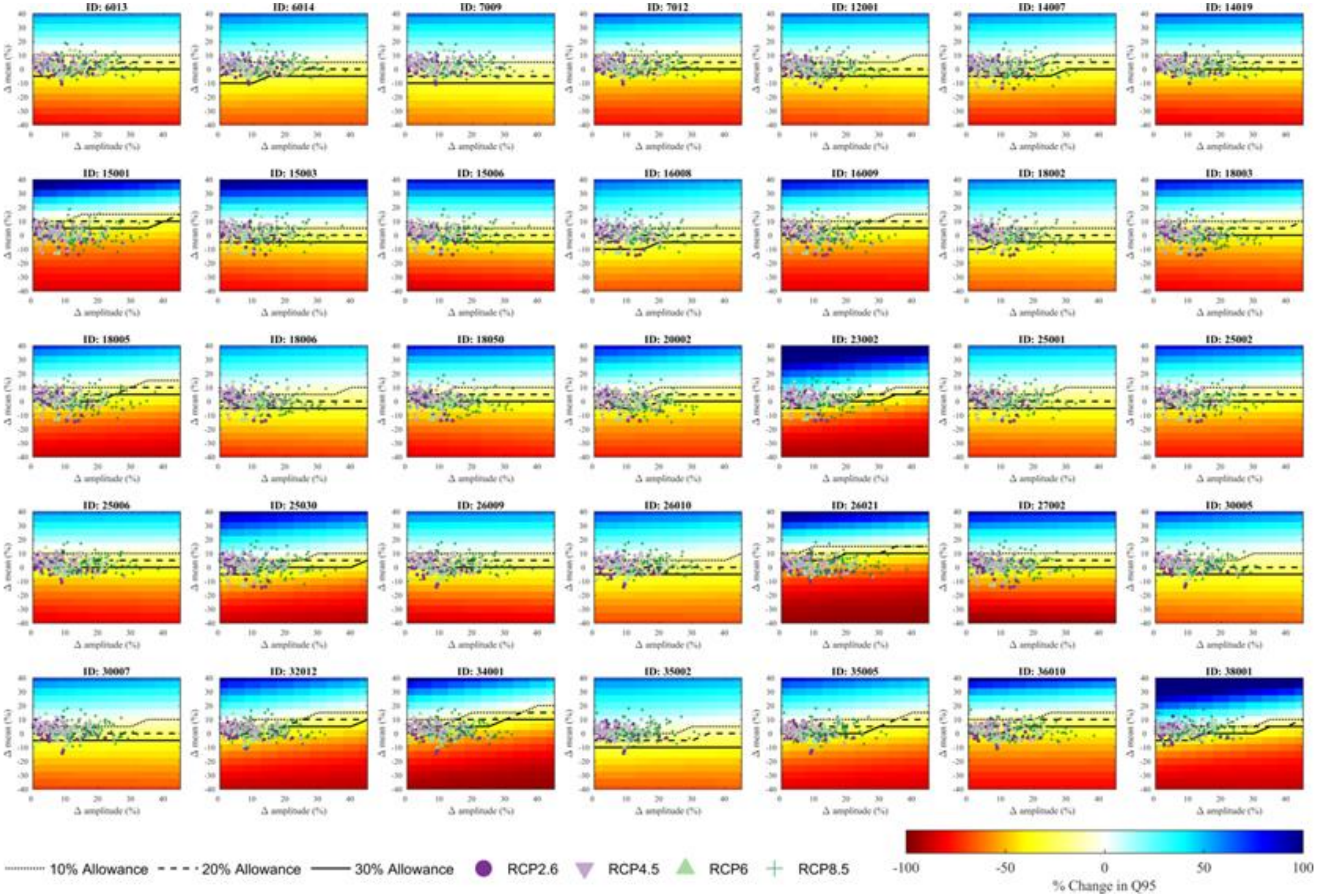

Figure A22 Response surfaces showing changes (%) in the magnitude of the Q95 low flow indicator for incremental changes (5%) in harmonic parameters representing the mean amount (-40% to +40%; *x*-axis) and seasonality (0% to 50%; *y*-axis) of the annual precipitation cycle. Surfaces are developed for each of the 35 catchments using the median NAM simulation. Overlain on each plot are changes (%) in the harmonic mean and amplitude projected for the period 2070-2099 under all 4 RCPs by each member of the CMIP5 ensemble. Surfaces relate to a +4°C increase in mean annual temperature relative to 1976-2005.

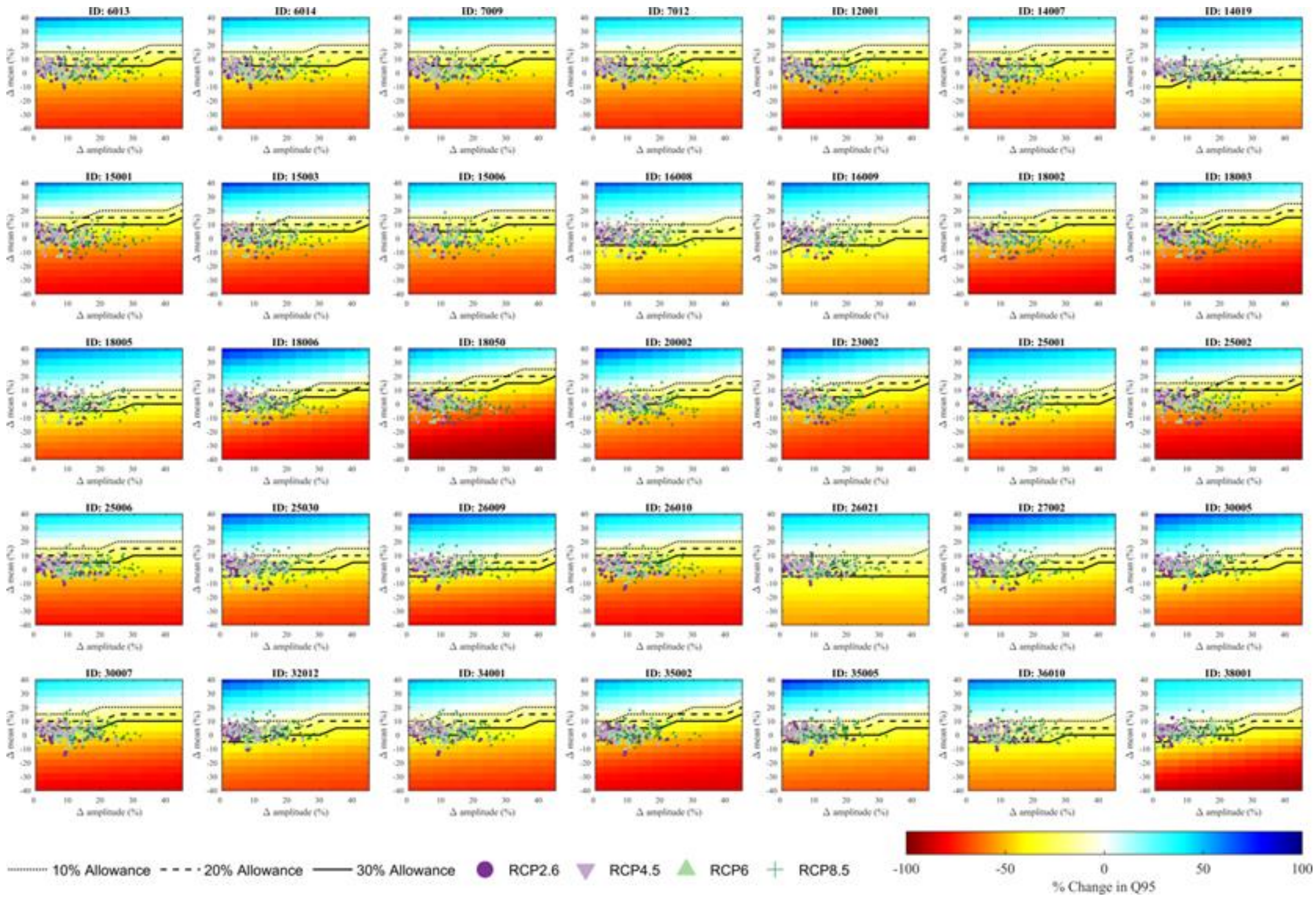

Figure A23 Response surfaces showing changes (%) in the magnitude of the Q95 low flow indicator for incremental changes (5%) in harmonic parameters representing the mean amount (-40% to +40%; *x*-axis) and seasonality (0% to 50%; *y*-axis) of the annual precipitation cycle. Surfaces are developed for each of the 35 catchments using the median GR4J simulation. Overlain on each plot are changes (%) in the harmonic mean and amplitude projected for the period 2070-2099 under all 4 RCPs by each member of the CMIP5 ensemble. Surfaces relate to a +4°C increase in mean annual temperature relative to 1976-2005.

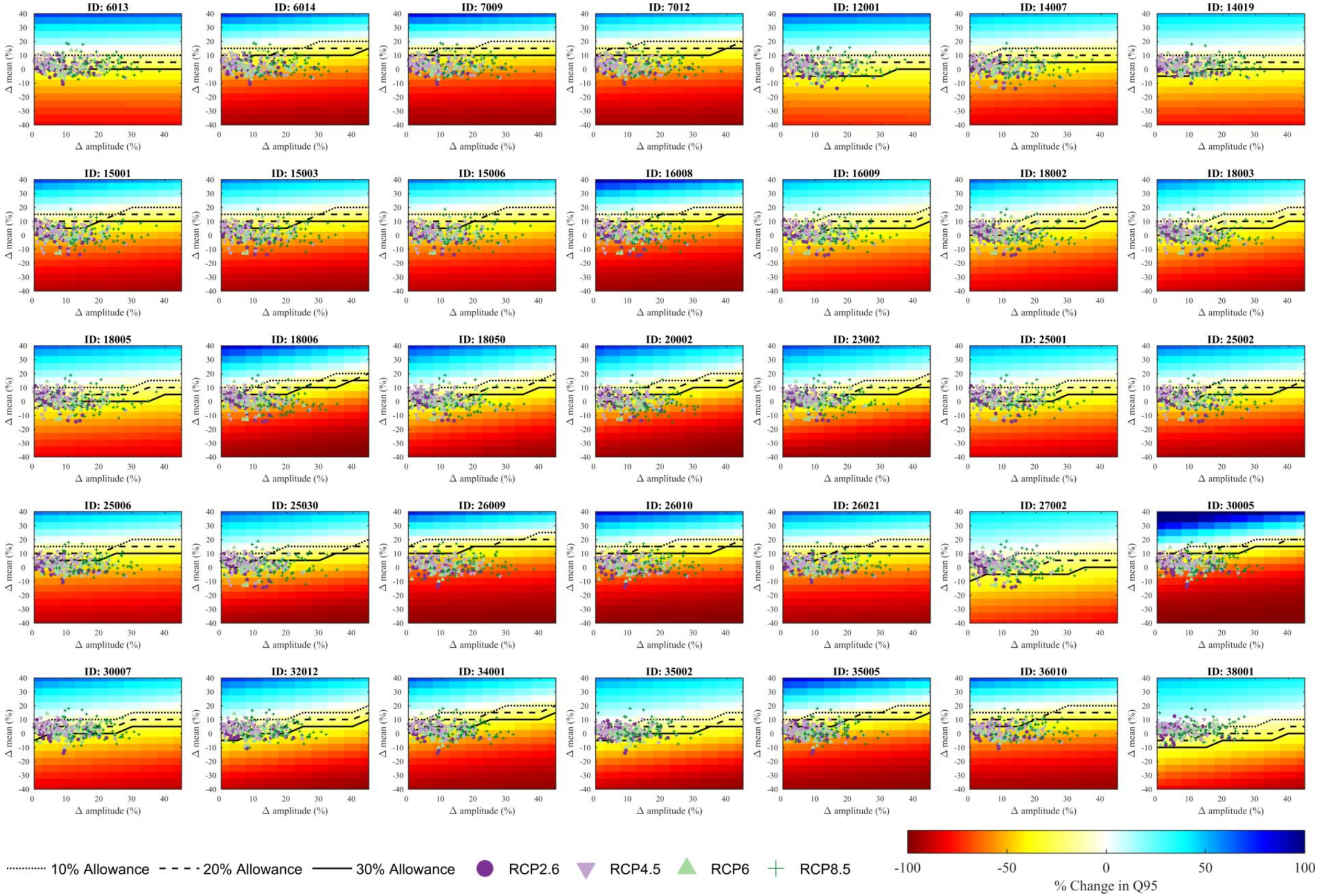

Figure A24 Response surfaces showing changes (%) in the magnitude of the Q95 low flow indicator for incremental changes (5%) in harmonic parameters representing the mean amount (-40% to +40%; *x*-axis) and seasonality (0% to 50%; *y*-axis) of the annual precipitation cycle. Surfaces are developed for each of the 35 catchments using the median HBV simulation. Overlain on each plot are changes (%) in the harmonic mean and amplitude projected for the period 2070-2099 under all 4 RCPs by each member of the CMIP5 ensemble. Surfaces relate to a +4°C increase in mean annual temperature relative to 1976-2005.

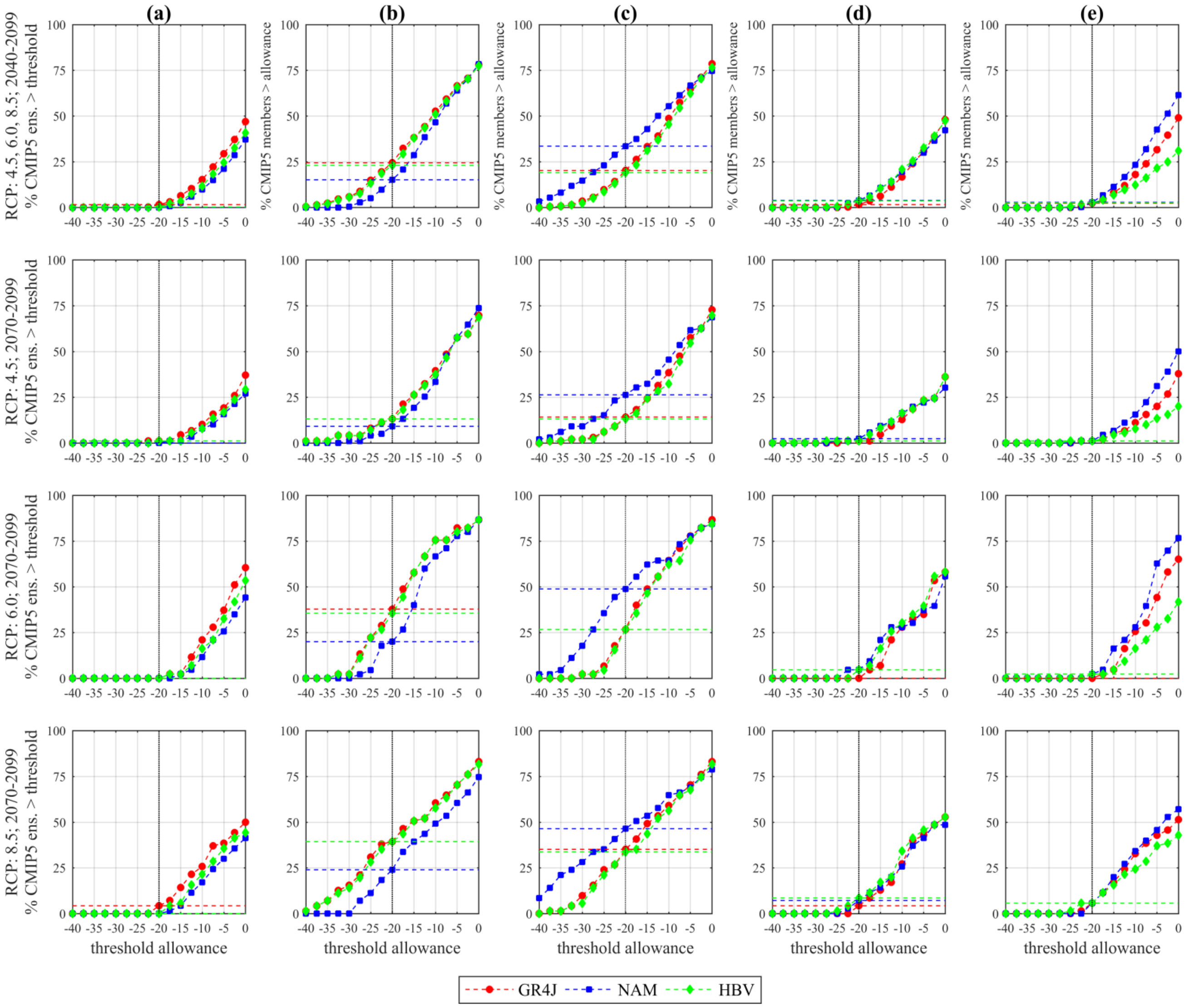

Figure A25 Percent of CMIP5 projections (y-axis) which exceed climate change allowances of 0% - 40% (relative to baseline period 1976-2005; x-axis) calculated for each catchment type (a-e) and rainfall-runoff model. Thresholds relate to a temperature scenario of +0°C relative to baseline conditions. Climate risk exposure based on the CMIP5 ensemble is calculated using projections for all 215 catchments and the corresponding centroid relating to their sensitivity type (Figure 3.11). Plots show the exposure of each type to projected climate and the adequacy of different adaptive thresholds. The 20% reduction allowance is emphasised using the black line. Combined threshold calculated for RCP4.5, RCP6 and RCP8.5 over the period 2040-2069 and 2070-2099 are shown in the upped row. The second, third and fourth row show thresholds for the period 2070-2099 relating to RCP4.5, RCP6 and RCP8.5 respectively.

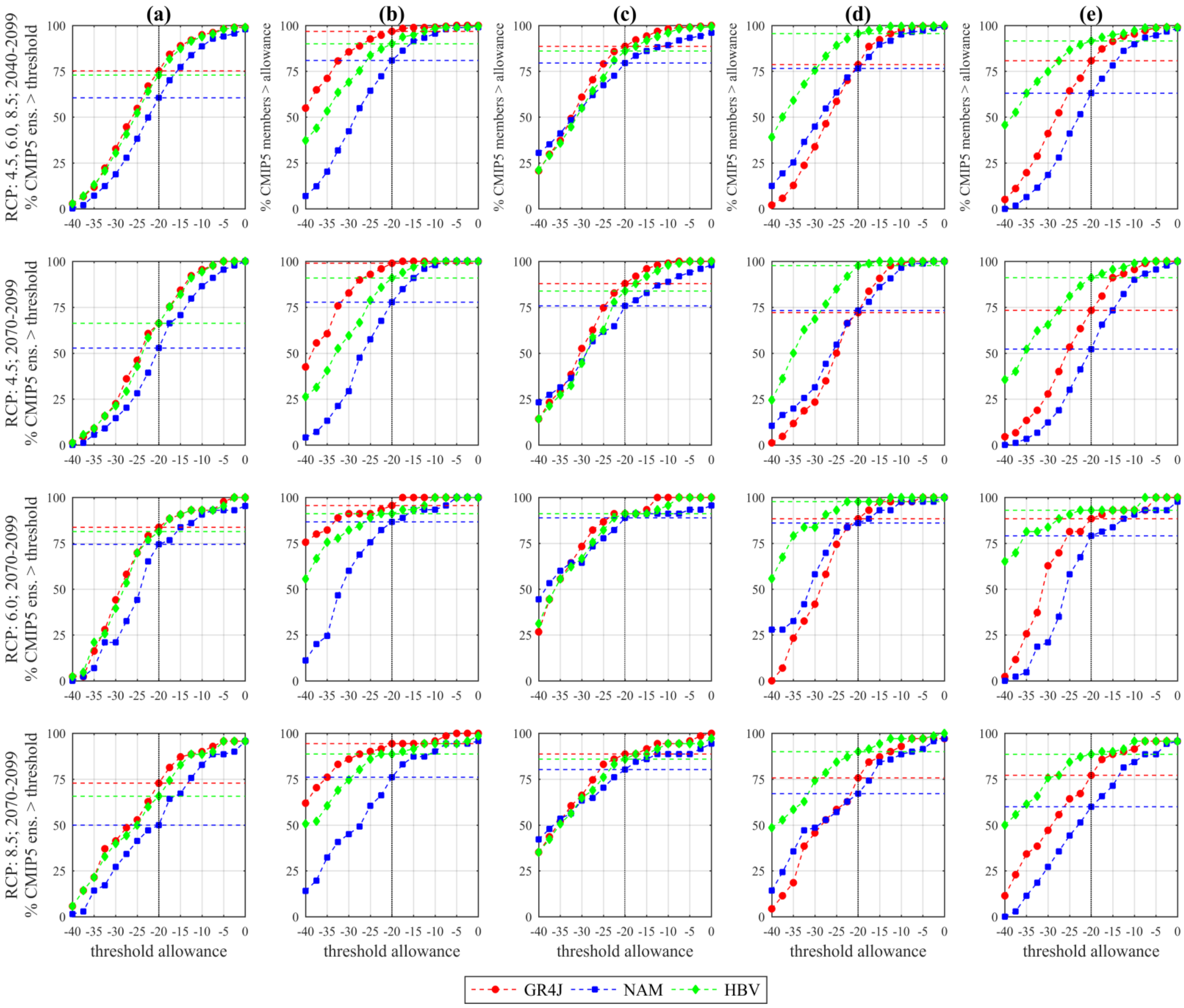

Figure A26 Percent of CMIP5 projections (y-axis) which exceed climate change allowances of 0% - 40% (relative to baseline period 1976-2005; x-axis) calculated for each catchment type (a-e) and rainfall runoff model. Thresholds relate to a temperature scenario of +4°C relative to baseline conditions. Climate risk exposure based on CMIP5 ensemble is calculated using projections for all 215 catchment and the corresponding centroid relating to their sensitivity type (Figure 3.11). Plots show the exposure of each type to projected climate and the adequacy of different adaptive thresholds. The 20% reduction allowance is emphasized using the black line. Combined threshold calculated for RCP4.5, RCP6 and RCP8.5 over the period 2040-2069 and 2070-2099 are shown in the upper row. The second third and fourth row show threshold for period 2070-2099 relating to RCP4.5, RCP6 and RCP8.5 respectively.

ervia

Aurora TELECOM

Gas Networks Ireland

UISCE ÉIREANN : IRISH WATER